Cambridge University

Doctoral Thesis

On the Simulation of Boson Stars in General Relativity

Author: Robin Croft

Supervisor: Dr. Ulrich Sperhake

Contents

Chapter 1

Introduction to Differential Geometry and General Relativity

1.1 Introduction

1.1.1 Introduction to General Relativity

The modern theory of gravity, published by Albert Einstein in 1915, is general relativity (GR). It is a geometric theory relying on curved spaces and differential geometry. GR is a generalisation of Einstein's theory of special relativity (SR) to include matter and gravity. Where the main idea behind SR was that the laws of physics are identical in any non-accelerating frame, GR includes the gravitational force (and subsequently matter) by postulating that the laws of physics are identical in any free-falling frame. In a universe without gravity or matter GR is equivalent to SR.

GR also supersedes Newton's theory of gravity when gravity becomes stronger. In Newtonian theory, two masses orbit each other in a constant circle or ellipse; the ellipses can precess in the presence of extra masses. However, the calculated precession rate of Mercury about the sun using Newton's theory of gravity was too slow; Einstein correctly calculated the precession rate using GR. This initial success proved to the world that Einstein's theory was the best current description of gravity. In the weak gravity limit, GR replicates Newton's theory of gravity; the precession of Mercury is the most stark deviation from Newton's theory in the solar system as it is closest to the sun where gravity is the strongest.

Other new effects predicted by GR include gravitational time dilation and light ray deflection. Gravitational time dilation is similar to time dilation in SR which states that an observer at rest would age more quickly (in their own frame) compared to a quickly moving observer. Gravitational time dilation states that an observer in a stronger gravitational field will age more slowly than one in a weaker gravitational field; this effect has been verified by comparing two atomic clocks where one is left on the surface of the earth and one is elevated. Light ray deflection occurs when a beam of light passes close by an object with a strong gravitational field - the stronger the field the more the light beam is deflected. This can be seen when distant bright objects pass behind matter such as black holes or large clusters of matter.

When gravity becomes moderately strong, Newtons theory starts to become quite inaccurate. After many orbits of two heavy objects the time averaged separation can be seen to decrease, hence the objects are inspiralling. The orbital energy lost is released as a gravitational wave (GW) signal. Inspiralling and radiation becomes more pronounced at lower separations and with heavier objects. Approximations to GR can be used in this regime, for example post Newtonian (PN) theory. Another example is the neutron star (NS), an object so dense that all of the electrons in an atom are forced to combine with nearby protons and reduce all matter to a dense lattice of neutrons. The gravitational field on the surface of a NS is of order 10^{11} times stronger than on earth's surface and the internal physics of the NS is not well known to date.

In the strong gravity regime GR deviates entirely from Newtonian theory leading to a plethora of exotic results. One major group of examples are black holes (BHs), the densest known macroscopic objects with such a strong gravitational pull that even light cannot escape. These dense objects can be produced by the collapse of large dying stars, implosions of supernovae, and collisions of very dense objects such as NSs or other heavy stars; the collapse of matter to a black hole itself is not described by Newtonian physics.

At the centre of a black hole, GR predicts a singularity; a single infinitely dense point surrounded by vacuum. It is presumed that Einstein's theory breaks down towards a singularity which is deemed unphysical. Theories such as loop quantum gravity (LQG) and string theory (ST) try to reconcile GR with quantum mechanics which is thought might alleviate this problem. Sadly there is no definitive answer as to what happens near a gravitational singularity, this is in part due to the lack of experimental data to draw from. The weak cosmic censorship conjecture states that all physical singularities are hidden inside an event horizon (EH). The EH is a surface containing all points that cannot send information to $\mathcal{I}^+$, the surface reached by out-directed photons in the infinite future; points inside an EH are *causally disconnected* from the exterior.

GR also describes physics at the largest scales. The application of GR to the entire universe is called Cosmology. Cosmology can be used to describe the big bang, early universe expansion and late universe inflation. Cosmology can also be used to describe a universe with small matter and gravitational perturbations on top of a uniform background which is currently the best large scale description of the universe.

One final noteworthy prediction of GR is gravitational waves. In 2015 GWs were detected by the Laser Interferometer Gravitational-Wave Observatory (LIGO) which lead to the 2017 Nobel prize in physics. Many subsequent signals from inspiralling BH-BH and BH-BS inspirals have been measured which agree with the waveforms predicted by NR simulations and PN theories. This recent discovery has lead to an increase in interest in gravitational physics - especially systems with observable GWs.

1.1.2 Introduction to Compact Objects and Boson Stars

The first non-trivial solution to Einstein's equation found was that of the spherically symmetric, static and asymptotically flat vacuum spacetime by Karl Schwarzschild in 1916. The solution was designed to be used outside a spherically symmetric, non-spinning, body of mass; however it also turned out to provide use in describing black holes. This metric was then modified by Tolman, Oppenheimer and Volkov in 1939 to describe the non-vacuum case of a constant density neutron star.

Black holes in the universe generally spin; any black hole forming from the collapse of matter will inherit the angular momentum of the matter as it collapses. Another way to see this is that the space of black hole solutions has zero size compared to the space of spinning black holes; the non-spinning black hole is a fine tuned black hole with spin zero. Rotating black holes were first described by Roy Kerr in 1963, and are subsequently called Kerr black holes. The collisions of black holes (with or without spin) is also successfully described by GR, however this phenomenon is far too complicated to solve analytically. Numerical relativity (NR), the exact simulation of GR using methods to solve partial differential equations (PDEs), is needed to describe black hole collisions and inspirals.

The study of compact exotic objects can be traced back to John Wheeler who investigated Geons in 1955 for their potential similarity to elementary particles. Geons are gravito-electromagnetic objects with the name arising from "gravitational electromagnetic entity". In 1968 David Kaup published [1] describing what he called "Klein-Gordon Geons", nowadays referred to as boson stars. Importantly, boson stars are a localised complex Klein-Gordon configuration, with the real counterparts being unstable. Variants such as (Spin 1) Proca stars [2], electromagnetically charged boson stars and many others have been studied.

Interest in boson stars remains for many reasons. Given the recent discovery of the Higgs boson, we know that scalar fields exist in nature and any gravitational wave signals created by compact objects could theoretically be detected with modern gravitational wave interferometers. Secondly, boson stars are a good candidate for dark matter halos [3] [4]. Boson stars are also useful as a proxy to other compact objects in general relativity; there is a lot of freedom in the construction of different types of boson star and they can be fine tuned to model dense neutron stars for one example. The advantage this would have over simulating a real fluid is that the Klein Gordon equation is linear in the principal part meaning smooth data must always remain smooth; this avoids shocks and conserves particle numbers relatively well with less sophisticated numerical schemes.

On a slightly different topic, collisions of boson stars could be a natural method to produce scalar hair around black holes which will be discussed later in more detail in section 3.2.5.

1.1.3 Conventions

Throughout this thesis physical quantities will be expressed as a dimensionless ratio of the Planck length $L_{\rm pl}$, time $T_{\rm pl}$ and mass $M_{\rm pl}$ unless stated otherwise; for example Newtons equation of gravity would be

written as

$$F = \frac{GMm}{r^2} \quad \rightarrow \quad \left(\frac{F}{F_{\mathrm{pl}}}\right) = \frac{\left(\frac{M}{M_{\mathrm{pl}}}\right)\left(\frac{m}{M_{\mathrm{pl}}}\right)}{\left(\frac{r}{L_{\mathrm{pl}}}\right)^2}, \tag{1.1.1}$$

where $F_{\mathrm{pl}} = M_{\mathrm{pl}} L_{\mathrm{pl}} T_{\mathrm{pl}}{}^{-2}$ is the Planck force. Consequently c, G and $\hbar$ take the numerical value of 1.

The Einstein summation convention for tensor indices will be used extensively; this means $A_\mu B^\mu \equiv \sum_\mu A_\mu B^\mu$ where the sum over μ is implied by contracting indices of same latter. Tensors and tensor fields will be denoted using bold font ($\boldsymbol{T}$) for index free notation and normal font ($T_{\mu\nu,\ldots}$) for the components. The dot product between two vectors or vector fields will be written interchangeably as $\boldsymbol{A} \cdot \boldsymbol{B} \leftrightarrow A_\mu B^\mu$ for readability. Additionally, ∇_μ denotes the covariant derivative and ∂_μ is the partial derivative, both with respect to coordinate x^μ. The metric signature will always be $(-,+,+,+)$.

When considering the ADM decomposition, as in section 2.1, objects can be associated with both a $3+1$ dimensional manifold $\mathcal{M}$ or a 3 dimensional hypersurface Σ. To distinguish between these, standard Roman letters such as R represent the object belonging to $\mathcal{M}$ and calligraphic letters such as $\mathcal{R}$ correspond to the object belonging to Σ.

Finally, unless stated otherwise, Greek indices such as $\{\alpha, \beta, ..., \mu, \nu, ...\}$ label generic dimension tensor components (often 4 dimensions) whereas late Latin indices such as $\{i, j, k, ...\}$ label three dimensional tensor components and early Latin indices such as $\{a, b, ...\}$ label two dimensional ones.

1.2 Differential Geometry

1.2.1 Introduction to Geometry and Manifolds

Everyone's first encounter with geometry will cover Pythagoras' theorem; arguably the most famous and useful equation in existence. Pythagoras' equation relates the sidelengths of a right angled triangle, it says that $s^2 = x^2 + y^2$ for a triangle with height y, width x and hypotenuse length s. This can be shown very simply by looking at Fig. 1.1. The area of the partially rotated square is s^2, but we can also calculate it from the the area of the larger square A_{sq} and subtracting four times the area of one of the triangles A_{tr}. Given that $A_{sq} = (x+y)^2$ and $A_{tr} = \frac{1}{2}xy$, then

$$s^2 = (x+y)^2 - 2xy = x^2 + y^2, \tag{1.2.1}$$

and we have proved Pythagoras' theorem. Using an infinitesimally small triangle, we can write $\mathrm{d}s^2 = \mathrm{d}x^2 + \mathrm{d}y^2$ and this can be trivially extended to arbitrary dimensions like

$$\mathrm{d}s^2 = \mathrm{d}x^2 + \mathrm{d}y^2 + \mathrm{d}z^2 + \ldots \ . \tag{1.2.2}$$

The infinitesimal form of Pythagoras' theorem is very powerful as it can be used to calculate the length of a generic curve by approximating the curve as a collection of infinitesimally small straight lines with length $\mathrm{d}s$. So far we have assumed that space is flat meaning Eq. (1.2.2) is true for all points in space, this is an assumption we will have to drop if we want to study the curved spaces arising in strong gravity. In the next sections we will explore the generalisation of Pythagoras' equation to curved spaces and use it to measure curve lengths as well as volumes and areas.

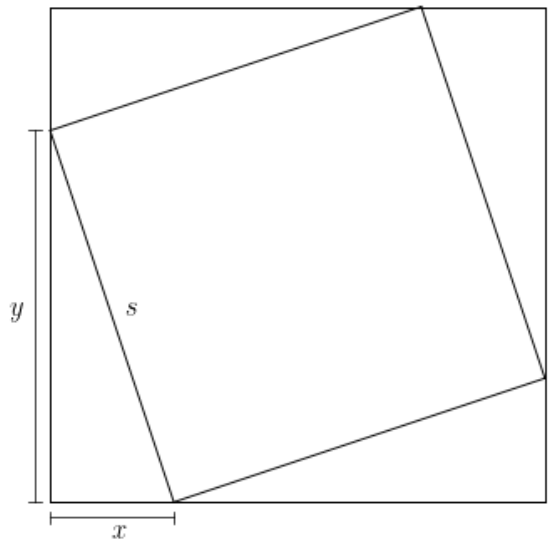

Figure 1.1: Diagram for proof of Pythagoras' theorem.

Differential Geometry (DG) is the extension of calculus, linear algebra and multilinear algebra to curved geometries. Einstein's Theory of Relativity is written using the language of DG as it is the natural way to deal with curves, tensor calculus and differential tensor equations in curved spaces. For a basic introduction to DG, we should start with a manifold $\mathcal{M}$ which is an N dimensional space that locally looks like $\mathbb{R}^N$, N dimensional Euclidean space. This is important as at a point $p \in \mathcal{M}$ we can find infinitesimally close neighbouring points $p + \delta p \in \mathcal{M}$. In the following sections we will explore curves, functions, tensors and calculus on manifolds using DG.

1.2.2 Functions, Curves and Tensors on Manifolds

A real scalar function f over $\mathcal{M}$ maps any point $p \in \mathcal{M}$ to a real number, denoted $f : p \to \mathbb{R}$. An important example of a set of scalar functions is the coordinate system ϕ, $\phi : p \to \mathbb{R}^N$, this is normally

written x^μ where $\mu \in \{0, 1, ..., N-1\}$ is an index labelling the coordinate. The map ϕ is called a chart, and unlike Euclidean space one chart may not be enough to cover the entire manifold; in this case a set of compatible charts should be smoothly joined, collectively known as an atlas.

Now that functions have been discussed, the next simplest object we can discuss is a curve, or path, through $\mathcal{M}$. A curve Γ is a set of smoothly connected points $p(\lambda) \in \mathcal{M}$ that smoothly depend on an input parameter $\lambda \in [\lambda_0, \lambda_1]$. This can be expressed in terms of coordinates as $x^\mu(\lambda)$ where $\phi : p(\lambda) \to x^\mu(\lambda)$. Differentiating a function f along Γ with respect to λ gives

$$\frac{\mathrm{d}}{\mathrm{d}\lambda} f(x^\mu(\lambda)) = \frac{\mathrm{d}x^\nu}{\mathrm{d}\lambda} \frac{\partial f(x^\mu)}{\partial x^\nu} = \frac{\mathrm{d}x^\nu}{\mathrm{d}\lambda} \partial_\nu f, \tag{1.2.3}$$

where the Einstein summation convention was invoked, summing over all values of ν, and $\partial_\nu = \partial/\partial x^\nu$. Equation (1.2.3) was derived independently of the choice of f, therefore we can generally write

$$\frac{\mathrm{d}}{\mathrm{d}\lambda} = \frac{\mathrm{d}x^\nu}{\mathrm{d}\lambda} \partial_\nu. \tag{1.2.4}$$

The operator $\mathrm{d}/\mathrm{d}\lambda$ can act on any function f and return a new function $\tilde{f}$ over $\mathcal{M}$, this is written as $\mathrm{d}/\mathrm{d}\lambda(f) = \tilde{f}$ where $\tilde{f} : p \to \mathbb{R}$ for $p \in \mathcal{M}$. We can also think of $\mathrm{d}/\mathrm{d}\lambda$ as a vector $\boldsymbol{X}$ with components $X^\mu = \mathrm{d}x^\mu/\mathrm{d}\lambda$ and basis vectors $\boldsymbol{e}_\mu := \partial_\mu$ taken from Eq. (1.2.4). The vector $\boldsymbol{X}$ can be written as $\boldsymbol{X} = X^\mu \boldsymbol{e}_\mu$ and can act on a general function f over $\mathcal{M}$ as $\boldsymbol{X}(f) = X^\mu \boldsymbol{e}_\mu(f) = X^\mu \partial_\mu f$. Considering the set of all possible curves through a points $p \in \mathcal{M}$, the tangent vector components $\mathrm{d}x^\mu/\mathrm{d}\lambda$ span an N dimensional space with basis $\boldsymbol{e}_\mu = \partial_\mu$; this space is called the tangent space and is denoted as $\mathcal{T}_p(\mathcal{M})$ at a point $p \in \mathcal{M}$.

The next object to discuss is the co-vector which is defined as a map from vectors to real numbers; not to be confused with the dot product in section 1.2.3. Similarly to vectors, a co-vector $\boldsymbol{\omega}$ can be expressed as a sum of components ω_μ and basis co-vectors $\boldsymbol{\theta}^\mu$ like $\boldsymbol{\omega} = \omega_\mu \boldsymbol{\theta}^\mu$. Contrary to vectors, co-vector components have downstairs indices and the basis has upstairs indices; this choice improves the readability of tensor equations when working with components. A co-vector can map a vector to a real number like $\boldsymbol{\omega} : \boldsymbol{X} \to \mathbb{R}$ or $\boldsymbol{\omega}(\boldsymbol{X}) \to \mathbb{R}$. Vectors are equally able to map co-vectors to real numbers, denoted as $\boldsymbol{X} : \boldsymbol{\omega} \to \mathbb{R}$. Co-vectors are defined such that $\boldsymbol{\theta}^\mu : \boldsymbol{e}_\nu = \delta^\mu_\nu$ where δ^μ_ν are the components of the Kroneka delta equating to zero unless $\mu = \nu$ in which case they are one. The operation of a generic co-vector $\boldsymbol{\omega}$ on a generic vector $\boldsymbol{X}$ is

$$\boldsymbol{\omega} : \boldsymbol{X} = \omega_\mu X^\nu \boldsymbol{\theta}^\mu : \boldsymbol{e}_\nu = \omega_\mu X^\nu \delta^\mu_\nu = \omega_\mu X^\mu \in \mathbb{R}. \tag{1.2.5}$$

This map is linear and identical under reversing the order of operation; $\boldsymbol{\omega} : \boldsymbol{X} = \boldsymbol{X} : \boldsymbol{\omega}$. Similarly to vectors, the set of all possible co-vectors at a point $p \in \mathcal{M}$ span an N-dimensional space called the co-tangent space, written as $\mathcal{T}^*_p(\mathcal{M})$.

Multilinear Maps and Tensors

Generalising the previous linear maps between vectors and co-vectors gives the multilinear map. Consider a tensor $\boldsymbol{T}$, this can be expressed in component form like

$$\boldsymbol{T} = T^{\alpha\beta,\cdots}_{\mu\nu,\cdots} \boldsymbol{e}_\alpha \otimes \boldsymbol{e}_\beta \otimes ... \otimes \boldsymbol{\theta}^\mu \otimes \boldsymbol{\theta}^\nu \otimes ... \tag{1.2.6}$$

for an arbitrary number of outer products of vector and co-vector bases. A tensor with m co-vector bases and n vector bases is called an (m, n) tensor and has a rank of $m + n$. Vectors, co-vectors and scalars are $(1, 0)$, $(0, 1)$ and $(0, 0)$ tensors respectively. Tensors can act as multilinear maps between tensors. We have already seen how a vector and co-vector can map each other to a scalar, let's extend this with an example. An $(0, 2)$ tensor, $\boldsymbol{T} = T_{\mu\nu} \boldsymbol{\theta}^\mu \otimes \boldsymbol{\theta}^\nu$ at $p \in \mathcal{M}$, can map two vectors $\boldsymbol{X}$ and $\boldsymbol{Y}$ to a scalar as

shown,

$$\boldsymbol{T}(\boldsymbol{X},\boldsymbol{Y}) = T_{\mu\nu}X^{\alpha}Y^{\beta}\boldsymbol{\theta}^{\mu}\otimes\boldsymbol{\theta}^{\nu}(\boldsymbol{e}_{\alpha},\boldsymbol{e}_{\beta}), \tag{1.2.7}$$

$$= T_{\mu\nu}X^{\alpha}Y^{\beta}(\boldsymbol{\theta}^{\mu}:\boldsymbol{e}_{\alpha})(\boldsymbol{\theta}^{\nu}:\boldsymbol{e}_{\beta}), \tag{1.2.8}$$

$$= T_{\mu\nu}X^{\alpha}Y^{\beta}\delta^{\mu}_{\alpha}\delta^{\nu}_{\beta}, \tag{1.2.9}$$

$$= T_{\mu\nu}X^{\mu}Y^{\nu}. \tag{1.2.10}$$

The multilinear map can also output generic tensors, for example consider

$$\boldsymbol{T}(\boldsymbol{X},\star) = T_{\mu\nu}X^{\alpha}(\boldsymbol{\theta}^{\mu}:\boldsymbol{e}_{\alpha})\boldsymbol{\theta}^{\nu} = T_{\mu\nu}X^{\mu}\boldsymbol{\theta}^{\nu}, \tag{1.2.11}$$

which uses the $(0,2)$ tensor $\boldsymbol{T}$ to map the vector $\boldsymbol{X}$ to a co-vector $\boldsymbol{W}$ with components $W_{\mu} = T_{\mu\nu}X^{\mu}$.

One final example of a mapping is from a single tensor to a lower rank tensor, this is called contraction. To illustrate this, let's take a $(1,3)$ tensor $\boldsymbol{Z} = Z^{\alpha}{}_{\mu\nu\rho}\boldsymbol{e}_{\alpha}\otimes\boldsymbol{\theta}^{\mu}\otimes\boldsymbol{\theta}^{\nu}\otimes\boldsymbol{\theta}^{\rho}$. We can choose to use the basis vector $\boldsymbol{e}_{\alpha}$ to act on any of the three co-vector bases, choosing $\boldsymbol{\theta}^{\mu}$ this is

$$Z^{\alpha}{}_{\mu\nu\rho}(\boldsymbol{e}_{\alpha}:\boldsymbol{\theta}^{\mu})\boldsymbol{\theta}^{\nu}\otimes\boldsymbol{\theta}^{\rho} = Z^{\mu}{}_{\mu\nu\rho}\boldsymbol{\theta}^{\nu}\otimes\boldsymbol{\theta}^{\rho} = \tilde{Z}_{\nu\rho}\boldsymbol{\theta}^{\nu}\otimes\boldsymbol{\theta}^{\rho}, \tag{1.2.12}$$

where $\tilde{Z}_{\nu\rho} = Z^{\mu}{}_{\mu\nu\rho}$. Tensors are central to general relativity, objects such as curvature, matter and paths will be described by tensor fields[1].

1.2.3 The Inner Product and the Metric

To introduce the notion of length on a tangent plane $\mathcal{T}_p(\mathcal{M})$ at a point $p\in\mathcal{M}$ the metric tensor $\boldsymbol{g}$ is introduced. The metric tensor has components,

$$g_{\mu\nu} = \boldsymbol{e}_{\mu}\cdot\boldsymbol{e}_{\nu}, \tag{1.2.13}$$

where $\boldsymbol{e}_{\mu}\cdot\boldsymbol{e}_{\nu}$ represents the inner product (or dot product) on $\mathcal{T}_p(\mathcal{M})$; clearly the metric is symmetric by construction as $\boldsymbol{e}_{\mu}\cdot\boldsymbol{e}_{\nu} = \boldsymbol{e}_{\nu}\cdot\boldsymbol{e}_{\mu}$. The inner product can be thought of as a multilinear map,

$$\boldsymbol{g}:(\boldsymbol{X},\boldsymbol{Y})\to\mathbb{R}, \quad \text{or} \quad \boldsymbol{g}(\boldsymbol{X},\boldsymbol{Y}) = g_{\mu\nu}X^{\mu}Y^{\nu}, \tag{1.2.14}$$

where $\boldsymbol{X}\in\mathcal{T}_p(\mathcal{M})$, $\boldsymbol{Y}\in\mathcal{T}_p(\mathcal{M})$ and $\boldsymbol{g}\in\mathcal{T}^*_p(\mathcal{M})\otimes\mathcal{T}^*_p(\mathcal{M})$. The inner product can also be represented by a second map

$$\boldsymbol{X}:\boldsymbol{Y}\to\mathbb{R}, \quad \text{or} \quad \boldsymbol{X}\cdot\boldsymbol{Y} = X^{\mu}Y^{\nu}\boldsymbol{e}_{\mu}\cdot\boldsymbol{e}_{\nu} = X^{\mu}Y^{\nu}g_{\mu\nu}, \tag{1.2.15}$$

which is a new mapping. The inner product also gives the length (or magnitude) $|\boldsymbol{X}|$ of any vector $\boldsymbol{X}\in\mathcal{T}_p(\mathcal{M})$ as,

$$|\boldsymbol{X}|^2 = \boldsymbol{X}\cdot\boldsymbol{X} = g_{\mu\nu}X^{\mu}X^{\nu}. \tag{1.2.16}$$

Another way to think of the inner product is that the metric maps a vector $\boldsymbol{X}$ to an equivalent or *dual* co-vector $\boldsymbol{\Xi}$ such that $\boldsymbol{X}:\boldsymbol{\Xi} = X^{\mu}\Xi_{\mu} = g_{\mu\nu}X^{\mu}X^{\nu}$. In component form $\boldsymbol{\Xi}$ is

$$\Xi_{\mu} = g_{\mu\nu}X^{\nu}; \tag{1.2.17}$$

this use of the metric to map a vector to it's corresponding co-vector (and vice-versa) is extremely useful. Without loss of information we can write $\Xi_{\nu} = X_{\nu}$ to make it obvious that $X_{\nu} = X^{\mu}g_{\mu\nu}$ and this convention will be used from now on.

[1] A tensor field assigns a tensor to each point on a manifold $\mathcal{M}$; in this work the assigning will be continuous and tensors assigned to two infinitesimally close points $(p, p+\delta p)$ will be infinitesimally similar to each other.

The metric also assigns an inner product and a length measure on the co-tangent plane $\mathcal{T}_p^*(\mathcal{M})$ but instead using the inverse components $g^{\mu\nu} = (g^{-1})_{\mu\nu}$,

$$g^{\mu\nu} = \boldsymbol{\theta}^\mu \cdot \boldsymbol{\theta}^\nu. \tag{1.2.18}$$

Similarly to before the inner product of two co-vectors $\boldsymbol{\omega}$ and $\boldsymbol{\sigma}$ is

$$\boldsymbol{\omega} \cdot \boldsymbol{Y} = \omega_\mu \sigma_\nu \boldsymbol{\theta}^\mu \cdot \boldsymbol{\theta}^\nu = \omega_\mu \sigma_\nu g^{\mu\nu} = \omega_\mu \sigma^\mu. \tag{1.2.19}$$

The reason that $g^{\mu\nu}$ must be the inverse matrix of $g_{\mu\nu}$ is as follows. For a vector $X^\mu \boldsymbol{e}_\mu$ and a co-vector $\omega_\mu \boldsymbol{\theta}^\mu$ we would like,

$$\boldsymbol{X} : \boldsymbol{\omega} = \boldsymbol{g}(\boldsymbol{X}, \star) : \boldsymbol{g}^{-1}(\boldsymbol{\omega}, \star), \tag{1.2.20}$$

$$X^\mu \omega_\mu = X_\mu \omega^\mu, \tag{1.2.21}$$

$$= X^\rho g_{\rho\mu} g^{\mu\sigma} \omega_\sigma \tag{1.2.22}$$

which is only true if $g_{\rho\mu} g^{\mu\sigma} = \delta^\sigma_\rho$ which is true by definition if $(g^{-1})_{\mu\nu} = g^{\mu\nu}$.

Not only has the metric provided us with an inner product and a length on tangent planes and cotangent planes, but it has also given a mapping between the two tangent planes. Therefore the metric can raise and lower indices on general tensors such as

$$T^{\mu\nu\ldots}_{\quad\alpha\beta} = g^{\mu\rho} g_{\beta\sigma} T_\rho{}^\nu{}_\alpha{}^{\sigma\ldots}. \tag{1.2.23}$$

1.2.4 Maps Between Manifolds

We now discuss the maps between two manifolds M and N. This has many uses such as pushing and pulling tensors between manifolds, allowing us to calculate a Lie derivative of tensor fields and finding the metric (or any tensor field) on an embedded surface; this property is crucial in the 3+1 spacetime decomposition in section 2.1.2.

Define a smooth map $\Phi : M \to N$ between manifolds on some coordinate patch labelling coordinates $x^\mu \in M$ and $y^\mu \in N$. The map $\Phi : x^\mu \to y^\mu$ gives $y^\mu = \Phi^\mu(x^\nu)$, or equivalently $y^\mu(x^\nu)$. Scalar functions must also map trivially,

$$f_N(y^\mu(x^\nu)) = f_M(x^\mu), \tag{1.2.24}$$

where $f_N \in N$ and $f_M \in M$, thus we will no longer identify which manifold a function is on. The map Φ allows us to push the vector $\boldsymbol{X} \in \mathcal{T}_p(M)$ to $\Phi_* \boldsymbol{X} \in \mathcal{T}_q(N)$, where $q = \Phi(p)$, in a way such that it's action on a function f is the same in either manifold.

$$\boldsymbol{X}(f)\Big|_p = \Phi_* \boldsymbol{X}(f)\Big|_q, \tag{1.2.25}$$

$$X^\mu \frac{\partial f}{\partial x^\mu} = (\Phi_* X)^\nu \frac{\partial f}{\partial y^\nu}, \tag{1.2.26}$$

$$\left(X^\mu \frac{\partial y^\nu}{\partial x^\mu}\right) \frac{\partial f}{\partial y^\nu} = (\Phi_* X)^\nu \frac{\partial f}{\partial y^\nu}, \tag{1.2.27}$$

and hence the components of the push-forward $\Phi_* \boldsymbol{X}$ can be read off,

$$(\Phi_* X)^\mu = \frac{\partial y^\mu}{\partial x^\nu} X^\nu. \tag{1.2.28}$$

Given a co-vector field $\boldsymbol{\omega} \in \mathcal{T}_p^*(N)$ we can pull the field back from $\mathcal{T}_p^*(M) \leftarrow \mathcal{T}_q^*(N)$, denoted $\Phi^* \boldsymbol{\omega}$, by demanding that $\Phi^* \boldsymbol{\omega}(\boldsymbol{X})\big|_p = \boldsymbol{\omega}(\Phi_* \boldsymbol{X})\big|_q$. Evaluating this gives

$$\Phi^* \boldsymbol{\omega}(\boldsymbol{X})\Big|_p = \boldsymbol{\omega}(\Phi_* \boldsymbol{X})\Big|_q, \tag{1.2.29}$$

$$(\Phi^* \omega)_\mu X^\mu = \omega_\nu (\Phi_* X)^\nu, \tag{1.2.30}$$

$$(\Phi^* \omega)_\mu X^\mu = \omega_\nu \frac{\partial y^\nu}{\partial x^\mu} X^\mu, \tag{1.2.31}$$

and the components of the pull-back $\Phi_*\boldsymbol{\omega}$ can be read off,

$$(\Phi^*\omega)_\mu = \frac{\partial y^\nu}{\partial x^\mu}\omega_\nu. \tag{1.2.32}$$

Considering an $(0,2)$ tensor $\boldsymbol{T} \in N$, the pullback $\Phi^*\boldsymbol{T} \in M$ follows simply from demanding that $\boldsymbol{T}(\Phi_*\boldsymbol{X}, \Phi_*\boldsymbol{Y})|_q = \Phi^*\boldsymbol{T}(\boldsymbol{X},\boldsymbol{Y})|_p$ where $\boldsymbol{X}$ and $\boldsymbol{Y}$ are vector fields on M. The components of the pull-back of $\boldsymbol{T}$ are therefore

$$(\Phi^*T)_{\mu\nu} = \frac{\partial y^\rho}{\partial x^\mu}\frac{\partial y^\sigma}{\partial x^\nu}T_{\rho\sigma}. \tag{1.2.33}$$

The pull-back of a generic $(0,q)$ tensor and the push-forward of a generic $(p,0)$ tensor can be found similarly by contracting with an extra $\frac{\partial y^\mu}{\partial x^\nu}$ for each downstairs index or $\frac{\partial x^\mu}{\partial y^\nu}$ for each upstairs index of the tensor considered.

Diffeomorphisms

So far we have only discussed the one way mapping $\Phi : M \to N$ which requires a well behaved $\partial y^\nu/\partial x^\mu$. A diffeomorphism is an isomorphism[2] between smooth manifolds $\Phi : M \to N$, meaning M and N have the same number of dimensions. Two infinitesimally close points $\{p, p+\delta p\} \in \mathcal{M}$ map to two infinitesimally close points $(q, q+\delta q) \in \mathcal{N}$ meaning that open sets are preserved. Given that a diffeomorphism is smooth bijective map then it must be inevitable with inverse map $\Phi^{-1} : N \to M$, and $y^\nu(x^\mu)$ has a smooth inverse $x^\nu(y^\mu)$. When an inverse map Φ^{-1} is defined then the pull-back of $(p,0)$ tensors from N to M along with the push-forward of $(0,q)$ tensors from M to N is possible. This means it is possible to push or pull generic tensors between M and N in any direction. The tangent spaces associated with $p \in \mathcal{M}$ or $q \in \mathcal{N}$ are therefore also preserved under mapping meaning that local structure on the manifold is preserved under the mapping. Two common examples of diffeomorphisms are coordinate changes and translations.

Projection Mappings

As mentioned, maps between manifolds can be used to project tensors to lower dimensional embedded surfaces. This requires us to consider an m-dimensional manifold M with metric $g_{\mu\nu}$ and coordinates x^μ as well as an embedded n-dimensional surface N where $n < m$. We can treat N as a separate n dimensional manifold with metric $h_{\mu\nu}$. As before, we can define a map $\Phi : x^\mu \to y^\mu$ and the pullback of the metric demands that,

$${}^{(m)}h_{\rho\sigma} = {}^{(n)}h_{\mu\nu}\frac{\partial y^\mu}{\partial x^\rho}\frac{\partial y^\nu}{\partial x^\sigma}, \tag{1.2.34}$$

where ${}^{(m)}\boldsymbol{h}$ represents m-dimensional the tensor on M and ${}^{(n)}\boldsymbol{h}$ represents n-dimensional the tensor on N; of course ${}^{(n)}\boldsymbol{h}$ and $\boldsymbol{h}$ are completely identical.

In the case that $n = m-1$, which is a projection into one less dimension, a convenient form for ${}^{(n)}\boldsymbol{h}$ can be found. If the image of N in M has everywhere an m-dimensional unit normal $\boldsymbol{n}$, then a vector $\boldsymbol{X} \in \mathcal{T}_p(\mathcal{M})$ for $p \in N$ can be projected onto N like,

$$({}^{(m)}\overrightarrow{X})^\mu = (\delta^\mu_\nu \mp n^\mu n_\nu)X^\nu, \tag{1.2.35}$$

where the sign is negative if $|\boldsymbol{n}|^2 = 1$ and positive if $|\boldsymbol{n}|^2 = -1$. It should be noted that strictly, $\overrightarrow{\boldsymbol{X}} \in \mathcal{T}_p(\mathcal{M})$. To avoid confusion we will denote the m-dimensional projected vector as ${}^{(m)}\overrightarrow{\boldsymbol{X}}$ and vector existing in the n-dimensional manifold N as ${}^{(n)}\overrightarrow{\boldsymbol{X}}$. The projection guarantees that,

$$\begin{aligned}
{}^{(n)}\boldsymbol{h}({}^{(n)}\overrightarrow{\boldsymbol{X}}, {}^{(n)}\overrightarrow{\boldsymbol{X}}) &= \boldsymbol{g}({}^{(m)}\overrightarrow{\boldsymbol{X}}, {}^{(m)}\overrightarrow{\boldsymbol{X}}), &(1.2.36)\\
&= {}^{(m)}h_{\mu\nu}(\delta^\mu_\alpha \mp n^\mu n_\alpha)X^\alpha(\delta^\nu_\beta \mp n^\nu n_\beta)X^\beta, &(1.2.37)\\
&= {}^{(m)}\boldsymbol{h}(\boldsymbol{X},\boldsymbol{X}), &(1.2.38)
\end{aligned}$$

[2] An isomorphism is a structure preserving bijective map between sets.

which gives a formula for the projected metric ${}^{(m)}\boldsymbol{h} \in \mathcal{M}$,

$$ {}^{(m)}h_{\mu\nu} = g_{\mu\nu} \mp n_\mu n_\nu. \tag{1.2.39} $$

The use of this projected metric to project general tensors to lower dimensions is explored in detail in section 2.1.2 and heavily relied upon in section **??**.

Mapping to lower dimensional surface of d-dimensions can be done similarly by adding an extra mutually-orthogonal unit vector for each reduced dimension like,

$$ {}^{(d)}h_{\mu\nu} = g_{\mu\nu} \mp n^{(1)}_\mu n^{(1)}_\nu \mp n^{(2)}_\mu n^{(2)}_\nu + \dots \,. \tag{1.2.40} $$

The metric $\tilde{\boldsymbol{h}}$ on an a-dimensional sub-surface $A \in \mathcal{M}$ can be explicitly calculated from the pushforward of ${}^{(m)}\tilde{\boldsymbol{h}}$ considering the diffeomorphism Φ^A that maps the image of A embedded in $\mathcal{M}$ to an a-dimensional manifold $\mathcal{A}$. The resulting metric is,

$$ (\Phi^A_* g)_{ij} = \tilde{h}_{ij} = \frac{\partial x^\mu}{\partial z^i}\frac{\partial x^\nu}{\partial z^j}{}^{(m)}\tilde{h}_{\mu\nu} = \frac{\partial x^\mu}{\partial z^i}\frac{\partial x^\nu}{\partial z^j}\left(g_{\mu\nu} \mp n^{(1)}_\mu n^{(1)}_\nu \mp n^{(2)}_\mu n^{(2)}_\nu + \dots\right), \tag{1.2.41} $$

where the $\boldsymbol{n}^{(i)}$ are a set of orthogonal unit vectors perpendicular to A; x^μ span $\mathcal{M}$ and z^i span $\mathcal{A}$.

1.2.5 Lie Derivatives

The Lie derivative of a tensor at a point p is the rate of change of a tensor field with respect to a pull-back from a diffeomorphism Φ mapping infinitesimally close points $(p = x^\mu, q = x^\mu + \epsilon\xi^\mu) \in \mathcal{M}$ with $\Phi : p \to q$ for some vector field $\boldsymbol{\xi}$. Like any good differential operator, the Lie derivative $\mathcal{L}_\xi$ along $\boldsymbol{\xi}$ (and $\mathcal{L}_\zeta$ along vector field $\boldsymbol{\zeta}$) should obey,

$$ \mathcal{L}_{a\xi+b\zeta}\boldsymbol{T} = a\mathcal{L}_\xi\boldsymbol{T} + b\mathcal{L}_\zeta\boldsymbol{T}, \tag{1.2.42} $$

$$ \mathcal{L}_\xi(a\boldsymbol{T} + b\boldsymbol{W}) = a\mathcal{L}_\xi\boldsymbol{T} + b\mathcal{L}_\xi\boldsymbol{W}, \tag{1.2.43} $$

$$ \mathcal{L}_\xi(f\boldsymbol{T}) = \boldsymbol{T}\mathcal{L}_\xi f + f\mathcal{L}_\xi\boldsymbol{T}, \tag{1.2.44} $$

for constant $\{a, b\}$, function f and generic tensor fields $\boldsymbol{T}$ and $\boldsymbol{W}$ of same rank. Note that while the partial derivative is linear in first argument like $\partial_{f\xi} = f\partial_\xi$ for a function f, the Lie derivative is only linear in first argument if f is a constant.

The simplest example is the Lie derivative of a scalar field ϕ, denoted $\mathcal{L}_\xi\phi$ with respect to vector field $\boldsymbol{\xi}$,

$$ \mathcal{L}_\xi\phi = \lim_{\epsilon\to 0}\left[\frac{\Phi^*\phi|_q - \phi|_p}{\epsilon}\right], \tag{1.2.45} $$

$$ = \lim_{\epsilon\to 0}\left[\frac{\phi(x^\mu + \epsilon\xi^\mu) - \phi(x^\mu)}{\epsilon}\right], \tag{1.2.46} $$

$$ = \xi^\mu\partial_\mu\phi, \tag{1.2.47} $$

which reduces to the partial derivative of ϕ with along $\boldsymbol{\xi}$. Next let's calculate the Lie derivative of a vector field $\boldsymbol{X}$ with respect to vector field $\boldsymbol{\xi}$. Starting with the same definition as Eq. (1.2.45), and using

$y^\mu = x^\mu + \epsilon\xi^\mu$, the Lie derivative of $\boldsymbol{X}$ is,

$$(\mathcal{L}_\xi X)^\mu = \lim_{\epsilon\to 0}\left[\frac{(\Phi^* X|_q)^\mu - X|_p{}^\mu}{\epsilon}\right], \tag{1.2.48}$$

$$= \lim_{\epsilon\to 0}\left[\frac{\frac{\partial x^\mu}{\partial y^\nu}X^\nu(x^\rho+\epsilon\xi^\rho) - X^\mu(x^\rho)}{\epsilon}\right], \tag{1.2.49}$$

$$= \lim_{\epsilon\to 0}\left[\frac{(\delta^\mu_\nu - \epsilon\partial_\nu\xi^\mu)X^\nu(x^\rho+\epsilon\xi^\rho) - X^\mu(x^\rho)}{\epsilon}\right], \tag{1.2.50}$$

$$= \lim_{\epsilon\to 0}\left[\frac{-\epsilon\partial_\nu\xi^\mu X^\nu(x^\rho+\epsilon\xi^\rho) + X^\mu(x^\rho+\epsilon\xi^\rho) - X^\mu(x^\rho)}{\epsilon}\right], \tag{1.2.51}$$

$$= \lim_{\epsilon\to 0}\left[\frac{-\epsilon\partial_\nu\xi^\mu X^\nu(x^\rho) + X^\mu(x^\rho+\epsilon\xi^\rho) - X^\mu(x^\rho) + \mathcal{O}(\epsilon^2)}{\epsilon}\right], \tag{1.2.52}$$

$$= \xi^\nu\partial_\nu X^\mu - X^\nu\partial_\nu\xi^\mu. \tag{1.2.53}$$

The Lie derivative for co-vectors and tensors can be derived in the same way, but can be quickly derived from the Leibniz rule as follows. Define a scalar field ψ, vector field $\boldsymbol{X}$ and co-vector field $\boldsymbol{\omega}$, where $\psi = X^\mu\omega_\mu$, then it follows that,

$$\mathcal{L}_\xi\psi = \xi^\mu\partial_\mu\psi = X^\nu\xi^\mu\partial_\mu\omega_\nu + \omega_\nu\xi^\mu\partial_\mu X^\nu, \tag{1.2.54}$$

$$= \mathcal{L}_\xi(X^\mu\omega_\mu), \tag{1.2.55}$$

$$= \omega_\mu(\mathcal{L}_\xi X)^\mu + X^\mu(\mathcal{L}_\xi\omega)_\mu, \tag{1.2.56}$$

$$X^\mu(\mathcal{L}_\xi\omega)_\mu = X^\nu\xi^\mu\partial_\mu\omega_\nu + \omega_\nu\xi^\mu\partial_\mu X^\nu - \omega_\mu(\mathcal{L}_\xi X)^\mu, \tag{1.2.57}$$

$$(\mathcal{L}_\xi\omega)_\mu = \xi^\nu\partial_\nu\omega_\mu + \omega_\nu\partial_\mu\xi^\nu. \tag{1.2.58}$$

Derivatives of a generic tensor $\boldsymbol{T}$ follows simply, for example,

$$(\mathcal{L}_\xi T)^{\alpha\beta\ldots}_{\mu\nu\ldots} = \xi^\sigma\partial_\sigma T^{\alpha\beta\ldots}_{\mu\nu\ldots} + T^{\alpha\beta\ldots}_{\sigma\nu\ldots}\partial_\mu\xi^\sigma + T^{\alpha\beta\ldots}_{\mu\sigma\ldots}\partial_\nu\xi^\sigma + \ldots - T^{\sigma\beta\ldots}_{\mu\nu\ldots}\partial_\sigma\xi^\alpha - T^{\alpha\sigma\ldots}_{\mu\nu\ldots}\partial_\sigma\xi^\beta - \ldots. \tag{1.2.59}$$

Lie derivatives will prove useful in section 2.1.4 and 2.1.9 to describe the time evolution of tensors in general relativity. The flow of time can be described as a diffeomorphism with respect to a suitable time vector $\tilde{\boldsymbol{t}}$ and the Lie derivative $\mathcal{L}_{\tilde{\boldsymbol{t}}}$ gives the rate of change of objects with respect to this flow of time.

1.2.6 Lengths on Manifolds

The natural entry point for studying curved geometry is to revisit Pythagoras' theorem. For this we need a manifold $\mathcal{M}$ equipped with a metric $\boldsymbol{g}$, written as $(\mathcal{M}, \boldsymbol{g})$ for short. The distance $\mathrm{d}s$ between two infinitesimally close points $p \in \mathcal{M}$ and $p + \delta p \in \mathcal{M}$, with coordinates $p = x^\mu$ and $p + \delta p = x^\mu + \mathrm{d}x^\mu$, is given by

$$\mathrm{d}s^2 = \boldsymbol{g}(\mathbf{d}\boldsymbol{x}, \mathbf{d}\boldsymbol{x}) = g_{\mu\nu}\mathrm{d}x^\mu\mathrm{d}x^\nu, \tag{1.2.60}$$

where $g_{\mu\nu}$ are the components of the metric tensor. This is the generalisation of Eq. (1.2.2) to curved space; notably the line element can now have varying coefficients from $g_{\mu\nu}$ and cross terms such as $\mathrm{d}x\mathrm{d}y$. The special choice of $g_{\mu\nu} = \delta_{\mu\nu}$ gives us flat Euclidean space; $\delta_{\mu\nu} = 1$ if $\mu = \nu$ and vanishes otherwise. With the line element defined, we can immediately apply it to calculating the length of a general curve in $\mathcal{M}$. Consider the curve Γ consisting of a set of connected points $p(\lambda) \in \mathcal{M}$ smoothly parameterised by λ. We can calculate the length Δs of the curve between $\lambda_1 \geq \lambda \geq \lambda_0$ by parameterising $\mathrm{d}s$,

$$\mathrm{d}s^2 = g_{\mu\nu}\frac{\partial x^\mu}{\partial\lambda}\frac{\partial x^\nu}{\partial\lambda}\mathrm{d}\lambda^2, \tag{1.2.61}$$

and integrating $\mathrm{d}s$ along Γ,

$$\Delta s = \int_{\lambda_0}^{\lambda_1}\sqrt{\left(g_{\mu\nu}\frac{\partial x^\mu}{\partial\lambda}\frac{\partial x^\nu}{\partial\lambda}\right)}\mathrm{d}\lambda. \tag{1.2.62}$$

In the simplified case where λ is one of the coordinates, say ξ, the length Δs becomes,

$$\Delta s = \int_{\xi_0}^{\xi_1} \sqrt{g_{\xi\xi}} \mathrm{d}\xi. \tag{1.2.63}$$

1.2.7 Volumes on Manifolds

Following from measuring the length of a curve now we can now measure volumes on a manifold; of course we still require a manifold with metric $(\mathcal{M}, \boldsymbol{g})$. In a coordinate system x^μ we can calculate the volume V of a subregion M by integrating some weight function $w(x^\mu)$,

$$V = \int_M w(x^\mu) \mathrm{d}x^1 \mathrm{d}x^2 ... \mathrm{d}x^n, \tag{1.2.64}$$

over M. To find $w(x^\mu)$, start by defining an orthogonal coordinate transformation $x^\mu \to \tilde{x}^\mu$ such that $\tilde{\boldsymbol{g}}$ is diagonal and $\det(\boldsymbol{g}) = \det(\tilde{\boldsymbol{g}})$; this is always possible as $\boldsymbol{g}$ is real and symmetric. In this coordinate system, the volume δV in an infinitesimal cuboid, with i'th sidelength $\delta\tilde{x}^i$, is

$$\delta V = \left(\sqrt{\tilde{g}_{11}}\delta\tilde{x}^1\right)\left(\sqrt{\tilde{g}_{22}}\delta\tilde{x}^2\right) ... \left(\sqrt{\tilde{g}_{nn}}\delta\tilde{x}^n\right), \tag{1.2.65}$$

where Eq. (1.2.63) was used to get the length between each $\tilde{x}^i$ and $\tilde{x}^i + \delta\tilde{x}^i$. Given that $\tilde{\boldsymbol{g}}$ is diagonal we know the i'th eigenvalue $\tilde{\lambda}_i = \tilde{g}_{ii}$ and therefore $\det(\tilde{\boldsymbol{g}}) = \prod_i \tilde{g}_{ii}$. Thus the volume δV can be rewritten,

$$\delta V = \sqrt{|\det(\tilde{\boldsymbol{g}})|}\delta\tilde{x}^1\delta\tilde{x}^2 ... \delta\tilde{x}^n, \tag{1.2.66}$$

and the formula for the finite volume of M is,

$$V = \int_M \sqrt{|\det(\tilde{\boldsymbol{g}})|}\mathrm{d}\tilde{x}^1\mathrm{d}\tilde{x}^2 ... \mathrm{d}\tilde{x}^n, \tag{1.2.67}$$

and the form of the weight function in $\tilde{x}^\mu$ coordinates is $\tilde{w}(\tilde{x}^\mu) = \sqrt{|\det(\tilde{\boldsymbol{g}})|}$. We are now free to transform back from $\tilde{x}^\mu \to x^\mu$, and given that the transformation is orthogonal we know that $\det(\boldsymbol{g}) = \det(\tilde{\boldsymbol{g}})$ and the Jacobean matrix $\boldsymbol{J}$ of the coordinate transformation has $\det(\boldsymbol{J}) = 1$, therefore

$$V = \int_M \sqrt{|\det(\boldsymbol{g})|}\, \mathrm{d}x^1\, \mathrm{d}x^2 \ldots \mathrm{d}x^n\,, \tag{1.2.68}$$

which holds for any non-diagonal, real and symmetric metric $\boldsymbol{g}$. In general we will now denote the determinant of a metric $\det(\boldsymbol{g})$ with the lower case letter g. When dealing with a pseudo-Riemannian manifold with a negative determinant, such as spacetime, it is more common to see $\sqrt{-g}$ written rather than $\sqrt{|g|}$ giving

$$V = \int_M \sqrt{-g}\, \mathrm{d}x^1\, \mathrm{d}x^2 \ldots \mathrm{d}x^n\,. \tag{1.2.69}$$

Equation (1.2.68) can also be used to find the volume (or area) of a lower dimensional sub-volume. First cover the new sub-volume A with coordinates z^μ, where $\mu \in \{1, 2, ..., m\}$ for $m < n$, and then calculate the metric $\tilde{\boldsymbol{h}}$ which can be done using Eq. (1.2.41). The area V_A of A is then,

$$V_A = \int_A \sqrt{|\tilde{h}|}\, \mathrm{d}z^1\, \mathrm{d}z^2 \ldots \mathrm{d}z^m\,, \tag{1.2.70}$$

which can be seen by mapping to an a-dimensional manifold $\mathcal{A}$ that is diffeomorphic to A and applying Eq. (1.2.68). These volume formulae are very useful in general relativity and have many uses in this thesis, especially throughout section **??**.

1.2.8 Geodesics

For a manifold equipped with metric $(\mathcal{M}, g)$ the curve with shortest distance between two points $p, q \in \mathcal{M}$ is called a geodesic. To find the geodesic joining p and q we need to use calculus of variations on the total length Δs from Eq. (1.2.62) of a general curve between two points. Given that the integrand $\mathcal{L}$ of Eq. (1.2.62) is a function $\mathcal{L}(x^\mu, \dot{x}^\mu)$, where the dot denotes differentiation by λ, we can use the Euler-Lagrange equation,

$$\frac{\partial \mathcal{L}}{\partial x^\mu} - \frac{\mathrm{d}}{\mathrm{d}\lambda}\frac{\partial \mathcal{L}}{\partial \dot{x}^\mu} = 0, \tag{1.2.71}$$

to give a differential equation with solution being a geodesic. Applying the EL equation to the integrand of Eq. (1.2.62) is algebraically messy, it is easier[3] to square the integrand and start from $\mathcal{L}^2$ giving the same solution if $\mathrm{d}\mathcal{L}/\mathrm{d}\lambda = 0$,

$$\frac{\partial \mathcal{L}^2}{\partial x^\alpha} - \frac{\mathrm{d}}{\mathrm{d}\lambda}\frac{\partial \mathcal{L}^2}{\partial \dot{x}^\alpha} = 0, \tag{1.2.72}$$

$$\frac{\partial}{\partial x^\alpha}\left(g_{\mu\nu}\dot{x}^\mu\dot{x}^\nu\right) - \frac{\mathrm{d}}{\mathrm{d}\lambda}\frac{\partial}{\partial \dot{x}^\alpha}\left(g_{\mu\nu}\dot{x}^\mu\dot{x}^\nu\right) = 0, \tag{1.2.73}$$

$$(\partial_\alpha g_{\mu\nu})\dot{x}^\mu\dot{x}^\nu - 2\frac{\mathrm{d}}{\mathrm{d}\lambda}\left(g_{\alpha\nu}\dot{x}^\nu\right) = 0, \tag{1.2.74}$$

$$(\partial_\alpha g_{\mu\nu})\dot{x}^\mu\dot{x}^\nu - 2\left(\dot{x}^\rho\partial_\rho\left(g_{\alpha\nu}\right)\dot{x}^\nu\right) - 2\ddot{x}^\nu g_{\alpha\nu} = 0. \tag{1.2.75}$$

Rearranging and multiplying by $g^{\alpha\beta}$ gives,

$$\ddot{x}^\beta + \frac{1}{2}g^{\alpha\beta}\left(\partial_\mu g_{\alpha\nu} + \partial_\nu g_{\alpha\mu} - \partial_\alpha g_{\mu\nu}\right)\dot{x}^\mu\dot{x}^\nu = 0, \tag{1.2.76}$$

$$\ddot{x}^\beta + \Gamma^\beta{}_{\mu\nu}\dot{x}^\mu\dot{x}^\nu = 0, \tag{1.2.77}$$

where $\Gamma^\beta{}_{\mu\nu}$ is the components of the connection-symbol from Eq. (1.3.77). A trivial solution to Eq. (1.2.77) is in flat space using Cartesian coordinates where $\Gamma^\beta{}_{\mu\nu} = 0$ and therefore $\ddot{x}^\beta = 0$ so $\dot{x}^\beta$ is a constant; this tells us the shortest distance between two points in flat space is a straight line. In other words, geodesics are straight lines in flat space.

Non-Affine Geodesics

The equation of a geodesic given above is true for an *affinely* parameterised curve. An affine parameter λ is defined so that the length of a curve δs between two parameter values λ and $\lambda + \delta\lambda$ is given by $\delta s = k(\delta\lambda)$ for constant k; the arclength along a curve is linearly proportional to the value of the λ. This property was inherent in the derivation of Eq. (1.2.77) is that $\mathrm{d}\mathcal{L}/\mathrm{d}\lambda = 0$ was assumed along a curve.

A non-affine parameter μ could equally be used to describe the curve. Writing $\mu(\lambda)$ the geodesic equation is transformed as shown,

$$\frac{\mathrm{d}^2x^\beta}{\mathrm{d}\lambda^2} + \Gamma^\beta{}_{\mu\nu}\frac{\mathrm{d}x^\mu}{\mathrm{d}\lambda}\frac{\mathrm{d}x^\nu}{\mathrm{d}\lambda} = 0, \tag{1.2.78}$$

$$\left(\frac{\mathrm{d}^2\mu}{\mathrm{d}\lambda^2}\frac{\mathrm{d}}{\mathrm{d}\mu} + \left(\frac{\mathrm{d}\mu}{\mathrm{d}\lambda}\right)^2\frac{\mathrm{d}^2}{\mathrm{d}\mu^2}\right)x^\beta + \Gamma^\beta{}_{\mu\nu}\frac{\mathrm{d}x^\mu}{\mathrm{d}\mu}\frac{\mathrm{d}x^\nu}{\mathrm{d}\mu}\left(\frac{\mathrm{d}\mu}{\mathrm{d}\lambda}\right)^2 = 0, \tag{1.2.79}$$

$$\frac{\mathrm{d}^2x^\beta}{\mathrm{d}\mu^2} + \Gamma^\beta{}_{\mu\nu}\frac{\mathrm{d}x^\mu}{\mathrm{d}\mu}\frac{\mathrm{d}x^\nu}{\mathrm{d}\mu} = -\left(\frac{\mathrm{d}\mu}{\mathrm{d}\lambda}\right)^{-2}\frac{\mathrm{d}^2\mu}{\mathrm{d}\lambda^2}\frac{\mathrm{d}x^\beta}{\mathrm{d}\mu}, \tag{1.2.80}$$

$$\frac{\mathrm{d}^2x^\beta}{\mathrm{d}\mu^2} + \Gamma^\beta{}_{\mu\nu}\frac{\mathrm{d}x^\mu}{\mathrm{d}\mu}\frac{\mathrm{d}x^\nu}{\mathrm{d}\mu} = -f(\mu)\frac{\mathrm{d}x^\beta}{\mathrm{d}\mu}, \tag{1.2.81}$$

[3]Given that $\mathcal{L}$ is homogeneous to degree k, $\dot{x}^i\partial\mathcal{L}/\partial\dot{x}^i = k\mathcal{L}$ for constant k, one can show that $\mathrm{d}\mathcal{L}/\mathrm{d}\lambda = 0$ if the Euler-Lagrange equation is assumed.

which is the same as the affine geodesic equation except with an extra non-zero right hand side proportional to $\mathrm{d}x^\beta/\mathrm{d}\mu$ and some function $f(\mu)$. If μ is a linear function of λ then μ is also an affine parameter; this is reflected in the term $\mathrm{d}^2\mu/\mathrm{d}\lambda^2 = 0$ and the affine geodesic equation is returned.

The non-affine geodesic equation can be can be found by re-deriving the Geodesic equation from $\mathcal{L}$ rather than $\mathcal{L}^2$. It can be seen that,

$$\frac{\partial \mathcal{L}}{\partial x^\alpha} = \frac{1}{2\mathcal{L}} \dot{x}^\mu \dot{x}^\nu \partial_\alpha g_{\mu\nu}, \tag{1.2.82}$$

$$\frac{\mathrm{d}}{\mathrm{d}\lambda}\frac{\partial \mathcal{L}}{\partial \dot{x}^\mu} = \frac{\mathrm{d}}{\mathrm{d}\lambda}\left(\frac{1}{\mathcal{L}} g_{\mu\alpha}\dot{x}^\mu\right), \tag{1.2.83}$$

$$= \frac{1}{\mathcal{L}} g_{\mu\alpha}\ddot{x}^\mu + \frac{1}{\mathcal{L}}\dot{x}^\nu \dot{x}^\mu \partial_\nu g_{\mu\alpha} + g_{\mu\alpha}\dot{x}^\mu \frac{\mathrm{d}}{\mathrm{d}\lambda}\frac{1}{\mathcal{L}}. \tag{1.2.84}$$

Rearranging and using the Euler-Lagrange equation as in the previous section gives

$$\ddot{x}^\beta + \Gamma^\beta{}_{\mu\nu}\dot{x}^\mu \dot{x}^\nu = -\mathcal{L}\frac{\mathrm{d}\mathcal{L}}{\mathrm{d}\lambda}\dot{x}^\alpha, \tag{1.2.85}$$

which is the non-affine geodesic equation.

1.3 Tensor Calculus and Curvature

1.3.1 General Covariance and Coordinate transformations

Many laws of physics can be expressed as tensor field equations where a tensor field is the assignment of a tensor to each point in space. This assignment must be smooth as it is to describe physical quantities. The power of tensor algebra and tensor calculus is that if a tensor field equation can be written in one coordinate system then it must hold (in index form) in all regular coordinate systems. This is a consequence of the tensor transformation law. Looking back, we can write a generic vector $\boldsymbol{X}$ as $X^\mu \boldsymbol{e}_\mu = X^\mu \partial_\mu$ and if we choose a coordinate transformation $x^\mu \to \tilde{x}^\mu$ then we see that in the transformed coordinate system the vector field $\boldsymbol{X}$, written $\tilde{\boldsymbol{X}}$, becomes

$$\begin{aligned}
\tilde{\boldsymbol{X}} &= \tilde{X}^\mu \frac{\partial}{\partial \tilde{x}^\mu}, && (1.3.1)\\
&= \tilde{X}^\mu \frac{\partial x^\nu}{\partial \tilde{x}^\mu}\frac{\partial}{\partial x^\nu}, && (1.3.2)\\
&= X^\nu \frac{\partial}{\partial x^\nu}, && (1.3.3)\\
&= \boldsymbol{X}, && (1.3.4)
\end{aligned}$$

where the components $X^\nu = \tilde{X}^\mu \frac{\partial x^\nu}{\partial \tilde{x}^\mu}$ are required to transform in order to ensure $\boldsymbol{X} = \tilde{\boldsymbol{X}}$. This says that the underlying geometric object (a vector in this case) is independent of the coordinates used to describe them; the tradeoff for this useful property is that the vectors components X^μ have to transform under the tensor transformation law, effectively opposing the transformation of the basis vectors. Working from a co-vector ω we can write it as $\omega_\mu \boldsymbol{\theta}^\mu = \omega_\mu \mathrm{d}x^\mu$ in component-basis form and the same coordinate transformation gives

$$\begin{aligned}
\tilde{\boldsymbol{\omega}} &= \tilde{\omega}_\mu \mathrm{d}\tilde{x}^\mu, && (1.3.5)\\
&= \tilde{\omega}_\mu \frac{\partial \tilde{x}^\mu}{\partial x^\nu}\,\mathrm{d}x^\nu\,, && (1.3.6)\\
&= \omega_\nu \mathrm{d}x^\nu, && (1.3.7)
\end{aligned}$$

where the co-vector components transform like $\omega_\nu = \tilde{\omega}_\mu \frac{\partial \tilde{x}^\mu}{\partial x^\nu}$, the opposite way to the vector components. These transformation laws ensure that a scalar field created from the product of a vector field and a co-vector field, like $\boldsymbol{\omega} : \boldsymbol{X}$, is a Lorentz scalar not transforming under coordinate transformations. This can be seen from

$$\begin{aligned}
\tilde{\boldsymbol{\omega}} : \tilde{\boldsymbol{X}} &= \tilde{X}^\mu \tilde{\omega}_\mu, && (1.3.8)\\
&= X^\nu \frac{\partial \tilde{x}^\mu}{\partial x^\nu}\frac{\partial x^\rho}{\partial \tilde{x}^\mu}\omega_\rho, && (1.3.9)\\
&= X^\nu \frac{\partial x^\rho}{\partial x^\nu}\omega_\rho, && (1.3.10)\\
&= X^\nu \delta_\nu{}^\rho \omega_\rho, && (1.3.11)\\
&= X^\nu \omega_\nu, && (1.3.12)\\
&= \boldsymbol{\omega} : \boldsymbol{X}. && (1.3.13)
\end{aligned}$$

The general tensor transformation law can be derived from chaining multiple of the previous examples together, for example,

$$\tilde{T}^{\mu\nu\ldots}{}_{\rho\sigma\ldots} = T^{\alpha\beta\ldots}{}_{\gamma\delta\ldots}\left(\frac{\partial \tilde{x}^\mu}{\partial x^\alpha}\frac{\partial \tilde{x}^\nu}{\partial x^\beta} \times \ldots \times \frac{\partial x^\gamma}{\partial \tilde{x}^\rho}\frac{\partial x^\delta}{\partial \tilde{x}^\sigma} \times \ldots\right), \qquad (1.3.14)$$

where each upstairs tensor index on $\boldsymbol{T}$ is contracted with a $\partial \tilde{x}^\mu / \partial x^\nu$ and each downstairs index is contracted with a $\partial x^\rho / \partial \tilde{x}^\sigma$.

Tensor Densities

A tensor density is the generalisation of a tensor field obeying the tensor transformation law in Eq. (1.3.14). One important example of a tensor density is the volume element $\sqrt{-g}$, this is a scalar density. This object does not have any indices so at first glance may pass for a true scalar field. However, when a coordinate transformation $x^\mu \to \tilde{x}^\mu$ is applied we find that $\sqrt{-g} \to \sqrt{-\tilde{g}} \neq \sqrt{-g}$, but for a general scalar field ϕ we find $\phi \to \tilde{\phi} = \phi$; therefore $\sqrt{-g}$ cannot be a scalar field. This can be shown explicitly by looking at the determinant of the metric,

$$\sqrt{-\tilde{g}} = \sqrt{\det(-\tilde{g}_{\mu\nu})}, \tag{1.3.15}$$

$$= \sqrt{\det\left(-g_{\alpha\beta}\frac{\partial x^\alpha}{\partial \tilde{x}^\mu}\frac{\partial x^\beta}{\partial \tilde{x}^\nu}\right)}, \tag{1.3.16}$$

$$= \sqrt{-g}\det\left(\frac{\partial x^\alpha}{\partial \tilde{x}^\mu}\right), \tag{1.3.17}$$

and as can be seen, the volume element picks up a factor of the determinant of the Jacobian. A tensor density $\boldsymbol{\mathcal{T}}$ of weight w can be written in the form,

$$\boldsymbol{\mathcal{T}} = \sqrt{-g}^w \boldsymbol{T}, \tag{1.3.18}$$

where $\boldsymbol{T}$ is a tensor obeying the tensor transformation law. It should be noted that a tensor density of weight zero is a regular tensor and the weight of a tensor has nothing to do with the rank of the tensor.

Lie Derivatives of Tensor Densities

To calculate the Lie derivative of a tensor density, first the Lie derivative of $\sqrt{-g}$ should be calculated, and in order to calculate the Lie derivative of the volume element a preliminary result is needed. Following the definition of a Lie derivative in section 1.2.5 and setting $y^\mu = x^\mu + \epsilon\xi^\mu$, the determinant of the Jacobian matrix is,

$$\det\left(\frac{\partial y^\mu}{\partial x^\rho}\right) = \det\left(\delta^\mu_\rho + \epsilon\frac{\partial \xi^\mu}{\partial x^\rho}\right), \tag{1.3.19}$$

$$= \det\begin{pmatrix} 1+\epsilon\frac{\partial\xi^1}{\partial x^1} & \epsilon\frac{\partial\xi^1}{\partial x^2} & \epsilon\frac{\partial\xi^1}{\partial x^3} & \epsilon\frac{\partial\xi^1}{\partial x^4} \\ \epsilon\frac{\partial\xi^2}{\partial x^1} & 1+\epsilon\frac{\partial\xi^2}{\partial x^2} & \epsilon\frac{\partial\xi^2}{\partial x^3} & \epsilon\frac{\partial\xi^2}{\partial x^4} \\ \epsilon\frac{\partial\xi^3}{\partial x^1} & \epsilon\frac{\partial\xi^3}{\partial x^2} & 1+\epsilon\frac{\partial\xi^3}{\partial x^3} & \epsilon\frac{\partial\xi^3}{\partial x^4} \\ \epsilon\frac{\partial\xi^4}{\partial x^1} & \epsilon\frac{\partial\xi^4}{\partial x^2} & \epsilon\frac{\partial\xi^4}{\partial x^3} & 1+\epsilon\frac{\partial\xi^4}{\partial x^4} \end{pmatrix}, \tag{1.3.20}$$

$$= \left(1 + \epsilon\sum_i \frac{\partial\xi^i}{\partial x^i} + \mathcal{O}(\epsilon^2)\right), \tag{1.3.21}$$

$$= 1 + \epsilon\partial_\mu\xi^\mu + \mathcal{O}(\epsilon^2), \tag{1.3.22}$$

where a four-dimensional spacetime was used for explicitness, but the calculation works exactly the same in any number of dimensions. Using this result and the definition of a Lie derivative, $\mathcal{L}_\xi\sqrt{-g}$ evaluates

to,

$$\mathcal{L}_\xi \sqrt{-g} = \lim_{\epsilon \to 0} \left(\frac{\Phi^* \sqrt{-\tilde{g}}\Big|_q - \sqrt{-g}\Big|_p}{\epsilon} \right), \tag{1.3.23}$$

$$= \lim_{\epsilon \to 0} \left(\frac{\sqrt{-\det\left(g_{\mu\nu}(y^\alpha) \frac{\partial y^\mu}{\partial x^\rho} \frac{\partial y^\nu}{\partial x^\sigma}\right)} - \sqrt{-g}(x^\alpha)}{\epsilon} \right), \tag{1.3.24}$$

$$= \lim_{\epsilon \to 0} \left(\frac{\sqrt{-g}(y^\alpha) \det\left(\frac{\partial y^\mu}{\partial x^\rho}\right) - \sqrt{-g}(x^\alpha)}{\epsilon} \right), \tag{1.3.25}$$

$$= \lim_{\epsilon \to 0} \left(\frac{\sqrt{-g}(y^\alpha)(1 + \epsilon \partial_\mu \xi^\mu + \mathcal{O}(\epsilon^2)) - \sqrt{-g}(x^\alpha)}{\epsilon} \right), \tag{1.3.26}$$

$$= \lim_{\epsilon \to 0} \left(\frac{[\sqrt{-g}(x^\alpha) + \epsilon \xi^\mu \partial_\mu \sqrt{-g}(x^\alpha)](1 + \epsilon \partial_\mu \xi^\mu + \mathcal{O}(\epsilon^2)) - \sqrt{-g}(x^\alpha)}{\epsilon} \right), \tag{1.3.27}$$

$$= \lim_{\epsilon \to 0} \left(\frac{\epsilon \xi^\mu \partial_\mu \sqrt{-g}(x^\alpha) + \epsilon \sqrt{-g}(x^\alpha) \partial_\mu \xi^\mu + \mathcal{O}(\epsilon^2))}{\epsilon} \right), \tag{1.3.28}$$

$$\mathcal{L}_\xi \sqrt{-g} = \xi^\mu \partial_\mu \sqrt{-g} + \sqrt{-g} \partial_\mu \xi^\mu. \tag{1.3.29}$$

Given that $\mathcal{L}_\xi \sqrt{-g}$ has been calculated, it is straightforward to calculate the Lie derivative of a tensor density $\boldsymbol{\mathcal{T}} = \sqrt{-g}^w \boldsymbol{T}$ of weight w, where $\boldsymbol{T}$ is a regular tensor, using the Leibniz rule in Eq. (1.2.44). The Lie derivative is,

$$\mathcal{L}_\xi \boldsymbol{\mathcal{T}} = \sqrt{-g}^w \left(\mathcal{L}_\xi \boldsymbol{T} + w \boldsymbol{T} \left(\frac{1}{\sqrt{-g}} \xi^\mu \partial_\mu \sqrt{-g} + \partial_\mu \xi^\mu \right) \right). \tag{1.3.30}$$

As would be expected, setting $w = 0$ returns the regular Lie derivative of a tensor. This can also be written as,

$$\mathcal{L}_\xi \boldsymbol{\mathcal{T}} = \widetilde{\mathcal{L}}_\xi \boldsymbol{\mathcal{T}} + w \boldsymbol{\mathcal{T}} \partial_\mu \xi^\mu, \tag{1.3.31}$$

where $\widetilde{\mathcal{L}}_\xi$ is the differential operator equivalent to the Lie derivative of the same tensor but with weight zero.

1.3.2 The Covariant Derivative

There are many types of derivative on a manifold that we care about in the context of General Relativity. The simplest is the partial derivative,

$$\partial_\mu = \frac{\partial}{\partial x^\mu}, \tag{1.3.32}$$

which works much the same as always. Two other derivatives are the exterior derivative[4] and the Lie derivative which is discussed in section 1.2.5.

The purpose of the covariant derivative, denoted ∇_μ, is to generalise the partial derivative to curved spaces (or curvilinear coordinates). The covariant derivative exactly reduces to the partial derivative (∂_μ) in flat space with Cartesian coordinates. As suggested by the name, the covariant derivative of an object is covariant; it obeys the tensor transformation law of section 1.3.1. The covariant derivative uses a vector field $\boldsymbol{X}$ to map a (p, q) tensor field $\boldsymbol{T}$ to a (p, q) tensor field $\boldsymbol{\nabla}_{\boldsymbol{X}} \boldsymbol{T}$. Requiring the covariant derivative of a tensor to return another tensor may sound pedantic but it allows the writing of physical

[4]The antisymmetric derivative of a differential n-form (totally antisymmetric co-tensor of rank n) that returns a differential $(n + 1)$-form.

differential equations that are covariant, i.e. that hold in all coordinate systems. Encoding the laws of physics with tensor differential equations is explored in more detail in section 1.4.3.

To be the analogue of the partial derivative, the covariant derivative must be linear in first argument, linear in second argument and obey the Leibniz rule,

$$\boldsymbol{\nabla}_{f\boldsymbol{X}+g\boldsymbol{Y}}\boldsymbol{T} = f\boldsymbol{\nabla}_{\boldsymbol{X}}\boldsymbol{T} + g\boldsymbol{\nabla}_{\boldsymbol{Y}}\boldsymbol{T}, \tag{1.3.33}$$

$$\boldsymbol{\nabla}_{\boldsymbol{X}}(a\boldsymbol{T} + b\boldsymbol{W}) = a\boldsymbol{\nabla}_{\boldsymbol{X}}\boldsymbol{T} + b\boldsymbol{\nabla}_{\boldsymbol{X}}\boldsymbol{W}, \tag{1.3.34}$$

$$\boldsymbol{\nabla}_{\boldsymbol{X}}(f\boldsymbol{T}) = f\boldsymbol{\nabla}_{\boldsymbol{X}}\boldsymbol{T} + \boldsymbol{T}\boldsymbol{\nabla}_{\boldsymbol{X}}f, \tag{1.3.35}$$

where a and b are constants, f and g are functions on $\mathcal{M}$ and $\boldsymbol{T}$ and $\boldsymbol{W}$ are tensors of equal rank. These are exactly the same as the conditions imposed on Lie derivatives in section 1.2.5. From now on the covariant derivative $\boldsymbol{\nabla}_{\boldsymbol{e}_\mu}$ with respect to a basis vector $\boldsymbol{e}_\mu$ will be written as ∇_μ.

Let us start by finding the covariant derivative of a of a scalar field φ. The partial derivative $\partial_\mu\varphi$ obeys the tensor transformation law for a co-vector,

$$\frac{\partial}{\partial\tilde{x}^\mu}\tilde{\varphi} = \frac{\partial}{\partial\tilde{x}^\mu}\varphi, \tag{1.3.36}$$

$$= \frac{\partial x^\nu}{\partial\tilde{x}^\mu}\frac{\partial}{\partial x^\nu}\varphi, \tag{1.3.37}$$

and therefore the $\nabla_\mu\varphi = \partial_\mu\varphi$. Note that $\varphi = \tilde{\varphi}$ for any point p as a scalar remains unchanged in a coordinate transformation. Complications arise when taking the partial derivative of any other higher rank tensor; let's demonstrate this with a vector $\boldsymbol{X}$.

$$\frac{\partial}{\partial\tilde{x}^\mu}\tilde{X}^\alpha = \frac{\partial}{\partial\tilde{x}^\mu}\left(\frac{\partial\tilde{x}^\alpha}{\partial x^\beta}X^\beta\right), \tag{1.3.38}$$

$$= \frac{\partial x^\nu}{\partial\tilde{x}^\mu}\frac{\partial}{\partial x^\nu}\left(\frac{\partial\tilde{x}^\alpha}{\partial x^\beta}X^\beta\right), \tag{1.3.39}$$

$$= \underbrace{\frac{\partial\tilde{x}^\alpha}{\partial x^\beta}\frac{\partial x^\nu}{\partial\tilde{x}^\mu}}_{\text{Tensor transformation law}}\frac{\partial}{\partial x^\nu}X^\beta + X^\beta\frac{\partial x^\nu}{\partial\tilde{x}^\mu}\frac{\partial}{\partial x^\nu}\left(\frac{\partial\tilde{x}^\alpha}{\partial x^\beta}\right), \tag{1.3.40}$$

and as can be seen, only the first term on the right hand side should exist if the components $\partial_\mu X^\alpha$ were to obey the tensor transformation law.

The problem with performing differentiation on tensors is that it requires the comparison of tensors at two different (infinitesimally close) tangent spaces. Lie derivatives circumvented this problem by comparing two tangent planes with a pullback defined by a diffeomorphism. Another way of overcoming this problem is to consider how the coordinate basis vectors change over the manifold, not just the components. Defining the covariant derivative of the basis vector as

$$\boldsymbol{\nabla}_{\boldsymbol{e}_\rho}\boldsymbol{e}_\nu = \nabla_\rho\boldsymbol{e}_\nu := \Gamma^\mu{}_{\nu\rho}\boldsymbol{e}_\mu, \tag{1.3.41}$$

where $\Gamma^\mu{}_{\nu\rho}$ is called the connection due to it defining a connection between neighbouring tangent spaces. The connection can be used to get the covariant derivative of the vector field $\boldsymbol{X} = X^\rho\boldsymbol{e}_\rho$,

$$\nabla_\rho(X^\nu\boldsymbol{e}_\nu) = (\partial_\rho X^\nu)\boldsymbol{e}_\nu + X^\nu(\nabla_\rho\boldsymbol{e}_\nu), \tag{1.3.42}$$

$$= (\partial_\rho X^\nu)\boldsymbol{e}_\nu + X^\nu\Gamma^\mu{}_{\nu\rho}\boldsymbol{e}_\mu, \tag{1.3.43}$$

$$= (\partial_\rho X^\mu + \Gamma^\mu{}_{\nu\rho}X^\nu)\boldsymbol{e}_\mu. \tag{1.3.44}$$

Note that on the first line above we have used $\nabla_\rho X^\nu = \partial_\rho X^\nu$ as the X^ν are being treated as a set of scalar function coefficients multiplying the basis vectors $\boldsymbol{e}_\mu$. Strictly we should write the covariant derivative of $\boldsymbol{X}$ as,

$$\boldsymbol{\nabla}\boldsymbol{X} = (\nabla X)_\sigma{}^\mu\boldsymbol{e}_\mu\otimes\boldsymbol{\theta}^\sigma, \tag{1.3.45}$$

but for convenience the coefficients $(\nabla X)_\sigma{}^\mu$ are usually denoted as,

$$\nabla_\sigma X^\mu = \partial_\sigma X^\mu + \Gamma^\mu{}_{\nu\sigma} X^\nu. \tag{1.3.46}$$

This is a slight abuse of notation as $\nabla_\sigma X^\mu$ might be understood as the covariant derivative of the components X^μ, but really it denotes the component $\boldsymbol{\theta}^\sigma \cdot (\boldsymbol{\nabla X}) \cdot \boldsymbol{e}_\mu$ where $\boldsymbol{\nabla X}$ is given in Eq. (1.3.45).

Given that the covariant derivative of a scalar reduces to the partial derivative we can see that,

$$\nabla_\rho (\boldsymbol{e}_\mu : \boldsymbol{\theta}^\nu) = 0, \tag{1.3.47}$$

and using the Leibniz rule (1.3.35),

$$\begin{aligned}
\nabla_\rho (\boldsymbol{e}_\nu : \boldsymbol{\theta}^\mu) &= (\nabla_\rho \boldsymbol{e}_\nu) : \boldsymbol{\theta}^\mu + \boldsymbol{e}_\nu : (\nabla_\rho \boldsymbol{\theta}^\mu), && (1.3.48)\\
&= (\Gamma^\sigma{}_{\nu\rho} \boldsymbol{e}_\sigma) : \boldsymbol{\theta}^\mu + \boldsymbol{e}_\nu : (\nabla_\rho \boldsymbol{\theta}^\mu), && (1.3.49)\\
&= \Gamma^\mu{}_{\nu\rho} + \boldsymbol{e}_\nu : (\nabla_\rho \boldsymbol{\theta}^\mu). && (1.3.50)
\end{aligned}$$

Combining Eqs. (1.3.47) and (1.3.50) gives

$$\boldsymbol{e}_\nu : (\nabla_\rho \boldsymbol{\theta}^\mu) = -\Gamma^\mu{}_{\nu\rho}, \tag{1.3.51}$$

and therefore we must have

$$\nabla_\rho \boldsymbol{\theta}^\mu = -\Gamma^\mu{}_{\nu\rho} \boldsymbol{\theta}^\nu. \tag{1.3.52}$$

In an identical way, we might ask what is the covariant derivative of a co-vector $\boldsymbol{\omega} = \omega_\alpha \boldsymbol{\theta}^\alpha$. The covariant derivative $\boldsymbol{\nabla \omega}$ can be found from,

$$\begin{aligned}
\nabla_\sigma \boldsymbol{\omega} &= \nabla_\sigma (\omega_\alpha \boldsymbol{\theta}^\alpha), && (1.3.53)\\
&= \partial_\sigma (\omega_\alpha) \boldsymbol{\theta}^\alpha + \omega_\alpha \nabla_\sigma \boldsymbol{\theta}^\alpha, && (1.3.54)\\
&= \partial_\sigma (\omega_\alpha) \boldsymbol{\theta}^\alpha - \omega_\alpha \Gamma^\alpha{}_{\nu\sigma} \boldsymbol{\theta}^\nu, && (1.3.55)\\
&= (\partial_\sigma \omega_\alpha - \omega_\nu \Gamma^\nu{}_{\alpha\sigma}) \boldsymbol{\theta}^\alpha. && (1.3.56)
\end{aligned}$$

Again, we used have $\nabla_\sigma \omega_\alpha = \partial_\sigma \omega_\alpha$ as the components ω_α are scalar coefficients of the basis co-vectors $\boldsymbol{\theta}^\alpha$. From now on the components $(\nabla\omega)_{\sigma\alpha}$ are written as $\nabla_\sigma \omega_\alpha$ even though this is a mild abuse of notation.

The covariant derivative of a general tensor can be found by following the simple rule of adding a connection symbol term for each index, for example,

$$\nabla_\mu T^{\alpha\beta\ldots}{}_{\lambda\nu\ldots} = \partial_\mu T^{\alpha\beta\ldots}{}_{\lambda\nu\ldots} + \Gamma^\alpha{}_{\sigma\mu} T^{\sigma\beta\ldots}{}_{\lambda\nu\ldots} + \Gamma^\beta{}_{\sigma\mu} T^{\alpha\sigma\ldots}{}_{\lambda\nu\ldots} + \ldots - \Gamma^\sigma{}_{\lambda\mu} T^{\alpha\beta\ldots}{}_{\sigma\nu\ldots} - \Gamma^\sigma{}_{\nu\mu} T^{\alpha\beta\ldots}{}_{\lambda\sigma\ldots} - \ldots . \tag{1.3.57}$$

1.3.3 The Connection

In flat space we are used to the idea that the partial derivative commutes, i.e. $\partial_\mu \partial_\nu = \partial_\nu \partial_\mu$, and this remains true by definition in curved space. However, the covariant derivative does not generally commute, $\nabla_\mu \nabla_\nu \neq \nabla_\nu \nabla_\mu$. Applying $\nabla_\mu \nabla_\nu - \nabla_\nu \nabla_\mu$ to a scalar field φ gives,

$$\begin{aligned}
(\nabla_\mu \nabla_\nu - \nabla_\nu \nabla_\mu)\varphi &= \nabla_\mu \nabla_\nu \varphi - \nabla_\nu \nabla_\mu \varphi, && (1.3.58)\\
&= \nabla_\mu \partial_\nu \varphi - \nabla_\nu \partial_\mu \varphi, && (1.3.59)\\
&= (\partial_\mu \partial_\nu - \partial_\nu \partial_\mu)\varphi - \Gamma^\sigma{}_{\nu\mu} \partial_\sigma \varphi + \Gamma^\sigma{}_{\mu\nu} \partial_\sigma \varphi, && (1.3.60)\\
&= (\Gamma^\sigma{}_{\mu\nu} - \Gamma^\sigma{}_{\nu\mu}) \partial_\sigma \varphi, && (1.3.61)
\end{aligned}$$

where we have used the fact that $\nabla_\mu \varphi = \partial_\mu \varphi$ for a scalar field. This non-commutativity of derivatives of a scalar field is known as torsion.

Torsion

If a connection is torsion free then $(\nabla_\mu\nabla_\nu - \nabla_\nu\nabla_\mu)\varphi = 0$ which implies $\Gamma^\sigma{}_{\nu\mu} = \Gamma^\sigma{}_{\mu\nu}$. This leads to two important tensor identities; first the antisymmetric derivative of a co-vector,

$$\nabla_\mu A_\nu - \nabla_\nu A_\mu = \partial_\mu A_\nu - \partial_\nu A_\nu - \underbrace{(\Gamma^\sigma{}_{\nu\mu} - \Gamma^\sigma{}_{\mu\nu})}_{=0} A_\sigma, \tag{1.3.62}$$

$$\nabla_\mu A_\nu - \nabla_\nu A_\mu = \partial_\mu A_\nu - \partial_\nu A_\mu, \tag{1.3.63}$$

and the second identity,

$$\begin{aligned}
\boldsymbol{\nabla_X Y - \nabla_Y X} &= (X^\mu \nabla_\mu Y^\nu - Y^\mu \nabla_\mu X^\nu)\boldsymbol{e}_\nu, && (1.3.64)\\
&= (X^\mu \partial_\mu Y^\nu - Y^\mu \partial_\mu X^\nu + \Gamma^\nu{}_{\sigma\mu} X^\mu Y^\sigma - \Gamma^\nu{}_{\sigma\mu} Y^\mu X^\sigma)\boldsymbol{e}_\nu, && (1.3.65)\\
&= (X^\mu \partial_\mu Y^\nu - Y^\mu \partial_\mu X^\nu + (\Gamma^\nu{}_{\sigma\mu} - \Gamma^\nu{}_{\mu\sigma}) X^\mu Y^\sigma)\boldsymbol{e}_\nu, && (1.3.66)\\
&= (X^\mu \partial_\mu Y^\nu - Y^\mu \partial_\mu X^\nu)\boldsymbol{e}_\nu, && (1.3.67)\\
\boldsymbol{\nabla_X Y - \nabla_Y X} &= [\boldsymbol{X}, \boldsymbol{Y}]. && (1.3.68)
\end{aligned}$$

Here the *commutator bracket* $[\boldsymbol{X}, \boldsymbol{Y}]$ of two vectors $\boldsymbol{X}$ and $\boldsymbol{Y}$ is defined by,

$$\begin{aligned}
[X^\mu \partial_\mu, Y^\nu \partial_\nu] &= X^\mu \partial_\mu (Y^\nu \partial_\nu) - Y^\nu \partial_\nu (X^\mu \partial_\mu), && (1.3.69)\\
&= X^\mu \partial_\mu Y^\nu - Y^\nu \partial_\nu (X^\mu)\partial_\mu + X^\mu Y^\nu \partial_\mu \partial_\nu - Y^\nu X^\mu \partial_\nu \partial_\mu, && (1.3.70)\\
&= (X^\mu \partial_\mu Y^\nu - Y^\mu \partial_\mu X^\nu)\partial_\nu, && (1.3.71)
\end{aligned}$$

where the basis vector $\boldsymbol{e}_\mu$ has been written as ∂_μ with the intention of acting on a function f over the manifold $\mathcal{M}$.

Metric Compatibility

Another property that can be imposed on the connection is metric compatibility; this is $\nabla_\mu g_{\rho\sigma} = 0$, where $\boldsymbol{g}$ is the metric tensor. This immediately tells us $\nabla_\mu g^{\alpha\beta} = 0$ since,

$$\begin{aligned}
\nabla_\mu \delta^\alpha_\rho &= 0, && (1.3.72)\\
&= \nabla_\mu (g^{\alpha\nu} g_{\nu\rho}), && (1.3.73)\\
&= g_{\nu\rho}\nabla_\mu g^{\alpha\nu} + g^{\alpha\nu} \underbrace{\nabla_\mu g_{\nu\rho}}_{=0}, && (1.3.74)
\end{aligned}$$

which implies that $\nabla_\mu g^{\alpha\nu} = 0$. Metric compatibility implies that the raising and lowering of indices with the metric commutes with the covariant derivative,

$$\nabla_\mu T^{\alpha\beta\ldots} = \nabla_\mu g^{\alpha\rho} T_\rho{}^{\beta\ldots} = g^{\alpha\rho}\nabla_\mu T_\rho{}^{\beta\ldots}, \tag{1.3.75}$$

and the derivative of the length of a vector $\boldsymbol{X}$ is given by,

$$\nabla_\alpha |\boldsymbol{X}|^2 = \nabla_\alpha (X^\mu X_\mu) = \nabla_\alpha (g_{\mu\nu} X^\mu X^\nu) = 2X^\mu \nabla_\alpha X_\mu = 2X_\mu \nabla_\alpha X^\mu. \tag{1.3.76}$$

The Levi-Civita Connection

As it turns out, a connection that obeys Eqs. (1.3.33,1.3.34 & 1.3.35), is both torsion-free and metric-compatible, is uniquely determined. This connection is called the Levi-Civita connection. The Levi-Civita connection will always be assumed from now on and is given by,

$$\Gamma^\rho{}_{\mu\nu} = \frac{1}{2} g^{\rho\sigma}(\partial_\mu g_{\sigma\nu} + \partial_\nu g_{\mu\sigma} - \partial_\sigma g_{\nu\mu}), \tag{1.3.77}$$

which is also called Christoffel symbol of the second kind. The connection coefficient with lowered indices

$$\Gamma_{\sigma\mu\nu} = \frac{1}{2}(\partial_\mu g_{\sigma\nu} + \partial_\nu g_{\mu\sigma} - \partial_\sigma g_{\nu\mu}), \tag{1.3.78}$$

is called the Christoffel symbol of the first kind. It is very important to note that even though the connection symbols may look like a tensor they are not a tensor. This can demonstrated by applying the tensor transformation law to the Christoffel symbol of the first kind,

$$2\tilde{\Gamma}_{\sigma\mu\nu} = \tilde{\partial}_\mu \tilde{g}_{\sigma\nu} + \tilde{\partial}_\nu \tilde{g}_{\mu\sigma} - \tilde{\partial}_\sigma \tilde{g}_{\nu\mu}, \tag{1.3.79}$$

$$= \frac{\partial x^\alpha}{\partial \tilde{x}^\mu}\partial_\alpha\left(\frac{\partial x^\beta}{\partial \tilde{x}^\sigma}\frac{\partial x^\gamma}{\partial \tilde{x}^\nu}g_{\beta\gamma}\right) + \frac{\partial x^\gamma}{\partial \tilde{x}^\nu}\partial_\gamma\left(\frac{\partial x^\beta}{\partial \tilde{x}^\sigma}\frac{\partial x^\alpha}{\partial \tilde{x}^\mu}g_{\alpha\beta}\right) - \frac{\partial x^\beta}{\partial \tilde{x}^\sigma}\partial_\beta\left(\frac{\partial x^\alpha}{\partial \tilde{x}^\mu}\frac{\partial x^\gamma}{\partial \tilde{x}^\nu}g_{\gamma\alpha}\right), \tag{1.3.80}$$

$$\begin{aligned} = {} & \frac{\partial x^\alpha}{\partial \tilde{x}^\mu}\frac{\partial x^\beta}{\partial \tilde{x}^\sigma}\frac{\partial x^\gamma}{\partial \tilde{x}^\nu}(\partial_\alpha g_{\beta\gamma} + \partial_\gamma g_{\alpha\beta} - \partial_\beta g_{\gamma\alpha}) \\ & + \frac{\partial x^\alpha}{\partial \tilde{x}^\mu}g_{\beta\gamma}\partial_\alpha\left(\frac{\partial x^\beta}{\partial \tilde{x}^\sigma}\frac{\partial x^\gamma}{\partial \tilde{x}^\nu}\right) + \frac{\partial x^\gamma}{\partial \tilde{x}^\nu}g_{\alpha\beta}\partial_\gamma\left(\frac{\partial x^\beta}{\partial \tilde{x}^\sigma}\frac{\partial x^\alpha}{\partial \tilde{x}^\mu}\right) - \frac{\partial x^\beta}{\partial \tilde{x}^\sigma}g_{\gamma\alpha}\partial_\beta\left(\frac{\partial x^\alpha}{\partial \tilde{x}^\mu}\frac{\partial x^\gamma}{\partial \tilde{x}^\nu}\right), \end{aligned} \tag{1.3.81}$$

$$\begin{aligned} = {} & 2\frac{\partial x^\alpha}{\partial \tilde{x}^\mu}\frac{\partial x^\beta}{\partial \tilde{x}^\sigma}\frac{\partial x^\gamma}{\partial \tilde{x}^\nu}\Gamma_{\beta\alpha\gamma} \\ & + \frac{\partial x^\alpha}{\partial \tilde{x}^\mu}g_{\beta\gamma}\partial_\alpha\left(\frac{\partial x^\beta}{\partial \tilde{x}^\sigma}\frac{\partial x^\gamma}{\partial \tilde{x}^\nu}\right) + \frac{\partial x^\gamma}{\partial \tilde{x}^\nu}g_{\alpha\beta}\partial_\gamma\left(\frac{\partial x^\beta}{\partial \tilde{x}^\sigma}\frac{\partial x^\alpha}{\partial \tilde{x}^\mu}\right) - \frac{\partial x^\beta}{\partial \tilde{x}^\sigma}g_{\gamma\alpha}\partial_\beta\left(\frac{\partial x^\alpha}{\partial \tilde{x}^\mu}\frac{\partial x^\gamma}{\partial \tilde{x}^\nu}\right), \end{aligned} \tag{1.3.82}$$

$$= 2\frac{\partial x^\alpha}{\partial \tilde{x}^\mu}\frac{\partial x^\beta}{\partial \tilde{x}^\sigma}\frac{\partial x^\gamma}{\partial \tilde{x}^\nu}\Gamma_{\beta\alpha\gamma} + \Xi_{\sigma\mu\nu}. \tag{1.3.83}$$

$$\tag{1.3.84}$$

If $\Xi_{\sigma\mu\nu} = 0$ then the $\Gamma_{\sigma\mu\nu}$ would transform as an $(0,3)$ tensor, however this is not the case in general and the Christoffel symbol of the first kind is not a tensor but instead a *symbol*[5]. The non-tensorial nature of the Christoffel symbol of first kind is sufficient to prove that the Christoffel symbol of second kind is also not a tensor.

Lie Derivatives in the Levi Civita Connection

The covariant derivative ∇, described in section 1.3.2 can replace all partial derivatives in a Lie derivative due to the connection symbols $\left(\Gamma^\mu{}_{\rho\sigma}\right)$ cancelling out.

A special example of a Lie derivative is of the metric tensor, $\boldsymbol{g}$, giving

$$(\mathcal{L}_\xi g)_{\mu\nu} = \xi^\rho\partial_\rho g_{\mu\nu} + g_{\rho\nu}\partial_\mu\xi^\rho + g_{\mu\rho}\partial_\nu\xi^\rho, \tag{1.3.85}$$

$$= \xi^\rho\nabla_\rho g_{\mu\nu} + g_{\rho\nu}\nabla_\mu\xi^\rho + g_{\mu\rho}\nabla_\nu\xi^\rho, \tag{1.3.86}$$

where $\nabla_\rho g_{\mu\nu} = 0$ from metric compatibility, described in section 1.3.3. In the case the Lie derivative vanishes we get Killing's equation

$$\nabla_\mu\xi_\nu + \nabla_\nu\xi_\mu = 0, \tag{1.3.87}$$

and a vector field $\boldsymbol{\xi}$ satisfying Killing's equation is called a Killing vector. Killings equation will be very important in section **??**.

Normal Coordinates

Consider the set of all affinely parameterised geodesics, parameterised with λ, passing through the point p on a manifold $\mathcal{M}$. At p, each geodesic has a tangent vector $X^\mu\big|_p$. For all geodesics, define p to be

[5]Here we use the word symbol to denote an object that looks like the components of a tensor but does not obey the tensor transformation law.

the origin with $\lambda = 0$ and $x^\mu = 0$. Following a geodesic associated with $X^\mu\big|_p$ to a parameter value of λ will map to a new point q close to p for small enough λ. Normal coordinates $x^\mu(\lambda)$ at $q(\lambda)$ are defined such that $x^\mu(\lambda) = \lambda X^\mu\big|_p$. Given that $X^\mu\big|_p$ is constant, the geodesic equation, from Eq. (1.2.77), becomes

$$\frac{\mathrm{d}^2 x^\mu(\lambda)}{\mathrm{d}\lambda^2} + \Gamma^\alpha{}_{\mu\nu}\frac{\mathrm{d}x^\mu(\lambda)}{\mathrm{d}\lambda}\frac{\mathrm{d}x^\nu(\lambda)}{\mathrm{d}\lambda} = \Gamma^\alpha{}_{\mu\nu}X^\mu\big|_p X^\nu\big|_p = 0. \tag{1.3.88}$$

Using the Levi-Civita connection, the connection symbol is symmetric in the lower two indices and this implies $\Gamma^\alpha{}_{\mu\nu} = 0$ as the geodesic equation must hold for generic $X^\mu\big|_p$. From the definition of the covariant derivative,

$$\partial_\alpha g_{\mu\nu} = \nabla_\alpha g_{\mu\nu} + \Gamma^\beta{}_{\alpha\nu}g_{\mu\beta} + \Gamma^\beta{}_{\alpha\mu}g_{\beta\nu}, \tag{1.3.89}$$

which must vanish in normal coordinates as $\Gamma^\alpha{}_{\mu\nu} = 0$ and the Levi-Civita connection demands $\nabla_\alpha g_{\mu\nu} = 0$. Therefore, it is possible to construct a coordinate system such that at one point p both $\partial_\alpha g_{\mu\nu} = 0$ and $\Gamma^\alpha{}_{\mu\nu} = 0$; importantly $\partial_\alpha\partial_\beta g_{\mu\nu} \neq 0$. As well as the metric's first derivative vanishing at p, it is also possible to demand that $g_{\mu\nu}\big|_p = \eta_{\mu\nu}$, the Minkowski metric defined in section 1.4.1. This can be done with a set of ${}^{(j)}X^\mu\big|_p$, one for each normal coordinate x^j, that satisfy

$$\boldsymbol{g}({}^{(j)}\boldsymbol{X}\big|_p, {}^{(k)}\boldsymbol{X}\big|_p) = \eta_{jk}. \tag{1.3.90}$$

1.3.4 Curvature Tensors

We have already seen that with the Levi-Civita connection, the antisymmetrised second derivative of a scalar field vanishes; but operating on a vector field $\boldsymbol{X}$ gives,

$$(\nabla_\mu\nabla_\nu - \nabla_\nu\nabla_\mu)X^\sigma = (\partial_\mu\nabla_\nu - \partial_\nu\nabla_\mu)X^\sigma + (\Gamma^\sigma{}_{\mu\rho}\nabla_\nu - \Gamma^\sigma{}_{\nu\rho}\nabla_\mu)X^\rho - \underbrace{(\Gamma^\rho{}_{\nu\mu} - \Gamma^\rho{}_{\mu\nu})}_{=0}\nabla_\rho X^\sigma, \tag{1.3.91}$$

$$= \underbrace{(\partial_\mu\partial_\nu - \partial_\nu\partial_\mu)}_{=0}X^\sigma + (\partial_\mu\Gamma^\sigma{}_{\nu\rho} - \partial_\nu\Gamma^\sigma{}_{\mu\rho})X^\rho + (\Gamma^\sigma{}_{\mu\rho}\nabla_\nu - \Gamma^\sigma{}_{\nu\rho}\nabla_\mu)X^\rho, \tag{1.3.92}$$

$$= (\partial_\mu\Gamma^\sigma{}_{\nu\rho} - \partial_\nu\Gamma^\sigma{}_{\mu\rho})X^\rho + (\Gamma^\sigma{}_{\mu\rho}\partial_\nu - \Gamma^\sigma{}_{\nu\rho}\partial_\mu)X^\rho + (\Gamma^\sigma{}_{\mu\rho}\Gamma^\rho{}_{\nu\lambda} - \Gamma^\sigma{}_{\nu\rho}\Gamma^\rho{}_{\mu\lambda})X^\lambda, \tag{1.3.93}$$

$$= X^\rho(\partial_\mu\Gamma^\sigma{}_{\nu\rho} - \partial_\nu\Gamma^\sigma{}_{\mu\rho}) + (\Gamma^\sigma{}_{\mu\rho}\Gamma^\rho{}_{\nu\lambda} - \Gamma^\sigma{}_{\nu\rho}\Gamma^\rho{}_{\mu\lambda})X^\lambda, \tag{1.3.94}$$

where one should note that whenever a term appears after a derivative here it is to be differentiated, even if it is outside a bracket. We introduce the Riemann tensor $R^\sigma{}_{\rho\mu\nu}$ by,

$$(\nabla_\mu\nabla_\nu - \nabla_\nu\nabla_\mu)X^\sigma = R^\sigma{}_{\rho\mu\nu}X^\rho, \tag{1.3.95}$$

and setting $\boldsymbol{X} = \boldsymbol{e}_\rho$, the coordinate basis vector associated with the x^ρ coordinate, the Riemann tensor can be written as

$$R^\sigma{}_{\rho\mu\nu} = \partial_\mu\Gamma^\sigma{}_{\nu\rho} - \partial_\nu\Gamma^\sigma{}_{\mu\rho} + \Gamma^\sigma{}_{\mu\lambda}\Gamma^\lambda{}_{\nu\rho} - \Gamma^\sigma{}_{\nu\lambda}\Gamma^\lambda{}_{\mu\rho}. \tag{1.3.96}$$

Symmetries of the Riemann Tensor

Now we will discuss the symmetries of the Riemann tensor. Firstly, from the definition of the Riemann tensor, it follows that $R^\sigma{}_{\rho\mu\nu} = -R^\sigma{}_{\rho\nu\mu}$; this can be written succinctly as $R^\sigma{}_{\rho[\mu\nu]} = 0$.

The second symmetry of the Riemann tensor is most conveniently derived using normal coordinates (described in section 1.3.3). At a point p where $\Gamma^\mu{}_{\nu\rho} = 0$ (but $\partial_\alpha\Gamma^\mu{}_{\nu\rho} \neq 0$) to get

$$R^\sigma{}_{\rho\mu\nu}\big|_p = \partial_\mu\Gamma^\sigma{}_{\nu\rho} - \partial_\nu\Gamma^\sigma{}_{\mu\rho}, \tag{1.3.97}$$

it is straightforward to show that $R^\sigma_{[\rho\mu\nu]} = 0$ as

$$R^\sigma{}_{[\rho\mu\nu]}\big|_p = \partial_{[\mu}\Gamma^\sigma{}_{\nu\rho]} - \partial_{[\nu}\Gamma^\sigma{}_{\mu\rho]} = 0, \tag{1.3.98}$$

due to the antisymmetrisation of any connection symbol like $\Gamma^{\sigma}{}_{[\nu\rho]} = 0$. Given that the tensor equation $R^{\sigma}{}_{[\rho\mu\nu]} = 0$ is true at p in normal coordinates then it is true in any coordinate system; on top of this the point p was arbitrary so therefore $R^{\sigma}{}_{[\rho\mu\nu]} = 0$ holds globally.

The next symmetry of the Riemann tensor is $R_{\sigma\rho\mu\nu} = R_{\mu\nu\sigma\rho}$. We can prove this again using normal coordinates at a point p; here derivatives of the metric and its inverse vanish, but second derivatives do not. The proof of the symmetry follows Eq. (1.3.97) for the Riemann tensor in normal coordinates at a point p,

$$R_{\sigma\rho\mu\nu}\big|_p = g_{\lambda\sigma}\partial_\mu\Gamma^{\lambda}{}_{\nu\rho} - g_{\lambda\sigma}\partial_\nu\Gamma^{\lambda}{}_{\mu\rho}, \tag{1.3.99}$$

$$= \partial_\mu g_{\lambda\sigma}\Gamma^{\lambda}{}_{\nu\rho} - \partial_\nu g_{\lambda\sigma}\Gamma^{\lambda}{}_{\mu\rho}, \tag{1.3.100}$$

$$= \partial_\mu\Gamma_{\sigma\nu\rho} - \partial_\nu\Gamma_{\sigma\mu\rho}, \tag{1.3.101}$$

$$= \frac{1}{2}\left(\partial_\mu\partial_\rho g_{\sigma\nu} - \partial_\mu\partial_\sigma g_{\rho\nu} + \partial_\nu\partial_\sigma g_{\rho\mu} - \partial_\nu\partial_\rho g_{\sigma\mu}\right), \tag{1.3.102}$$

and it is a straightforward to show that this final expression doesn't change under swapping indices $\sigma \leftrightarrow \mu$ and $\rho \leftrightarrow \nu$.

The final symmetry of the Riemann tensor is the Bianchi identity, $\nabla_{[\lambda}R_{\sigma\rho]\mu\nu}$=0. Using normal coordinates at a point p, we can write

$$\nabla_\lambda R_{\sigma\rho\mu\nu}\big|_p = \partial_\lambda R_{\sigma\rho\mu\nu}\big|_p, \tag{1.3.103}$$

as all the Christoffel symbols generated by the covariant derivative cancel and therefore

$$2\nabla_\lambda R_{\sigma\rho\mu\nu}\big|_p = \partial_\lambda\partial_\mu\partial_\rho g_{\sigma\nu} - \partial_\lambda\partial_\mu\partial_\sigma g_{\rho\nu} + \partial_\lambda\partial_\nu\partial_\sigma g_{\rho\mu} - \partial_\lambda\partial_\nu\partial_\rho g_{\sigma\mu}. \tag{1.3.104}$$

Antisymmetrising over λ, ρ and σ makes each term vanish as the triple partial derivatives always contain two of the antisymmetrised indices and must vanish.

To summarise, we have the following symmetries of the Riemann tensor;

$$R_{\sigma\rho[\mu\nu]} = 0, \tag{1.3.105}$$

$$R_{\sigma\rho\mu\nu} = R_{\mu\nu\sigma\rho}, \tag{1.3.106}$$

$$\nabla_{[\lambda}R_{\sigma\rho]\mu\nu} = 0. \tag{1.3.107}$$

The first two of these can be used together to give another useful relation $R_{[\sigma\rho]\mu\nu} = 0$.

Contractions of the Riemann Tensor

Now that we have explored the Riemann tensor, it is time to introduce the Ricci tensor and Ricci scalar. The Ricci tensor $R_{\mu\nu}$ is simply defined by the unique, non-zero self contraction (or trace) of the Riemann tensor,

$$R_{\rho\mu} := R^{\mu}{}_{\rho\mu\nu} = R_{\sigma\rho\mu\nu}g^{\sigma\mu}. \tag{1.3.108}$$

Contracting the the Riemann tensor with $g^{\mu\nu}$ or $g^{\sigma\rho}$ would give zero due to the antisymmetries of those indices in the tensor. Any other contractions, such as with $g^{\rho\mu}$ can be shown to be exactly the same (up to a minus sign) as contracting with $g^{\sigma\mu}$ using the symmetries of the Riemann tensor. The symmetries of the Riemann tensor guarantee that the Ricci tensor itself is symmetric. We can contract the Ricci tensor with itself (the same as taking the trace with the metric) to give us the Ricci scalar R,

$$R = g^{\rho\nu}R_{\rho\nu}. \tag{1.3.109}$$

We can also take the trace of the Bianchi identity in Eq. (1.3.107) which gives us

$$g^{\lambda\mu}g^{\rho\nu}(\nabla_\lambda R_{\sigma\rho\mu\nu} + \nabla_\rho R_{\lambda\sigma\mu\nu} + \nabla_\sigma R_{\rho\lambda\mu\nu}) = 0, \tag{1.3.110}$$

$$\nabla^\mu R_{\sigma\mu} + \nabla^\nu R_{\sigma\nu} - \nabla_\sigma R = 0, \tag{1.3.111}$$

$$\nabla^\mu R_{\mu\sigma} - \frac{1}{2}\nabla_\sigma R = 0. \tag{1.3.112}$$

Defining the Einstein tensor $\boldsymbol{G}$,

$$G_{\mu\nu} := R_{\mu\nu} - \frac{1}{2}g_{\mu\nu}R, \tag{1.3.113}$$

and using the contracted Bianchi identity with $\boldsymbol{\nabla g} = 0$ from metric compatibility,

$$\nabla^\mu G_{\mu\nu} = \nabla^\mu R_{\mu\nu} - \frac{1}{2}\left(g_{\mu\nu}\nabla^\mu R + R\nabla^\mu g_{\mu\nu}\right), \tag{1.3.114}$$

$$= \nabla^\mu R_{\mu\nu} - \frac{1}{2}\nabla_\nu R, \tag{1.3.115}$$

$$= 0. \tag{1.3.116}$$

The Einstein tensor $G_{\mu\nu}$ therefore has a vanishing divergence $\nabla_\mu G^{\mu\nu} = 0$.

One more useful contraction of the Riemann tensor is with a second Riemann tensor which gives the Kretschmann scalar k,

$$k := R_{\mu\nu\rho\sigma}R^{\mu\nu\rho\sigma}. \tag{1.3.117}$$

Both k and R are scalar fields so they provide us with a coordinate invariant curvature measure; section 1.4.5 will have use of the Kretschmann scalar in categorising spacetime singularities.

1.3.5 The Divergence Theorem

There is a generalisation of the divergence theorem to curved spaces, using differential geometry, which will be important in sections [FIX THIS]**??**. However, before we discuss the divergence theorem, we must derive a preliminary matrix identity for a real symmetric matrix $\boldsymbol{M}$ with determinant M,

$$M^{-1}\partial_\mu M = M^{-1}_{ij}\partial_\mu M_{ij} = \mathrm{Tr}(\boldsymbol{M}^{-1}\partial_\mu \boldsymbol{M}). \tag{1.3.118}$$

Simplifying the left hand side in terms of the eigenvalues λ_i of $\boldsymbol{M}$. Given that $M = \det\{\boldsymbol{M}\} = \prod_i \lambda_i$ we know

$$M^{-1}\partial_\mu M = \partial_\mu \ln(|M|), \tag{1.3.119}$$

$$= \partial_\mu \ln\left(\left|\prod_i \lambda_i\right|\right), \tag{1.3.120}$$

$$= \partial_\mu \sum_i \ln(|\lambda_i|), \tag{1.3.121}$$

$$= \sum_i \lambda_k^{-1}\partial_\mu \lambda_k. \tag{1.3.122}$$

Now we will show that the right hand side of Eq. (1.3.118) equals this. To do so we start by decomposing $\boldsymbol{M}$ into a diagonal matrix $\boldsymbol{D}$ like

$$\boldsymbol{M} = \boldsymbol{O}^{-1}\boldsymbol{D}\boldsymbol{O}, \tag{1.3.123}$$

$$\boldsymbol{M}^{-1} = \boldsymbol{O}^{-1}\boldsymbol{D}^{-1}\boldsymbol{O}, \tag{1.3.124}$$

then using the fact that $\mathrm{Tr}(\boldsymbol{AB}....\boldsymbol{CD}) = \mathrm{Tr}(\boldsymbol{DAB}....\boldsymbol{C})$ for matrices $\boldsymbol{A}$, $\boldsymbol{B}$, $\boldsymbol{C}$, ... and $\boldsymbol{D}$,

$$\begin{aligned}
\mathrm{Tr}(\boldsymbol{M}^{-1}\partial_\mu \boldsymbol{M}) &= \mathrm{Tr}(\boldsymbol{O}^{-1}\boldsymbol{D}^{-1}\boldsymbol{O}\partial_\mu(\boldsymbol{O}^{-1}\boldsymbol{D}\boldsymbol{O})), && (1.3.125)\\
&= \mathrm{Tr}(\boldsymbol{D}^{-1}\partial_\mu \boldsymbol{D}) + \mathrm{Tr}(\boldsymbol{O}^{-1}\partial_\mu \boldsymbol{O}) + \mathrm{Tr}(\boldsymbol{O}\partial_\mu \boldsymbol{O}^{-1}), && (1.3.126)\\
&= \mathrm{Tr}(\boldsymbol{D}^{-1}\partial_\mu \boldsymbol{D}) + \mathrm{Tr}(\underbrace{\partial_\mu(\boldsymbol{O}^{-1}\boldsymbol{O})}_{=0}), && (1.3.127)\\
&= \mathrm{Tr}(\boldsymbol{D}^{-1}\partial_\mu \boldsymbol{D}). && (1.3.128)
\end{aligned}$$

Given that $\boldsymbol{D}$ is the diagonal matrix composed of the eigenvalues λ_i then it follows that,

$$\begin{aligned}
\boldsymbol{D} &= \mathrm{Diag}\{\lambda_1, \lambda_2, ..., \lambda_n\}, && (1.3.129)\\
\partial_\mu \boldsymbol{D} &= \mathrm{Diag}\{\partial_\mu\lambda_1, \partial_\mu\lambda_2, ..., \partial_\mu\lambda_n\}, && (1.3.130)\\
\boldsymbol{D}^{-1} &= \mathrm{Diag}\{\lambda_1^{-1}, \lambda_2^{-1}, ..., \lambda_n^{-1}\}. && (1.3.131)
\end{aligned}$$

Finally $\mathrm{Tr}(\boldsymbol{D}^{-1}\partial_\mu \boldsymbol{D})$ can be evaluated in terms of the λ_i as follows,

$$\begin{aligned}
\mathrm{Tr}(\boldsymbol{D}^{-1}\partial_\mu \boldsymbol{D}) &= \sum_{ij} D_{ij}^{-1}\partial_\mu D_{ij}, && (1.3.132)\\
&= \sum_{i} D_{ii}^{-1}\partial_\mu D_{ii}, && (1.3.133)\\
&= \sum_{i} \lambda_i^{-1}\partial_\mu \lambda_i, && (1.3.134)
\end{aligned}$$

which proves that Eq. (1.3.118) is true.

Now we can find a convenient form of the divergence $\nabla_\mu X^\mu$ of a vector $\boldsymbol{X}$. Expanding the covariant derivative gives

$$\begin{aligned}
\nabla_\mu X^\mu &= \partial_\mu X^\mu + \Gamma^\mu{}_{\mu\nu} X^\nu, && (1.3.135)\\
&= \partial_\mu X^\mu + \frac{1}{2} g^{\mu\rho}\left(\partial_\mu g_{\rho\nu} + \partial_\nu g_{\mu\rho} - \partial_\rho g_{\mu\nu}\right) X^\nu, && (1.3.136)\\
&= \partial_\mu X^\mu + \frac{1}{2} g^{\mu\rho}\partial_\nu g_{\mu\rho} X^\nu. && (1.3.137)
\end{aligned}$$

Applying Eq. (1.3.118) to the metric $\boldsymbol{g}$ gives,

$$g^{\mu\rho}\partial_\nu g_{\mu\rho} = g^{-1}\partial_\nu g, \tag{1.3.138}$$

and the covariant divergence $\nabla_\mu X^\mu$ of a vector $\boldsymbol{X}$ simplifies to

$$\begin{aligned}
\nabla_\mu X^\mu &= \partial_\mu X^\mu + \frac{1}{2g}\partial_\mu g, && (1.3.139)\\
&= \frac{1}{\sqrt{|g|}}\partial_\mu\left(\sqrt{|g|}X^\mu\right), && (1.3.140)
\end{aligned}$$

which in the standard pseudo-Riemannian spacetime is often written

$$\boldsymbol{\nabla}\cdot\boldsymbol{X} = \nabla_\mu X^\mu = \frac{1}{\sqrt{-g}}\partial_\mu(\sqrt{-g}X^\mu). \tag{1.3.141}$$

This equation will have much use later in section **??** where the divergence of a vector will be integrated over a finite n-dimensional volume V in $\mathcal{M}$. In order to do this, the divergence theorem of curved space is used,

$$\int_V \boldsymbol{\nabla}\cdot\boldsymbol{X}\sqrt{|{}^{(n)}g|}\,\mathrm{d}^n x = \sum_i \int_{\partial V_i} \boldsymbol{s}^{(i)}\cdot\boldsymbol{X}\sqrt{|{}^{(n-1)}g^{(i)}|}\,\mathrm{d}^{n-1}x, \tag{1.3.142}$$

where the surface of V is divided into a set of $(n-1)$-dimensional surfaces ∂V_i; for each of these surfaces there is an $(n-1)$-dimensional metric ${}^{(n-1)}\boldsymbol{g}^{(i)}$ with determinant ${}^{(n-1)}g^{(i)}$ and unit normal vector $\boldsymbol{s}^{(i)}$ with ${}^{(n-1)}\boldsymbol{g}^{(i)}(\boldsymbol{s}^{(i)}, \boldsymbol{s}^{(i)}) = \pm 1$. When dealing with a pseudo-Riemannian manifold, we need to take care of the direction of $\boldsymbol{s}^{(i)}$; in the case that $\boldsymbol{s}^{(i)}$ is timelike it should be in-directed, and if it's spacelike then it should be out-directed. The correct direction of the $\boldsymbol{s}^{(i)}$ can be readily checked by computing Eq. (1.3.142) in a non-curved manifold.

1.4 Relativity

1.4.1 Special Relativity

In the nineteenth century, it was widely believed that the universe was permeated by an invisible luminous aether. It was thought that light travels at a fixed speed through this aether; the aether could be thought of as a universal rest frame. Consequently moving towards/away from a light source would cause the speed of oncoming light to vary. With that line of thought one could measure the earths speed through the aether by setting up an interferometer experiment. An interferometer sends a light beam through a splitter, dividing the beam into two perpendicular paths. The two beams then reach a separate mirror and are reflected to a half-mirror that recombines the two beams after they have travelled identical distance. If the time taken for the two beams to complete their identical length journeys differs then an interference pattern will be seen at a detector placed behind the half-mirror due to the phase change between the two beams. In 1887, Michelson and Morley conducted their famous interferometer experiment to measure the earth's velocity through the aether. They expected to see interference when the different beams made different angles with the earth's velocity through the aether. However, no matter which way they oriented the experiment there was no interference pattern. This implied that light moved at exactly the same speed in any direction; this is only possible if earth is in the rest frame of the aether, but this cannot possibly be true as the planet accelerates round a circular path around the Sun that is following a larger circular path (in the Milky Way) and so on. This famous result demonstrated that the speed of light (in vacuum) is the same in any direction in all inertial (non-accelerating) frames - a result that defied Newtonian physics. This was a crucial hint that a new theory of dynamics was needed.

In 1905, Einstein published "On the Electrodynamics of Moving Bodies" [5] which contained a description of Special Relativity (SR). SR is essentially the idea that the laws of physics (excluding gravity) are the same in any inertial rest frame. A consequence of this is that it is impossible to measure the velocity of your own rest frame and no inertial frame is special. One big problem with SR is that it does not properly describe gravity and thus describes an infinite vacuum universe; this is a problem that will be addressed in the next sections. SR alone contains many interesting results such as time dilation, length contraction and the inclusion of time in distance measures.

Minkowski Space

In Newtonian physics the metric of flat space, using Cartesian coordinates, is,

$$g_{ij} = \delta_{ij} = \begin{pmatrix} 1 & 0 & 0 \\ 0 & 1 & 0 \\ 0 & 0 & 1 \end{pmatrix}, \tag{1.4.1}$$

with the line element,

$$\mathrm{d}s^2 = \delta_{ij}\mathrm{d}x^i\mathrm{d}x^j = \mathrm{d}x^2 + \mathrm{d}y^2 + \mathrm{d}z^2. \tag{1.4.2}$$

In SR, time is promoted to an extra dimension and the metric is over space and time (spacetime); this flat 4-dimensional spacetime is called Minkowski space. The spacetime metric has a single negative eigenvalue and hence negative determinant. In Cartesian coordinates, the flat spacetime metric is,

$$g_{\mu\nu} = \eta_{\mu\nu} = \begin{pmatrix} -1 & 0 & 0 & 0 \\ 0 & 1 & 0 & 0 \\ 0 & 0 & 1 & 0 \\ 0 & 0 & 0 & 1 \end{pmatrix}, \tag{1.4.3}$$

and the line element is,

$$\mathrm{d}s^2 = \eta_{\mu\nu}\mathrm{d}x^\mu\mathrm{d}x^\nu = -\mathrm{d}t^2 + \mathrm{d}x^2 + \mathrm{d}y^2 + \mathrm{d}z^2, \tag{1.4.4}$$

where the speed of light has been set to unity again. Having a metric on a 4-dimensional spacetime is a non-intuitive concept where time is included into geometry and paths through spacetime can have negative length.

Transforming between two inertial frames moving at constant velocity with respect to each other is done with a *boost* in special relativity. Boosting from frame S with coordinates x^μ to $\tilde{S}$ with coordinates $\tilde{x}^\mu$ we can write,

$$\mathrm{d}\tilde{x}^\mu = \frac{\partial \tilde{x}^\mu}{\partial x^\nu}\mathrm{d}x^\nu = \Lambda^\mu{}_\nu \mathrm{d}x^\nu, \tag{1.4.5}$$

where we will call $\mathbf{\Lambda}$ the boost matrix. Considering a boost along the x direction with a speed v,

$$\mathrm{d}\tilde{t} = \gamma(\mathrm{d}t - v\mathrm{d}x), \tag{1.4.6}$$
$$\mathrm{d}\tilde{x} = \gamma(\mathrm{d}x - v\mathrm{d}t), \tag{1.4.7}$$
$$\mathrm{d}\tilde{y} = \mathrm{d}y, \tag{1.4.8}$$
$$\mathrm{d}\tilde{z} = \mathrm{d}z, \tag{1.4.9}$$

where $\gamma = 1/\sqrt{1-v^2}$ is the Lorentz factor. This transformation may seem odd at first glance but ensures that every inertial frame agrees on the same speed of light in all directions. For boosts in general directions $\mathbf{\Lambda}$ should be rotated with a spatial rotation matrix using the tensor transformation law.

1.4.2 General Relativity

It is a well known result of Newtonian physics that in a rotating reference frame, with angular velocity ω, a test particle will experience three fictitious forces; the centrifugal force that grows with distance from the origin, the Coriolis force that depends on the velocity of the test particle, and the Euler force depending on $\partial_t\omega$. From the point of view of an observer in the rotating frame a free test particle would appear to accelerate which is a violation of Newton's first law if there is no external force. The curved path followed by the particle in the rotating reference frame is of course a constant-speed straight line in the non-rotating inertial frame, and therefore the particle follows a geodesic. It is possible (but very involved) to do a coordinate transformation from the inertial frame to the rotating frame and find the metric $\tilde{\eta}_{\mu\nu}$ in the rotating frame using the tensor transformation law; it would then be possible to compute the geodesics in the rotating frame using Eq. (1.2.77).

The gravitational force can also be described as a fictitious force. In a non-accelerating frame, the path of a particle moving without external force is seen to accelerate towards massive bodies. The presence of matter density causes geodesics to curve. This is a property also possessed by curved spaces; the paths followed by a free particle on a curved background is often curved itself. Einstein's idea to incorporate gravity into relativity was to change the flat spacetime of special relativity to a curved spacetime; this theory is general relativity. In general relativity inertial frames are defined as freely falling frames (under gravity) following geodesics in curved space. The gravitational force is a fictitious force arising from an observer not being in an inertial frame. This explains why an observer standing on earth experiences a reaction force, the frame of the observer is not following a geodesic (not an inertial frame) and therefore to counteract the fictitious gravitational force the ground must push back with a reaction force. In the inertial frame, the observer standing on the earth is accelerated upwards by the earth's surface.

Worldlines and Causality

Consider a particle moving through spacetime, the motion can be described with coordinates $x^\mu(\tau)$ which is called a worldline. Here τ denotes *proper time*, the time experienced by the particle following the worldline. The 4-velocity along a worldline is,

$$v^\mu(\tau) = \frac{\mathrm{d}x^\mu}{\mathrm{d}\tau}(\tau). \tag{1.4.10}$$

In general relativity, the line element $\mathrm{d}s$ elapsed along a coordinate interval $\mathrm{d}x^\mu$ is,

$$\mathrm{d}s^2 = g_{\mu\nu}\mathrm{d}x^\mu \mathrm{d}x^\nu, \tag{1.4.11}$$

and for a particle with 4-velocity $\boldsymbol{v}$ is,

$$\mathrm{d}s^2 = g_{\mu\nu}\frac{\mathrm{d}x^\mu}{\mathrm{d}\tau}\frac{\mathrm{d}x^\nu}{\mathrm{d}\tau}\mathrm{d}\tau^2 = g_{\mu\nu}v^\mu v^\nu \mathrm{d}\tau^2 = \boldsymbol{v}\cdot\boldsymbol{v}\,\mathrm{d}\tau^2. \tag{1.4.12}$$

As shown in section 1.2.8, if a worldline $x^\mu(\lambda)$ parameterised by λ is a geodesic then $g_{\mu\nu}\dot{x}^\mu\dot{x}^\nu$ is constant where the dot denotes a derivative with respect to λ. Equating $\lambda = \tau$ gives $\dot{x}^\mu = v^\mu$ which tells us that $\boldsymbol{v}\cdot\boldsymbol{v}$, or $|\boldsymbol{v}|^2$, is constant along a world line. If $|\boldsymbol{v}|^2 < 0$ then the geodesic is *timelike*; similarly if $|\boldsymbol{v}|^2 > 0$ then the geodesic is *spacelike*. In the special case that $|\boldsymbol{v}|^2 = 0$, the curve is called *null*. Physical massive particles must travel along timelike intervals and massless particles must travel along null ones. Information cannot travel faster than light (which follows null geodesics) and hence all spacelike intervals are intraversable. Given that $|\boldsymbol{v}|^2$ is a scalar, it is unchanged by a coordinate transformation, this means that all observers in all frames (and using any coordinate system) will agree on whether an interval is timelike, spacelike or null.

1.4.3 Physics in Curved Space

General relativity postulates that (locally) the laws of physics in a free falling frame are indistinguishable from special relativity. Any equation of motions that we want to hold in general relativity must agree with special relativity in the flat-space limit. As a general rule, if there is a law of physics expressed as a differential equation in Minkowski space that we want to use in curved space, we must replace all partial derivatives of fields with co-variant derivatives of tensor fields. This process is called the minimal coupling approach and is explored in more detail at the end of section 1.4.6.

The Wave Equation

To derive the curved space wave equation we start with the wave equation for a scalar field ϕ in Minkowski space,

$$\frac{1}{c^2}\frac{\partial^2}{\partial t^2}\phi(x^i,t) - \left(\frac{\partial^2}{\partial x^2} + \frac{\partial^2}{\partial y^2} + \frac{\partial^2}{\partial z^2}\right)\phi(x^i,t) = 0, \tag{1.4.13}$$

using Cartesian coordinates and c as the speed of light which we will set to one. While this equation is Lorentz invariant[6] it is not generally covariant, changing coordinates can change the explicit form of the equation of motion. In SR, using the language of tensor calculus, we can write the wave equation as,

$$\eta^{\mu\nu}\partial_\mu\partial_\nu\phi = 0, \tag{1.4.14}$$

where $\eta^{\mu\nu}$ is the inverse metric of flat space. To adapt this to curved space we follow the minimal coupling procedure and replace $\boldsymbol{\eta} \to \boldsymbol{g}$ and $\partial_\mu \to \nabla_\mu$ giving,

$$g^{\mu\nu}\nabla_\mu\nabla_\nu\phi = 0. \tag{1.4.15}$$

This equation is fully covariant as it is a contraction of a tensor with some covariant derivatives; it is a tensor differential equation. Writing the laws of physics as tensor equations is useful as they can be written without reference to an explicit coordinate system. If a coordinate system is then picked, assuming knowledge of $g_{\mu\nu}$, then the wave equation becomes

$$g^{\mu\nu}\nabla_\mu\nabla_\nu\phi = g^{\mu\nu}\nabla_\mu\partial_\nu\phi = 0, \tag{1.4.16}$$

$$= g^{\mu\nu}\partial_\mu\partial_\nu\phi - g^{\mu\nu}\Gamma^\rho{}_{\mu\nu}\partial_\rho\phi, \tag{1.4.17}$$

[6] Lorentz in variance is to be invariant under a boost, also called a Lorentz transformation.

in terms of partial derivatives and covariant derivatives.

Equation (1.4.15) is not the only tensor equation that returns Eq. (1.4.13) in the limit of flat space (and Cartesian coordinates). What is to stop us arbitrarily adding terms that vanish in the flat-space limit? For a simple example one is free to choose the wave equation to be,

$$g^{\mu\nu}\nabla_\mu\nabla_\nu\phi + f(\phi)R^n = 0, \tag{1.4.18}$$

for constant n, function f and the Ricci scalar R from section 1.3.4. This equation certainly returns the regular wave equation in the low curvature limit as $R \to 0$. Following the rules of minimal coupling, the general rule is to keep things simple and terms such as R which are proportional to second order derivatives of the metric are thought to be less dominant that terms such as $\Gamma^\mu{}_{\rho\sigma}$ which are proportional to first derivatives of the metric. Navigating this minefield of which terms to include in the laws of physics is tricky and leads to the topic of modified gravity as discussed at the end of section 1.4.6.

Electromagnetism

Electromagnetism can also be written in terms of tensor differential equations suitable for use in curved space. Traditionally, Maxwell's equations of electromagnetism are written as,

$$\boldsymbol{\nabla}\cdot\boldsymbol{E} = \frac{\rho}{\epsilon_0}, \tag{1.4.19}$$

$$\boldsymbol{\nabla}\cdot\boldsymbol{B} = 0, \tag{1.4.20}$$

$$\boldsymbol{\nabla}\times\boldsymbol{E} + \frac{\mathrm{d}\boldsymbol{B}}{\mathrm{d}t} = 0, \tag{1.4.21}$$

$$\boldsymbol{\nabla}\times\boldsymbol{B} - \frac{\mathrm{d}\boldsymbol{E}}{\mathrm{d}t} = \mu_0\boldsymbol{J} \tag{1.4.22}$$

for charge density ρ, electric field $\boldsymbol{E}$, magnetic field $\boldsymbol{B}$, current density $\boldsymbol{J}$, permittivity of free space ϵ_0 and permeability of free space μ_0. Note these differential equations are written using vector calculus in flat space, not differential geometry and tensor calculus; the bold faced fields are therefore 3-vectors. In spacetime, the current density and charge are promoted to a single 4-vector $j^\mu = \{\rho, j^i\}$ and the 6 degrees of freedom of the electromagnetic field are encoded in the components $F_{\mu\nu}$ of an antisymmetric tensor $\boldsymbol{F}$. The four electromagnetic potentials ϕ and A_i, defined by $E_i = -\partial_i\phi - \partial_t A_i$ and $\boldsymbol{B} = \boldsymbol{\nabla}\times\boldsymbol{A}$, are also combined into one 4-vector $A_\mu = \{-\phi, A_i\}$. In Cartesian coordinates, the Electromagnetic field tensor $\boldsymbol{F}$ is,

$$F_{\mu\nu} = \nabla_\mu A_\nu - \nabla_\nu A_\nu = \partial_\mu A_\nu - \partial_\nu A_\nu, \tag{1.4.23}$$

where the swapping between $\partial_\mu \leftrightarrow \nabla_\mu$ is possible due to the cancellation of Christoffel symbols. To elucidate, in Minkowski space with Cartesian coordinates the field tensor is,

$$F_{\mu\nu} = \partial_\mu A_\nu - \partial_\nu A_\nu = \begin{pmatrix} 0 & E_x & E_y & E_z \\ -E_x & 0 & B_z & -B_y \\ -E_y & -B_z & 0 & B_x \\ -E_z & B_y & -B_x & 0 \end{pmatrix}. \tag{1.4.24}$$

The vector potential A_μ has a gauge transformation like $A_\mu \to A_\mu + \partial_\mu f$, for some scalar field f, that leaves the physically measurable field $F_{\mu\nu}$ unchanged,

$$F_{\mu\nu} \to \partial_\mu(A_\nu + \partial_\nu) - \partial_\nu(A_\mu + \partial_\mu), \tag{1.4.25}$$

$$= \partial_\mu A_\nu - \partial_\nu A_\mu + \underbrace{\partial_\mu\partial_\nu f - \partial_\nu\partial_\mu f}_{=0}, \tag{1.4.26}$$

$$= F_{\mu\nu}. \tag{1.4.27}$$

In curved space, the Maxwell Eqs. (1.4.19) and (1.4.22) in tensor form are,

$$\nabla_\mu F^{\mu\nu} = \mu_0 j^\nu, \tag{1.4.28}$$

as $\mu_0\epsilon_0 = c^{-2} = 1$ in natural units. The other two Maxwell Eqs. (1.4.20) and (1.4.21) are identically true from computing $\partial_{[\mu}F_{\alpha\beta]}$,

$$\partial_{[\mu}F_{\alpha\beta]} = \partial_\mu\partial_\alpha A_\beta - \partial_\mu\partial_\beta A_\alpha + \partial_\alpha\partial_\beta A_\mu - \partial_\alpha\partial_\mu A_\beta\partial_\beta\partial_\mu A_\alpha - \partial_\beta\partial_\alpha A_\mu, \tag{1.4.29}$$

$$\partial_{[\mu}F_{\alpha\beta]} = 0, \tag{1.4.30}$$

which is equivalent to $\nabla_{[\mu}F_{\alpha\beta]}$ due to the cancellation of Christoffel symbols.

The Stress-Energy-Momentum Tensor

At the heart of field theory in physics is the stress-energy-momentum tensor $\boldsymbol{T}$, also called the energy-momentum tensor or stress tensor for short. Roughly speaking, component T^{00} is energy density, components $T^{0i} = T^{i0}$ contain energy flux or momentum density and components $T^{ij} = T^{ji}$ contain momentum fluxes. The diagonal part of T^{ij} can also be though of as containing pressure and the off-diagonal terms containing shear stress. In flat space, the conservation of energy and momentum can be written as,

$$\partial_\mu T^{\mu\nu} = 0, \tag{1.4.31}$$

in the absence of external forces. Equation (1.4.31) is also called the continuity equation and can be split into two sets of familiar equations,

$$\partial_0 T^{00} = -\partial_i T^{i0}, \tag{1.4.32}$$

$$\partial_0 T^{0j} = -\partial_i T^{ij}, \tag{1.4.33}$$

where the first equation states *"The rate of change of energy density is equal and opposite to the divergence of energy flux density"* and the second equation states *"The rate of change of momentum density is equal and opposite to the divergence of momentum flux density"*.

The stress tensor plays an important role in curved space and the continuity equation becomes,

$$\nabla_\mu T^{\mu\nu} = \partial_\mu T^{\mu\nu} + \Gamma^\mu{}_{\mu\rho}T^{\rho\nu} + \Gamma^\nu{}_{\mu\rho}T^{\mu\rho} = 0, \tag{1.4.34}$$

where the partial derivative has been replaced with a covariant derivative in accordance with minimal coupling. This can be rewritten using Eq. (1.3.141) as,

$$\partial_\mu(\sqrt{-g}T^{\mu\nu}) = -\sqrt{-g}\Gamma^\nu{}_{\mu\rho}T^{\mu\rho}, \tag{1.4.35}$$

$$\partial_\mu(\mathcal{T}^{\mu\nu}) = -\Gamma^\nu{}_{\mu\rho}\mathcal{T}^{\mu\rho}, \tag{1.4.36}$$

where the second equation writes the stress tensor as a tensor density $\boldsymbol{\mathcal{T}} = \sqrt{-g}\boldsymbol{T}$ making the equation resemble the flat space continuity equation more closely. This modification of traditional continuity of energy and momentum to curved spaces will be revisited in section **??**.

1.4.4 The Einstein Equation

We have already seen how the equations of motion for matter can be promoted to curved space; building on the vague notion of matter causing spacetime curvature it would be helpful to have a mathematical law saying how much curvature is caused by a given matter distribution. The first guess that Einstein arrived at was to write $R_{\mu\nu} = kT_{\mu\nu}$ for some constant k. The problem is that given $\nabla_\mu T^{\mu\nu} = 0$ is the generic equation of continuity for matter, it would imply $\nabla_\mu R^{\mu\nu}$ vanishes which is not generally true. As shown in Eq. (1.3.115), the Einstein tensor $G_{\mu\nu}$ does satisfy $\nabla_\mu G^{\mu\nu} = 0$; the next simplest guess at

a physical law for spacetime curvature would be $G_{\mu\nu} = kT_{\mu\nu}$. Remarkably this turns out to be correct and has successfully described many[7] gravitational phenomena. The Einstein equation,

$$R_{\mu\nu} - \frac{1}{2}g_{\mu\nu}R = \frac{8\pi G}{c^4}T_{\mu\nu}, \tag{1.4.37}$$

where $G_{\mu\nu} = R_{\mu\nu} - g_{\mu\nu}R/2$, is at the core of general relativity. This equation relates spacetime curvature, encoded in the Einstein tensor $G_{\mu\nu}$, to the matter distribution described by the stress tensor $T_{\mu\nu}$. This leads nicely to Wheeler's insightful one line summary of general relativity:

"Spacetime tells matter how to move; matter tells spacetime how to curve."

This deceptively simple equation can describe an enormous amount of vastly diverse spacetime geometries including regular flat Minkowski space, black holes, stars, planets, gravitational waves and even the entire universe; to properly describe the entire universe a small modification has to be made to this equation as discussed at the end of this section.

General Relativity in Vacuum

In the case of a vacuum spacetime with $T_{\mu\nu} = 0$ the Einstein equation simplifies greatly to

$$G_{\mu\nu} = 0. \tag{1.4.38}$$

Taking the trace of the above equation and the definition of $G_{\mu\nu} = R_{\mu\nu} - g_{\mu\nu}R/2$, we see that,

$$g^{\mu\nu}G_{\mu\nu} = 0 = g^{\mu\nu}\left(R_{\mu\nu} - \frac{1}{2}Rg_{\mu\nu}\right) = R\left(1 - \frac{D}{2}\right), \tag{1.4.39}$$

where D is the number of spacetime dimensions. Clearly for $D \neq 2$ a vanishing Einstein tensor implies a vanishing Ricci scalar R; if the Ricci scalar vanishes then the Einstein equation in vacuum simplifies to

$$R_{\mu\nu} = 0. \tag{1.4.40}$$

Note that even though $R_{\mu\nu} = 0$, this does not mean there is no spacetime curvature; the Riemann tensor $R^{\mu}{}_{\nu\rho\sigma}$ can still be non-zero.

The Cosmological Constant

A discussion of general relativity is incomplete without discussing the cosmological constant Λ. At a geometric level, the cosmological constant encodes the homogeneous spacetime curvature in the absence of matter, and indeed setting $\Lambda \to 0$ (in vacuum) returns asymptotically flat vacuum general relativity. The cosmological constant is added into Einstein's equation (1.4.37), with $\Lambda g_{\mu\nu}$,

$$R_{\mu\nu} - \frac{1}{2}Rg_{\mu\nu} + \Lambda g_{\mu\nu} = \frac{8\pi G}{c^4}T_{\mu\nu}. \tag{1.4.41}$$

Each term still has a zero-divergence as $\nabla_\mu g_{\alpha\beta} = 0$ due to the Levi-Civita connection defined in section 1.3.3. The traced Einstein equation becomes

$$\left(1 - \frac{D}{2}\right)R + D\Lambda = \frac{8\pi G}{c^4}T \tag{1.4.42}$$

where $T = g^{\mu\nu}T_{\mu\nu}$ is the trace of the stress tensor and D is the number of spacetime dimensions. The traced Einstein equation makes it obvious that Λ has the same effect on curvature as a uniform matter density with constant T. Using geometric units $D\Lambda = 8\pi T$ is a special case which has solution $R = 0$ similarly to vacuum GR. From now on $\Lambda = 0$ will be assumed.

[7] These phenomena include, but are not limited to, stars, black holes (BHs), collisions of BHs and/or stars and gravitational waves.

1.4.5 Black Holes

As it turns out, vacuum General Relativity can describe more than just Minkowski space. Arguably the most important family of solutions to Einstein's equations in vacuum are black holes. The first black hole solution was found by Karl Schwarzschild, whose surname fittingly means "*black shield*" in German. This solution, known as the Schwarzschild solution, was discovered in 1916 with the intention of computing the spacetime curvature in the vacuum about a spherically symmetric mass such as stars and planets. The solution for $g_{\mu\nu}$ was assumed to take the following ansatz,

$$\mathrm{d}s^2 = g_{\mu\nu}\mathrm{d}x^\mu \mathrm{d}x^\nu = -A(r)\mathrm{d}t^2 + B(r)\mathrm{d}r^2 + r^2\left(\mathrm{d}\theta + \sin^2(\theta)\mathrm{d}\phi^2\right), \tag{1.4.43}$$

which is manifestly spherically symmetric and static; in the case $A(r) = B(r) = 1$ the solution is exactly Minkowski space in spherical polar coordinates. By solving the Einstein equation in vacuum ($R_{\mu\nu} = 0$) the Schwarzschild solution can be found,

$$g_{\mu\nu}\mathrm{d}x^\mu \mathrm{d}x^\nu = -\left(1 - \frac{2Gm}{rc^2}\right)\mathrm{d}t^2 + \left(1 - \frac{2Gm}{rc^2}\right)^{-1}\mathrm{d}r^2 + r^2\left(\mathrm{d}\theta + \sin^2(\theta)\mathrm{d}\phi^2\right). \tag{1.4.44}$$

The constants G and c are included for completeness, but are equal to one in geometric units or Planck units. The Schwarzschild solution describes the spacetime around a non-spinning sphere of mass m and as $r \to \infty$ or $m \to 0$ we approach the vacuum Minkowski spacetime as desired. What Schwarzschild did not realise before his untimely death was that his solution could in fact be trusted down to vanishing radii and describes the eternal (or static), non-spinning black hole of mass m called the Schwarzschild black hole.

Many other black hole solutions have been found to date. These solutions include the spinning *Kerr* black hole, non-spinning electromagnetically charged *Reissner-Nordström* black hole and spinning electromagnetically charged *Kerr-Newman* black hole. Non asymptotically flat black holes in cosmological backgrounds have also been found [6]. In modified gravity theories, briefly discussed in section 1.4.6, exotic black hole solutions (often coupled to other fields such as scalar fields) exist.

Polar-Areal Coordinates

The type of coordinates used in the Schwarzschild solution are called polar-areal coordinates; these are coordinates that assign an area $4\pi r_0^2$ to the 2-surface defined by $r = r_0$ and $t = t_0$. Using Eq. (1.2.70) the surface area of a coordinate sphere with $t = t_0$, $r = r_0$ can be calculated from

$$A = \int_0^\pi \left[\int_0^{2\pi} \sqrt{\sigma}\Big|_{t=t_0, r=r_0} \mathrm{d}\phi\right] \mathrm{d}\theta, \tag{1.4.45}$$

where σ is the metric determinant on the surface. Evaluating this explicitly for the Schwarzschild metric with $\sqrt{\sigma} = \sqrt{g_{\theta\theta}g_{\phi\phi}} = r^2\sin(\theta)$ gives

$$A = \int_0^\pi \left[\int_0^{2\pi} \sqrt{g_{\phi\phi}g_{\theta\theta}}\Big|_{t=t_0, r=r_0} \mathrm{d}\phi\right] \mathrm{d}\theta = r_0^2 \int_0^\pi \left[\int_0^{2\pi} \mathrm{d}\phi\right] \sin^2(\theta)\,\mathrm{d}\theta = 4\pi r_0^2. \tag{1.4.46}$$

Coordinate Singularities and Physical Singularities

There is obviously some kind problem at radius $r_s = 2m$ (or $r_s = 2mG/c^2$ in S.I. units), known as the Schwarzschild radius, as g_{rr} diverges here. For physical planets and stars observed the radius of the object is much larger than the Schwarzschild radius so the solution should not be trusted inside the object as it has been derived in vacuum. But in order to describe black holes we must consider radii down to $r = 0$. The problem at the Schwarzschild radius is due to the choice of coordinates and is not physically problematic. An easy way to show this is to compute a curvature scalar[8] and show that it

[8] Scalar curvature invariants are useful since if they diverge in one coordinate system then they must diverge in all coordinate systems as they do not transform under coordinate transformations. It should be noted that $\sqrt{-g}$ is a scalar density and not a true scalar so is not a scalar curvature invariant.

is finite and smooth at $r = r_s$. The first choice of curvature scalar might be the Ricci scalar, but this is zero in vacuum so is not useful for this purpose. Vacuum general relativity asserts that $R_{\mu\nu} = 0$, while that guarantees that $R = 0$ it does not guarantee that $R_{\mu\nu\rho\sigma} = 0$. Another curvature scalar is the Kretschmann scalar k, defined in Eq. (1.3.117), which does not generally vanish in vacuum. Calculating the Kretschmann scalar for the Schwarzschild metric gives,

$$k_{\text{sc}} = \frac{48m^2}{r^6}, \tag{1.4.47}$$

in polar-areal coordinates. As can be seen, k_{sc} is continuous and infinitely differentiable at $r = 2m$. However, as $r \to 0$, $k_{\text{sc}} \to \infty$ and there is a real coordinate independent singularity called a physical singularity.

To remove the coordinate singularity at $r = 2m$, new coordinates can be introduced. One example is to use ingoing-Eddington-Finkelstein coordinates $\{v, \tilde{r}, \theta, \phi\}$ defined by

$$\frac{\mathrm{d}\tilde{r}}{\mathrm{d}r} = \left(1 - \frac{2m}{r}\right), \tag{1.4.48}$$

$$v = t + \tilde{r}, \tag{1.4.49}$$

which transforms the line element to,

$$g_{\mu\nu}\mathrm{d}x^\mu \mathrm{d}x^\nu = -\left(1 - \frac{2m}{r}\right)\mathrm{d}v^2 + 2\mathrm{d}v\mathrm{d}r + r^2\left(\mathrm{d}\theta + \sin^2(\theta)\mathrm{d}\phi^2\right), \tag{1.4.50}$$

and the metric no longer diverges at $r = 2m$. Bearing in mind that now the metric is not diagonal, the metric determinant can be calculated, giving $\sqrt{-g} = r^2\sin(\theta)$. Given that the metric is finite for $r > 0$ and the metric determinant is non-zero for $r > 0$, the metric inverse is also guaranteed to be finite for $r > 0$. It has been demonstrated that the coordinate singularity at $r = 2m$ in Schwarzschild polar-areal vanishes when using ingoing-Eddington-Finkelstein coordinates.

Throughout this section we have ignored the fact that the inverse metric also diverges as $\theta \to 0$ or $\theta \to \pi$, this is a coordinate singularity that is present in flat space (which is equivalent to the Schwarzschild spacetime with $m = 0$). This coordinate singularity arises in flat space due to the azimuthal angle ϕ being undefined at $\theta = 0$ and $\theta = \pi$. There are no physical singularities in flat space and these coordinate singularities vanish when using Cartesian coordinates.

Isotropic Coordinates

A coordinate system that will be useful later on is the isotropic coordinate system. Isotropic coordinates lead to the line element,

$$g_{\mu\nu}\mathrm{d}x^\mu \mathrm{d}x^\nu = -\Omega^2(x^\mu)\mathrm{d}t^2 + \Psi^2(x^\mu)\mathrm{d}s^2_{\text{flat}}, \tag{1.4.51}$$

where $\mathrm{d}s^2_{\text{flat}}$ is the flat space Euclidean line element. For example, in spherical polar and Cartesian spatial coordinates, the isotropic line element in spherical symmetry becomes,

$$g_{\mu\nu}\mathrm{d}x^\mu \mathrm{d}x^\nu = -\Omega(\rho)^2\mathrm{d}t^2 + \Psi^2(\rho)\left(\mathrm{d}\rho^2 + \rho^2\left(\mathrm{d}\theta^2 + \sin^2(\theta)\mathrm{d}\phi^2\right)\right), \tag{1.4.52}$$

$$= -\Omega(\rho)^2\mathrm{d}t^2 + \Psi^2(\rho)\left(\mathrm{d}x^2 + \mathrm{d}y^2 + \mathrm{d}z^2\right), \tag{1.4.53}$$

where $\rho^2 = x^2 + y^2 + z^2$.

The Schwarzschild black hole solution can also be expressed in isotropic coordinates,

$$= -\left(\frac{1 - \frac{m}{2\rho}}{1 + \frac{m}{2\rho}}\right)^2 \mathrm{d}t^2 + \left(1 + \frac{m}{2\rho}\right)^4 \mathrm{d}s^2_{\text{flat}}. \tag{1.4.54}$$

As $\rho \to \infty$ the line element reduces to that of the Minkowski spacetime. At the radius $\rho = m/2$, g_{tt} vanishes (similarly to polar areal coordinates) and this is the Schwarzschild radius in isotropic coordinates. At first glance one might think that there is also the same physical singularity at $\rho = 0$. However, if a new radial coordinate ξ is used, where $\rho = \frac{m^2}{4\xi}$, the line element becomes,

$$g_{\mu\nu}\mathrm{d}x^\mu x^\nu = -\left(\frac{1-\frac{m}{2\xi}}{1+\frac{m}{2\xi}}\right)^2 \mathrm{d}t^2 + \left(1+\frac{m}{2\xi}\right)^4 \left(\mathrm{d}\xi^2 + \xi^2(\mathrm{d}\theta^2 + \sin^2(\theta)\mathrm{d}\phi^2)\right). \tag{1.4.55}$$

This is an intriguing result, inverting the radial coordinate about $\rho = 2/m$ has returned an identical metric. Given that at $\rho = \infty$ we have flat space this implies that at $\xi = \infty$ (or $\rho = 0$) there is another separate flat space, not the physical singularity that might have been expected. The black hole exterior $m/2 < \rho < \infty$ must be identical to the volume $m/2 < \xi < \infty$ (also written as $m/2 > \rho > 0$), hence there are two asymptotically flat universes joined by the surface $\rho = m/2$; this surface is the Einstein-Rosen bridge. The Einstein-Rosen bridge is not traversable, to cross this bridge would require a spacelike worldline or faster than light travel which is forbidden. The geometry of the isotropic black hole is shown in Fig. (1.2).

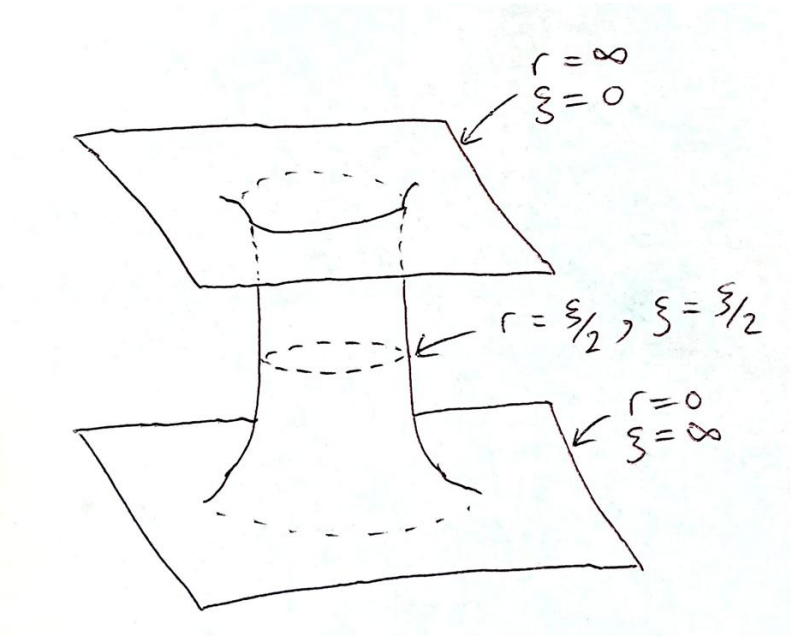

Figure 1.2: This diagram shows the geometry of the spacetime covered by isotropic coordinates. There are two asymptotically flat ends joined by the Einstein-Rosen bridge at $r = \xi = m/2$.

The reason that the physical singularity at $\rho = 0$ does not appear in isotropic coordinates is deceptively simple; in isotropic coordinates $\rho = 0$ does not correspond to the same point on the manifold as $r = 0$ does in the polar areal gauge for any value of t, θ or ϕ. Infact, the physical singularity of the black hole is outside of the patch on the manifold covered by isotropic coordinates. This can be illustrated by computing the Kretschmann scalar in isotropic coordinates. Using isotropic radial coordinate ξ and polar areal radius r we can write,

$$\xi\left(1+\frac{m}{2\xi}\right)^2 = r, \tag{1.4.56}$$

by comparing the $\mathrm{d}\theta$ part of the line element. Substituting this into Eq. (1.4.47), the Kretschmann scalar in isotropic coordinates is,

$$k_{\mathrm{iso}} = \frac{48m^2\xi^6}{(\xi+\frac{m}{2})^{12}}. \tag{1.4.57}$$

This is finite for $0 \leq \xi \leq \infty$ and hence there is no physical singularity covered by isotropic coordinates. In fact we can make a stronger statement. The value of the Kretschmann scalar on the event horizon is,

$$k_{\rm EH} = \frac{3}{4m^4}. \tag{1.4.58}$$

In isotropic coordinates, the minimum value that $k_{\rm iso}$ can take is found by $\partial k_{\rm iso}/\partial\xi = 0$ which has a turning point at $\xi = m/2$. At $\xi = m/2$ the value of $k_{\rm iso}$ is $3/(4m^4)$ which is the the minimum value of $k_{\rm iso}$. Given that $k < k_{\rm EH}$ in the interior of a black hole and $k_{\rm iso} \geq k_{\rm EH}\,\forall\,\xi$ then isotropic coordinates do not penetrate the event horizon.

1.4.6 The Lagrangian Formulation of General Relativity

A common procedure in theoretical physics is to encapsulate the solution space in an action functional S,

$$S = \int \mathcal{L}\sqrt{-g}\,\mathrm{d}x^4. \tag{1.4.59}$$

Using the calculus of variation on this action returns differential equations governing the system. As found by Hilbert [7] the following Lagrangian density $\mathcal{L} = R$, equal to the Ricci scalar, returns the vacuum Einstein equations under varying with respect to $g^{\mu\nu}$.

$$\delta S = \int \left[\sqrt{-g}(\delta R) + R(\delta\sqrt{-g})\right]\,\mathrm{d}x^4 \tag{1.4.60}$$

$$= \int \left[\sqrt{-g}\delta(g^{\mu\nu}R_{\mu\nu}) - \frac{1}{2}\sqrt{-g}g_{\mu\nu}R(\delta g^{\mu\nu})\right]\,\mathrm{d}x^4 \tag{1.4.61}$$

$$= \int \left[\sqrt{-g}g^{\mu\nu}(\delta R_{\mu\nu}) + \sqrt{-g}\left(R_{\mu\nu} - \frac{1}{2}Rg_{\mu\nu}\right)\delta g^{\mu\nu}\right]\,\mathrm{d}x^4 \tag{1.4.62}$$

where we have used Eq. (1.3.138) to vary $\sqrt{-g}$. Remembering that the difference of two Christoffel symbols such as,

$$\delta\Gamma^{\lambda}{}_{\mu\nu} = \Gamma^{\lambda}{}_{\mu\nu}|_{g^{\mu\nu}+\delta g^{\mu\nu}} - \Gamma^{\lambda}{}_{\mu\nu}|_{g^{\mu\nu}} \tag{1.4.63}$$

is a tensor, and using normal coordinates discussed in section 1.3.3 the left hand term of Eq. (1.4.62) becomes

$$g^{\mu\nu}\delta R_{\mu\nu} = g^{\mu\nu}\left(\partial_\lambda\delta\Gamma^{\lambda}{}_{\mu\nu} - \partial_\nu\delta\Gamma^{\lambda}{}_{\mu\lambda}\right), \tag{1.4.64}$$

$$= g^{\mu\nu}\left(\nabla_\lambda\delta\Gamma^{\lambda}{}_{\mu\nu} - \nabla_\nu\delta\Gamma^{\lambda}{}_{\mu\lambda}\right), \tag{1.4.65}$$

$$= \nabla_\lambda\left(g^{\mu\nu}\delta\Gamma^{\lambda}{}_{\mu\nu} - g^{\mu\lambda}\delta\Gamma^{\nu}{}_{\mu\nu}\right). \tag{1.4.66}$$

$$= \nabla_\lambda X^\lambda. \tag{1.4.67}$$

The first expression follows from contracting Eq. (1.3.97) for the Riemann tensor with normal coordinates and the second line swaps $\nabla_\mu \to \partial_\mu$ which are equivalent using normal coordinates. Putting everything together, δS becomes

$$\delta S = \int \left[\nabla_\mu X^\mu + \left(R_{\mu\nu} - \frac{1}{2}Rg_{\mu\nu}\right)\right]\sqrt{-g}\,\mathrm{d}x^4, \tag{1.4.68}$$

$$= \int_B X^\mu \hat{s}_\mu \sqrt{|{}^{(3)}g|}\mathrm{d}x^3 + \int \left[R_{\mu\nu} - \frac{1}{2}Rg_{\mu\nu}\right]\sqrt{-g}\,\mathrm{d}x^4, \tag{1.4.69}$$

$$\tag{1.4.70}$$

where the integral over B represents the surface integral over the boundary of our spacetime with metric ${}^{(3)}g_{ij}$; on B $\delta g^{\mu\nu} \to 0$ and therefore $X^\mu \to 0$. Setting $\mathrm{d}S = 0$ implies

$$R_{\mu\nu} - \frac{1}{2}Rg_{\mu\nu} = 0, \tag{1.4.71}$$

which is the vacuum Einstein equation.

Non-Vacuum Spacetimes

Matter is often added into a spacetime at the level of the Lagrangian with a term $\frac{16\pi G}{c^4}\mathcal{L}_m$. The cosmological constant can be added in exactly the same way with $\mathcal{L}_\Lambda$. The total Lagrangian becomes,

$$S = \int \left(R + \frac{16\pi G}{c^4}\mathcal{L}_m + \mathcal{L}_\Lambda \right) \sqrt{-g}\, \mathrm{d}x^4. \tag{1.4.72}$$

As we have already seen earlier in this section, the variation of R with respect to the inverse metric components $g^{\mu\nu}$ returns the vacuum Einstein equation; adding the two new terms from $\mathcal{L}_m$ and $\mathcal{L}_\Lambda$, setting $\delta S = 0$ gives the non-vacuum equation

$$R_{\mu\nu} - \frac{1}{2}Rg_{\mu\nu} + \frac{16\pi G}{c^4}\frac{1}{\sqrt{-g}}\frac{\delta(\mathcal{L}_m\sqrt{-g})}{\delta g^{\mu\nu}} + \frac{1}{\sqrt{-g}}\frac{\delta(\mathcal{L}_\Lambda\sqrt{-g})}{\delta g^{\mu\nu}} = 0. \tag{1.4.73}$$

Comparing the $\mathcal{L}_\Lambda$ term to the Einstein equation with cosmological constant in Eq. (1.4.41) we must have

$$\begin{aligned} g_{\mu\nu}\Lambda &= \frac{1}{\sqrt{-g}}\frac{\delta(\mathcal{L}_\Lambda\sqrt{-g})}{\delta g^{\mu\nu}}, && (1.4.74)\\ &= \mathcal{L}_\Lambda\frac{1}{\sqrt{-g}}\frac{\delta(\sqrt{-g})}{\delta g^{\mu\nu}} + \frac{\delta(\mathcal{L}_\Lambda)}{\delta g^{\mu\nu}}, && (1.4.75)\\ &= -\frac{1}{2}g_{\mu\nu}\mathcal{L}_\Lambda + \frac{\delta(\mathcal{L}_\Lambda)}{\delta g^{\mu\nu}}, && (1.4.76)\\ & && (1.4.77) \end{aligned}$$

which is solved by $\mathcal{L}_\Lambda = -2\Lambda$. Comparing the matter term instead returns another definition of the stress tensor,

$$\begin{aligned} T_{\mu\nu} :&= -\frac{2}{\sqrt{-g}}\frac{\delta(\mathcal{L}_m\sqrt{-g})}{\delta g^{\mu\nu}}, && (1.4.78)\\ &= -2\frac{\delta\mathcal{L}_m}{\delta g^{\mu\nu}} + g_{\mu\nu}\mathcal{L}_m. && (1.4.79) \end{aligned}$$

Collecting these results, the full Lagrangian is,

$$\mathcal{L} = R + \frac{16\pi G}{c^4}\mathcal{L}_m - 2\Lambda, \tag{1.4.80}$$

or in geometric units (with $c = G = 1$),

$$\mathcal{L} = R + 16\pi\mathcal{L}_m - 2\Lambda. \tag{1.4.81}$$

The form of $\mathcal{L}_m$ is problem specific, depending on the type of matter. The equation of motion of the matter, described by a set of fields ϕ_i, and their partial derivatives with respect to x^μ is,

$$\sqrt{-g}\frac{\delta\mathcal{L}}{\delta\phi_i} - \partial_\mu\left(\sqrt{-g}\frac{\delta\mathcal{L}}{\delta\partial_\mu\phi_i}\right) = 0. \tag{1.4.82}$$

If the ϕ_i are scalar fields then the equation of motion simplifies, using Eq. (1.3.141), to

$$\frac{\delta\mathcal{L}}{\delta\phi_i} - \nabla_\mu\left(\frac{\delta\mathcal{L}}{\delta\nabla_\mu\phi_i}\right) = 0. \tag{1.4.83}$$

Modified Theories of Gravity

At the level of the Lagrangian, minimal coupling means to write down the simplest Lagrangian possible. This avoids higher powers of the curvature tensors[9] as well as coupling between matter fields and curvature where possible. As an example, the action for the minimally coupled scalar field ψ in curved space is,

$$S_\psi = \int \left(aR - bg^{\mu\nu}\partial_\mu\psi\partial_\nu\psi\right)\sqrt{-g}\,\mathrm{d}^4x, \tag{1.4.84}$$

for constants a and b. Extra coupling terms between matter and curvature could be added, for instance the action,

$$S_f = \int \left(aRf(\psi) - bg^{\mu\nu}\partial_\mu\psi\partial_\nu\psi\right)\sqrt{-g}\,\mathrm{d}^4x, \tag{1.4.85}$$

for some function f; note that if f is constant then this action reduces to Eq. (1.4.84) for the minimally coupled scalar field. Varying S_f with respect to $g^{\mu\nu}$ gives a modification of the Einstein equation,

$$f(\psi)R_{\mu\nu} - \frac{1}{2}Rf(\psi)g_{\mu\nu} + R\frac{\delta f}{\delta g^{\mu\nu}}(\psi) = \frac{b}{a}\left(\nabla_\mu\psi\nabla_\nu\psi - \frac{1}{2}g_{\mu\nu}g^{\rho\sigma}\nabla_\rho\psi\nabla_\sigma\psi\right), \tag{1.4.86}$$

where a new type of term $R\frac{\delta f}{\delta g^{\mu\nu}}(\psi)$ coupling gravity and matter has arisen; note this becomes the regular Einstein equation for a spacetime with a real massless scalar field ψ if f is constant. Varying S_f with respect to ψ instead gives the modified wave equation,

$$g^{\mu\nu}\nabla_\mu\nabla_\nu\psi + \frac{a}{b}R\frac{\partial f}{\partial\psi} = 0, \tag{1.4.87}$$

which is equivalent to Eq. (1.4.18); note that this returns the regular curved space wave equation if $\partial f/\partial\psi = 0$ and the regular wave equation in the flat-space limit for general f since $R^\mu{}_{\nu\rho\sigma} = 0$. Other popular methods of modifying gravity include second order curvature terms like R^2, $R_{\mu\nu}R^{\mu\nu}$, $R_{\mu\nu\rho\sigma}R^{\mu\nu\rho\sigma}$, even higher powers of curvature or different couplings between matter and curvature in the Lagrangian.

The Lagrangian formulation of general relativity is especially useful for the more theoretical aspects of general relativity such as exotic matter and modified gravity. General relativity is not thought of as the correct or final theory of gravity. It is a classical field theory and does not describe particles or quantum mechanics. To date no successful quantisation of general relativity has been developed. Another problem with general relativity is that at the centre of black holes there are singularities which are usually viewed as unphysical. A similar singularity exists for the Coulomb force of a point particle and is resolved by quantum field theory (QFT); it is thought a similar thing may happen in a QFT for gravity but it is currently unknown.

Theories such as string theory and loop quantum gravity have attempted to describe a quantum theory of gravity but it is notoriously difficult to derive observable effects from them. Many modified gravity theories aim to describe the first leading-order deviation from general relativity towards quantum gravity. It is thought that deviations from general relativity might be seen in extremely high curvature regimes but there is no conclusive experimental evidence to date.

[9]The Riemann tensor, Ricci tensor, Ricci scalar and combinations thereof.

Chapter 2

Numerical Relativity and Boson Stars

2.1 Numerical Relativity

2.1.1 Spacetime Foliation

Einstein's equation is a classical field equation which, along with an equation of motion for any matter, governs the dynamics of spacetime curvature,

$$R_{\mu\nu} - \frac{1}{2}Rg_{\mu\nu} = \frac{8\pi G}{c^4}T_{\mu\nu}. \tag{2.1.1}$$

The above version is fully covariant, agnostic of the definition of time, and many solutions are known analytically, for instance black hole geometries. When the system of interest becomes more complicated, such as the case of orbiting objects which will be discussed later, finding an analytic expression becomes impossible. For low energy dynamics, Newtonian theory, post-Newtonian theory and perturbation theory can make more progress; however this work focuses on the highly nonlinear regime where numerical relativity is presently the only hope to solve Einstein's equations. To do this it is common to split the 4-dimensional spacetime into 3+1 dimensions, evolving a 3-dimensional manifold (maybe with matter) on a computer along the final 4th dimension. To do this we need to define a suitable hypersurface $\Sigma \in \mathcal{M}$ where $\mathcal{M}$ is the 4-dimensional manifold representing the entire spacetime. This is usually done by demanding the hypersurface Σ_t be the set of points $p \in \mathcal{M}$ where some scalar function $f : \mathcal{M} \mapsto \mathbb{R}$ satisfies $f(p) = t$. This hypersurface should be a Cauchy surface, intersecting all causal curves only once, or a partial Cauchy surface which intersects all causal curves at most once. Generally we will choose a partial Cauchy surface covering a finite region of Σ_t due to the finite memory of computers. A foliation $\mathcal{F}$ is then the union of a set of Σ_t for some range of the parameter t,

$$\mathcal{F} = \cup_t(\Sigma_t) \subseteq \mathcal{M}. \tag{2.1.2}$$

This means we should be careful to pick a parameter t such that the foliation is not self intersecting for the parameter range that covers the region of $\mathcal{M}$ that we are interested in simulating. The time coordinate in a suitable coordinate system works in many cases; it also gives the physical interpretation of Σ_t being an instant of time. Now we define the unit normal vector $\boldsymbol{n}$ to Σ_t,

$$n^\mu = -\frac{\nabla^\mu t}{\sqrt{|g_{\mu\nu}\nabla^\mu t \nabla^\nu t|}} \quad \& \quad n_\mu = -\frac{dt_\mu}{\sqrt{|g_{\mu\nu}\nabla^\mu t \nabla^\nu t|}}, \tag{2.1.3}$$

where $\mathrm{d}t_\mu = \partial_\mu t$ is the exterior derivative of t. For simplicity we define the lapse function α to be

$$\alpha := \frac{1}{\sqrt{|g_{\mu\nu}\nabla^\mu t \nabla^\nu t|}}. \tag{2.1.4}$$

giving us $n_\mu = -\alpha \mathrm{d}t_\mu$ as well as the *normal evolution* vector $m_\mu = \alpha n_\mu$. Defining two infinitesimally close points $p \in \Sigma_t$ and $q \in \Sigma_{t'}$, where $q^\mu = p^\mu + m^\mu \delta t$ and $t' = t + \delta t$, we see,

$$t(q) = t(p^\mu + m^\mu \delta t) = t(p) + \frac{\partial t}{\partial x^\mu} m^\mu \delta t = t(p) + \mathrm{d}t_\mu m^\mu \delta t = t(p) + \delta t, \tag{2.1.5}$$

showing that m^μ connects Σ_t and $\Sigma_{t'}$ for any point $p \in \Sigma_t$; therefore when creating evolution equations we should consider Lie derivatives $\mathcal{L}_m$ along m^μ rather than $\mathcal{L}_n$.

2.1.2 The 3+1 Decomposition

With the notion of a spacetime foliation we should define how to project tensors onto Σ_t; clearly scalars need no projecting. Following the ideas of section 1.2.4 we can split a vector $X^\mu \boldsymbol{e}_\mu = X^\mu_\parallel \boldsymbol{e}_\mu + X^\mu_\perp \boldsymbol{e}_\mu$ into components tangent or normal to Σ_t. We then define the orthogonal projector $\perp^\mu_\nu$ and parallel projector $-n^\mu n_\nu$,

$$X^\mu_\parallel = \left[\delta^\mu_\nu + n^\mu n_\nu\right] X^\mu = \perp^\mu_\nu X^\nu, \tag{2.1.6}$$

$$X^\mu_\perp = -n^\mu n_\nu X^\nu. \tag{2.1.7}$$

Considering scalars such as $\phi = w_\mu X^\mu$ or $\psi = T^{\mu\nu} w_\mu w_\nu$, and remembering scalars do not vary under projection, it is straightforward to show that any tensor T can be projected by contracting a projection operator $\perp$ on any free index,

$$T_\parallel^{ij\ldots}{}_{kl\ldots} = \mathcal{T}^{ij\ldots}{}_{kl\ldots} = \perp^i_\mu \perp^j_\nu \perp^\rho_k \perp^\sigma_l \cdots T^{\mu\nu\ldots}{}_{\rho\sigma\ldots}. \tag{2.1.8}$$

We can find the 3-metric $\gamma_{\mu\nu}$ of Σ_t by projecting $g_{\mu\nu}$,

$$\gamma_{ij} = \perp^\mu_i \perp^\nu_j g_{\mu\nu} = g_{\mu\nu} + n_\mu n_\nu \quad \Rightarrow \quad \gamma^i_j = \perp^i_j, \tag{2.1.9}$$

and we find it is equal to the projector $\perp$; this has to be the case as $\perp_{ij} \mathrm{d}x^i \mathrm{d}x^j$ gives the line element along Σ_t. With this machinery we can define the extrinsic curvature tensor $\mathcal{K}_{ij}$ representing curvature due to the choice of spacetime foliation; it could be nonzero for certain foliations of Minkowski space. It is not the same as the 3-Ricci tensor $\mathcal{R}_{ij}$ which is due to spacelike curvature on Σ_t for a single instant in time. The extrinsic curvature tensor is defined the following way,

$$\mathcal{K}_{ij} = \mathcal{K}_{ji} := -\perp^\mu_i \perp^\nu_j \nabla_\mu n_\nu = -\perp^\mu_i \nabla_\mu n_j = -\nabla_i n_j - n_i a_j, \tag{2.1.10}$$

$$\mathcal{K} = \mathcal{K}^i_i = -\boldsymbol{\nabla} \cdot \boldsymbol{n}, \tag{2.1.11}$$

where $a_i = \boldsymbol{n} \cdot \boldsymbol{\nabla} n_i$ is called the Eulerian acceleration; it should be noted that $\mathcal{K}_{ij}$ is symmetric. It can also be shown to take the following form,

$$\mathcal{K}_{ij} = -\frac{1}{2}\mathcal{L}_n \gamma_{ij} = -\frac{1}{2\alpha}\mathcal{L}_m \gamma_{ij}, \tag{2.1.12}$$

which gives the intuitive explanation of $\mathcal{K}_{ij}$ being related to the rate of change of the 3-metric γ_{ij} with respect to the foliation.

The next object to discuss is the covariant 3-derivative $\mathcal{D}_i$. This is the covariant derivative belonging to Σ_t and hence it's arguments should be tensors belonging to Σ_t; it should be noted that $\mathcal{D}_i \neq \perp^\mu_i \nabla_\mu$ for a generic non-scalar tensorial arguments. The covariant 3-derivative is instead found from,

$$\mathcal{T}^{ij\ldots}{}_{kl\ldots} = \perp^i_\mu \perp^j_\nu \perp^\rho_k \perp^\sigma_l \cdots T^{\mu\nu\ldots}{}_{\rho\sigma\ldots}, \tag{2.1.13}$$

$$\mathcal{D}_m \mathcal{T}^{ij\ldots}{}_{kl\ldots} := \perp^\mu_m \perp^i_\mu \perp^j_\nu \perp^\rho_k \perp^\sigma_l \cdots \nabla_\mu \mathcal{T}^{\mu\nu\ldots}{}_{\rho\sigma\ldots}. \tag{2.1.14}$$

The covariant 3-derivative in the Levi-Civita connection can be expressed in the same way as section 1.3.3; a simple example is the derivative of a vector $X^i \boldsymbol{e}_i \in \mathcal{T}(\Sigma_t)$,

$$\mathcal{D}_i X^j = \partial_i X^j + \Upsilon^i{}_{jk} X^k, \tag{2.1.15}$$

$$\Upsilon^i{}_{jk} = \frac{1}{2}\gamma^{il}\left[\partial_j \gamma_{lk} + \partial_k \gamma_{jk} - \partial_l \gamma_{jk}\right], \tag{2.1.16}$$

where $\Upsilon^i{}_{jk}$ is the 3-dimensional Christoffel symbol of Σ_t. Another useful example is a^μ which can be equated to,

$$a_\mu = \boldsymbol{n} \cdot \boldsymbol{\nabla} n_\mu = \mathcal{D}_\mu \ln \alpha = \frac{1}{\alpha}\mathcal{D}_\mu \alpha, \tag{2.1.17}$$

and allows us to evaluate the Lie derivative of the projector $\perp^i_j$,

$$\mathcal{L}_m \perp^i_j = \alpha n^k \nabla_k \perp^i_j + \perp^i_k \nabla_j \alpha n^k - \perp^k_j \nabla_k \alpha m^i, \tag{2.1.18}$$

$$= \alpha n^k \nabla_k \left[n^i n_j\right] + \alpha \nabla_j n^i - \left[\alpha \mathcal{K}^i_j + n^i \mathcal{D}_j \alpha\right], \tag{2.1.19}$$

$$= 0. \tag{2.1.20}$$

The result $\mathcal{L}_m \perp^i_j = 0$ is very important, it tells us that the projector commutes with $\mathcal{L}_m$ and as a result any tensor $\boldsymbol{T}$ which when projected onto Σ_t, written $\boldsymbol{\mathcal{T}}$, satisfies

$$\mathcal{L}_m \mathcal{T}^{ij\ldots}{}_{kl\ldots} = \perp^i_\mu \perp^j_\nu \perp^\rho_k \perp^\sigma_l \mathcal{L}_m T^{\mu\nu\ldots}{}_{\rho\sigma\ldots}. \tag{2.1.21}$$

In other words, evolving a projected tensor along integral curves of m leaves the tensor parallel to Σ_t.

2.1.3 Gauss, Codazzi and Ricci Equations

The decomposition of the 4-dimensional curvature tensors into a combination of 3-dimensional curvature tensors and $\boldsymbol{\mathcal{K}}$ is very useful as it captures all the degrees of freedom of the 4-dimensional Riemann tensor in terms of variables on Σ_t. This property is crucial when numerically simulating a single time slice Σ_t as we only have access to variables on Σ_t.

The Gauss Equations

From the definition of the Riemann tensor in section 1.3.4 we know,

$$[\mathcal{D}_i\mathcal{D}_j - \mathcal{D}_j\mathcal{D}_i]v^k = \mathcal{R}^k{}_{mij}v^m, \tag{2.1.22}$$

$$[\nabla_\alpha\nabla_\beta - \nabla_\beta\nabla_\alpha]X^\gamma = R^\gamma{}_{\lambda\alpha\beta}X^\lambda, \tag{2.1.23}$$

where $\boldsymbol{X} \in \mathcal{M}$ and $v^m = \perp^m_\rho v^\rho$ is tangent to Σ_t. Expanding the $\mathcal{D}$'s in terms of ∇'s gives,

$$\mathcal{D}_i\mathcal{D}_j v^k = \perp^\mu_i \perp^\sigma_j \perp^k_\xi \nabla_\mu(\perp^\nu_\sigma \perp^\xi_\rho \nabla_\nu v^\rho), \tag{2.1.24}$$

and using the following properties; impotence of projections $\perp^i_\mu \perp^\mu_j = \perp^i_j$, null projection of orthogonal vectors $\perp(\boldsymbol{n}) = 0$, metric compatibility $\nabla_\mu \perp^i_j = n_j\nabla_\mu n^i + n^i\nabla_\mu n_j$ and Eq. (2.1.10) for $\mathcal{K}_{ij}$ we obtain the Gauss relation,

$$\perp^\mu_i \perp^\nu_j \perp^k_\rho \perp^\sigma_l R^\rho{}_{\sigma\mu\nu} = \mathcal{R}^k{}_{lij} + \mathcal{K}^k_i\mathcal{K}_{lj} - \mathcal{K}^k_j\mathcal{K}_{il}. \tag{2.1.25}$$

Contracting over i, k above and relabelling indices we get the contracted Gauss relation,

$$\perp^\mu_i \perp^\nu_j R_{\mu\nu} + \gamma_{i\mu}n^\nu \perp^\rho_j n^\sigma R^\mu{}_{\nu\rho\sigma} = \mathcal{R}_{ij} + \mathcal{K}\mathcal{K}_{ij} - \mathcal{K}^k_j\mathcal{K}_{ik}. \tag{2.1.26}$$

Contracting again and realising $R_{\mu\nu\rho\sigma}n^\mu n^\nu n^\rho n^\sigma = 0$ from antisymmetry in indices 0 and 1 or 2 and 3 in the Riemann tensor, gives the scalar Gauss equation,

$$R + 2R_{\mu\nu}n^\mu n^\nu = \mathcal{R} + \mathcal{K}^2 - \mathcal{K}_{ij}\mathcal{K}^{ij}. \tag{2.1.27}$$

The Codazzi Equations

The Codazzi relations are derived from a different start point. Instead of projecting the Riemann tensor fully onto Σ_t with projection operators $\perp$ and a spacelike vector $\boldsymbol{v}$, it is now projected with a timelike vector $\boldsymbol{n}$,

$$[\nabla_\alpha\nabla_\beta - \nabla_\beta\nabla_\alpha]n^\gamma = R^\gamma{}_{\lambda\alpha\beta}n^\lambda, \tag{2.1.28}$$

and again projecting to Σ_t with three projection operators. The following relations are used

$$\nabla_j n^k = -\mathcal{K}^k{}_j - a^k n_j, \tag{2.1.29}$$

$$\perp^i_\mu \perp^j_\nu \perp^\rho_k \nabla_i\nabla_j n^k = -\mathcal{D}_i\mathcal{K}^k{}_j + a^k\mathcal{K}_{ij}, \tag{2.1.30}$$

which lead immediately to the Codazzi relation,

$$\perp^\mu_i \perp^\nu_j \perp^k_\rho n^\sigma R^\rho{}_{\sigma\mu\nu} = \mathcal{D}_j\mathcal{K}^k{}_i - \mathcal{D}_i\mathcal{K}^k{}_j, \tag{2.1.31}$$

and the contracted Codazzi relation,

$$\perp^\mu_i n^\nu R_{\mu\nu} = \mathcal{D}_i\mathcal{K} - \mathcal{D}_\mu\mathcal{K}^\mu{}_i. \tag{2.1.32}$$

The Ricci Equation

Finally we turn our attention to the Ricci equation, the projection of the Riemann tensor twice onto Σ_t and twice contracting with $\boldsymbol{n}$. This is done by projecting Eq (2.1.28) with two projectors $\perp$ and one timelike $\boldsymbol{n}$. If we contract with n^γ then the antisymmetry in the first two Riemann tensor indices would identically give to zero, therefore the unique choice (up to a minus sign) is to project with n^β,

$$R_{\gamma\lambda\alpha\beta}n^\lambda n^\beta = n^\beta \left[\nabla_\alpha\nabla_\beta - \nabla_\beta\nabla_\alpha\right] n_\gamma, \tag{2.1.33}$$

and project the remaining free indices with $\perp$ like,

$$\perp_i^\gamma \perp_j^\alpha R_{\gamma\lambda\alpha\beta}n^\lambda n^\beta = \perp_i^\gamma \perp_j^\alpha n^\beta \left[\nabla_\alpha\nabla_\beta - \nabla_\beta\nabla_\alpha\right] n_\gamma. \tag{2.1.34}$$

Rearranging Eqs. (2.1.10) and (2.1.17) we obtain,

$$\nabla_\sigma n_\mu = -\mathcal{K}_{\mu\sigma} - n_\sigma \mathcal{D}_\mu \ln(\alpha), \tag{2.1.35}$$

which can be used to expand the right hand side of Eq. (2.1.36),

$$\begin{aligned}
\perp_i^\gamma \perp_j^\alpha R_{\gamma\lambda\alpha\beta}n^\lambda n^\beta =& \perp_i^\gamma \perp_j^\alpha n^\beta \left[-\nabla_\alpha\mathcal{K}_{\gamma\beta} + \nabla_\beta\mathcal{K}_{\gamma\alpha}\right] && (2.1.36)\\
&+ \perp_i^\gamma \perp_j^\alpha n^\beta \left[-\nabla_\alpha(n_\beta\mathcal{D}_\gamma \ln(\alpha)) + \nabla_\beta(n_\alpha\mathcal{D}_\gamma \ln(\alpha))\right], \\
=& \perp_i^\gamma \perp_j^\alpha n^\beta n^\sigma\nabla_\sigma\mathcal{K}_{\gamma\alpha} + \perp_\gamma^i \perp_j^\alpha \mathcal{K}_{\gamma\beta}\nabla_\alpha n^\beta && (2.1.37)\\
&+ \perp_i^\gamma \perp_j^\alpha n^\beta \left[-n_\beta\nabla_\alpha(\mathcal{D}_\gamma \ln(\alpha)) + n_\alpha\nabla_\beta\mathcal{D}_\gamma \ln(\alpha) + (\mathcal{D}_\gamma \ln(\alpha))\nabla_\beta n_\alpha\right], \\
=& \perp_i^\gamma \perp_j^\alpha n^\beta n^\sigma\nabla_\sigma\mathcal{K}_{\gamma\alpha} - \mathcal{K}_{ik}\mathcal{K}^k{}_j && (2.1.38)\\
&+ \mathcal{D}_j\mathcal{D}_i \ln(\alpha) + \mathcal{D}_i \ln(\alpha)\mathcal{D}_j \ln(\alpha), \\
=& \perp_i^\gamma \perp_j^\alpha n^\beta n^\sigma\nabla_\sigma\mathcal{K}_{\gamma\alpha} - \mathcal{K}_{ik}\mathcal{K}^k{}_j + \frac{1}{\alpha}\mathcal{D}_j\mathcal{D}_i\alpha, && (2.1.39)
\end{aligned}$$

where $\boldsymbol{n}^2 = -1$, $\perp_i^\mu n_\mu = 0$, $\mathcal{D}_\alpha \ln\alpha = n^\beta\nabla_\beta n_\alpha$ from Eq. (2.1.17) and $n^\beta\nabla_\alpha n_\beta = 0$ have been used. This expression can be simplified by calculating the Lie derivative of $\boldsymbol{\mathcal{K}}$,

$$\begin{aligned}
\mathcal{L}_m\mathcal{K}_{ij} =& \perp_i^\mu \perp_j^\nu \mathcal{L}_m\mathcal{K}_{\mu\nu}, && (2.1.40)\\
=& \alpha \perp_i^\mu \perp_j^\nu \mathcal{L}_n\mathcal{K}_{\mu\nu}, && (2.1.41)\\
=& \alpha \perp_i^\mu \perp_j^\nu \left[\alpha\boldsymbol{n}\cdot\boldsymbol{\nabla}\mathcal{K}_{\mu\nu} + 2\mathcal{K}_{k(\nu}\nabla_{\mu)}n^k\right], && (2.1.42)\\
=& \alpha \perp_i^\mu \perp_j^\nu n^\sigma\nabla_\sigma\mathcal{K}_{\mu\nu} - 2\alpha\mathcal{K}_{ik}\mathcal{K}^k{}_j, && (2.1.43)
\end{aligned}$$

where the results $\mathcal{L}_m\boldsymbol{\mathcal{K}} = \alpha\mathcal{L}_n\boldsymbol{\mathcal{K}}$ from Eq. (2.1.12), $\mathcal{L}_m\mathcal{K}_{\alpha\beta} \in \Sigma_t$ from Eq. (2.1.21) and Eq. (2.1.10) have been used. Putting everything together we arrive at the Ricci equation,

$$\perp_i^\mu \perp_j^\nu n^\rho n^\sigma R_{\mu\rho\nu\sigma} = \frac{1}{\alpha}\mathcal{L}_m\mathcal{K}_{ij} + \frac{1}{\alpha}\mathcal{D}_j\mathcal{D}_i\alpha + \mathcal{K}_{ik}\mathcal{K}^k{}_j. \tag{2.1.44}$$

This is the final contraction of the Riemann tensor that can be made with $\perp$ and $\boldsymbol{n}$ as any projections with three or more contractions with $\boldsymbol{n}$ would identically give zero due to the symmetries of the Riemann tensor.

2.1.4 Decomposition of Einstein's Equation

To evolve General Relativity numerically we must project the Einstein Equation into 3+1 dimensions. Relations between three and four dimensional geometric objects have been derived above and will be used to decompose the Einstein tensor $G_{\mu\nu} = R_{\mu\nu} - g_{\mu\nu}R/2$ from the left hand side of Eq. (2.1.1). The second component, for simulating non-vacuum spacetimes, is the 3+1 decomposition of the Stress tensor

T_{ab}. We contract twice with $\boldsymbol{n}$, then once with $\boldsymbol{n}$ while projecting onto Σ_t and finally twice projecting onto Σ_t to get an energy, momentum and stress-like split,

$$\rho = \boldsymbol{T}(\boldsymbol{n}, \boldsymbol{n}) = T_{\mu\nu} n^\mu n^\nu, \tag{2.1.45}$$

$$\mathcal{S}_i = -\perp_i^\mu n^\nu T_{\mu\nu}, \tag{2.1.46}$$

$$\mathcal{S}_{ij} = \perp_i^\mu \perp_j^\nu T_{\mu\nu}, \tag{2.1.47}$$

and by construction,

$$T_{\mu\nu} = \rho n_\mu n_\nu + \mathcal{S}_\mu n_\nu + \mathcal{S}_\nu n_\mu + \mathcal{S}_{\mu\nu}. \tag{2.1.48}$$

With this and the Gauss-Codazzi equations of section 2.1.3 we can project the Einstein equation. Let us first look at the scalar equation,

$$G_{\mu\nu} n^\mu n^\nu = R_{\mu\nu} n^\mu n^\nu + \frac{1}{2} R = 8\pi\rho, \tag{2.1.49}$$

and equating the geometric terms to the scalar Gauss equation we get the Hamiltonian constraint, $\mathcal{H} = 0$,

$$\mathcal{H} = \mathcal{K}_{\mu\nu}\mathcal{K}^{\mu\nu} - \mathcal{K}^2 - \mathcal{R} + 16\pi\rho = 0. \tag{2.1.50}$$

Now looking at the mixed space-time projected part we see,

$$\perp_i^\mu n^\nu G_{\mu\nu} = \perp_i^\mu n^\nu R_{\mu\nu} = -8\pi\mathcal{S}_i, \tag{2.1.51}$$

and substituting the geometric terms for the contracted Codazzi relation we get the momentum constraint, $\mathcal{M}_i = 0$,

$$\mathcal{M}_i = \mathcal{D}_i\mathcal{K} - \mathcal{D}_j\mathcal{K}_i^j + 8\pi\mathcal{S}_i = 0. \tag{2.1.52}$$

Finally, the space-space projection gives the 6 evolution PDEs. This time start with the trace reversed Einstein Equation

$$R_{\mu\nu} = 8\pi \left[T_{\mu\nu} - \frac{1}{2} T g_{\mu\nu} \right], \tag{2.1.53}$$

$$\perp_i^\mu \perp_j^\nu R_{\mu\nu} = 8\pi \left[\mathcal{S}_{ij} - \frac{1}{2}(\mathcal{S} - \rho)\gamma_{ij} \right], \tag{2.1.54}$$

where we used $T = \left[\gamma^{\mu\nu} - n^\mu n^\nu\right] T_{\mu\nu} = \mathcal{S} - \rho$. When projecting the Ricci tensor, we use the contracted Gauss equation but replace the term with $R^\mu{}_{\nu\rho\sigma}$ with the Ricci equation (2.1.44). Rearranging gives a normal evolution for the extrinsic curvature,

$$\mathcal{L}_m \mathcal{K}_{ij} = -\mathcal{D}_j\mathcal{D}_i\alpha + \alpha \left[\mathcal{R}_{ij} + \mathcal{K}\mathcal{K}_{ij} - 2\mathcal{K}_i^k\mathcal{K}_{kj} + 4\pi \left[\gamma_{ij} \left[\mathcal{S} - \rho \right] - 2\mathcal{S}_{ij} \right] \right]. \tag{2.1.55}$$

Along with the definition of $\mathcal{K}_{ij}$ in Eq. (2.1.12),

$$\mathcal{L}_m \gamma_{ij} = -2\alpha\mathcal{K}_{ij}, \tag{2.1.56}$$

this gives the normal evolution equations for γ_{ij} and $\mathcal{K}_{ij}$. In 4 or n spacetime dimensions the normal evolution equations contain 6 or $\frac{n^2-n}{2}$ differential equations. The Hamiltonian constraint is a single differential equation, the momentum constraint contains 3 or $n-1$ differential equations and the Einstein equation contains 10 or $\frac{n^2+n}{2}$ differential equations. In four spacetime dimensions this corresponds to 6 evolution equations and 4 constraint equations over the surface Σ_t.

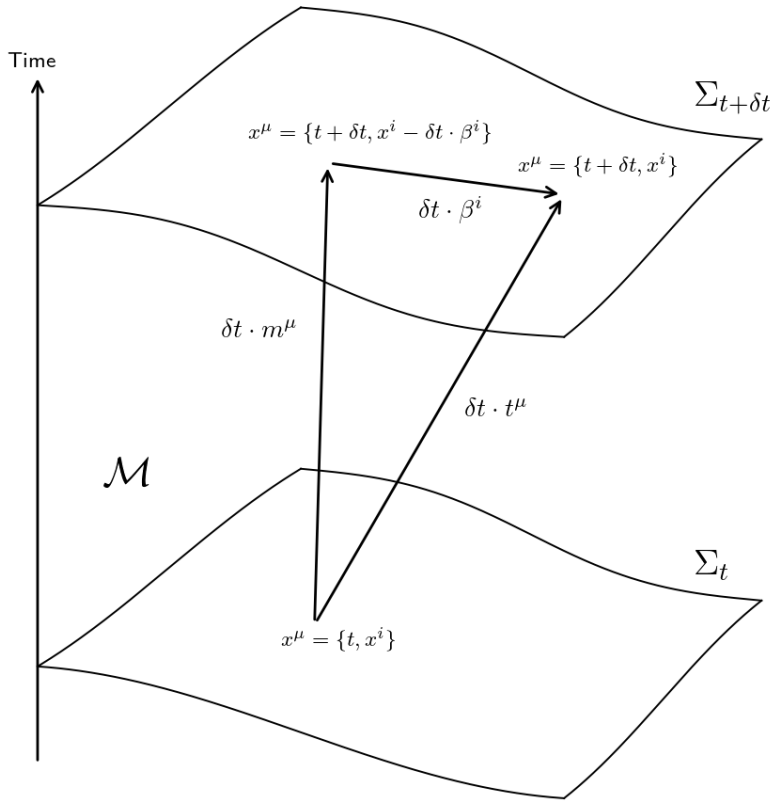

Figure 2.1: An illustration of two hypersurfaces Σ_t and $\Sigma_{t+\delta}$ and how they are connected by m^μ. As can be seen, integral curves of t^μ have constant spatial coordinates x^i.

2.1.5 Foliation Adapted Coordinates

Picking coordinates in general relativity introduces a gauge freedom which allows us to use a level set of the time coordinate $x^0 = t$ to define our foliation hypersurfaces Σ_t. The other three coordinates x^i for $i \in [1, 2, 3]$ can be used to span each hypersurface Σ_t however we define. It is conventional to split the normal evolution vector m^μ into time t^μ and space parts β^μ,

$$t^\mu = (1, 0, 0, 0)\,, \tag{2.1.57}$$

$$\beta^\mu = \left(0, \beta^1, \beta^2, \beta^3\right), \tag{2.1.58}$$

such that,

$$m^\mu = t^\mu - \beta^\mu = (\partial_0)^\mu - \beta^i(\partial_i)^\mu, \tag{2.1.59}$$

$$m^\mu = \left(1, -\beta^1, -\beta^2, -\beta^3\right). \tag{2.1.60}$$

We can view t^μ as the (not necessarily causal) worldline for a simulation gridpoint, hence we would like to evolve our PDEs along t^μ on a computer. In other words, integral curves of t^μ must have constant spatial coordinates on Σ_t. Equation (2.1.60), along with the definitions $\boldsymbol{m} = \alpha \boldsymbol{n}$ and $\boldsymbol{n}^2 = -1$, specifies n^μ and n_μ,

$$n^\mu = \frac{1}{\alpha}\left(1, -\beta^1, -\beta^2, -\beta^3\right), \tag{2.1.61}$$

$$n_\mu = -\alpha\,(1, 0, 0, 0)\,. \tag{2.1.62}$$

The decomposed metric can be calculated, using the property that $\boldsymbol{\beta}$ is tangent to Σ_t and orthogonal to $\boldsymbol{m}$,

$$g_{00} = \boldsymbol{g}(\boldsymbol{\partial}_0, \boldsymbol{\partial}_0) = \boldsymbol{g}(\boldsymbol{m} + \beta^i \boldsymbol{\partial}_i, \boldsymbol{m} + \beta^j \boldsymbol{\partial}_j) = \boldsymbol{g}(\boldsymbol{m}, \boldsymbol{m}) + \beta^i \beta_j \langle \boldsymbol{\partial}_i, \mathbf{d}\boldsymbol{x}^j \rangle = -\alpha^2 + \beta^i \beta_i, \tag{2.1.63}$$

$$g_{0i} = \boldsymbol{g}(\boldsymbol{\partial}_0, \boldsymbol{\partial}_i) = \boldsymbol{g}(\boldsymbol{m} + \beta^j \boldsymbol{\partial}_j, \boldsymbol{\partial}_i) = \beta^j \boldsymbol{g}(\boldsymbol{\partial}_j, \boldsymbol{\partial}_i) = \beta_i, \tag{2.1.64}$$

$$g_{ij} = \boldsymbol{g}(\boldsymbol{\partial}_i, \boldsymbol{\partial}_j) = \boldsymbol{\gamma}(\boldsymbol{\partial}_i, \boldsymbol{\partial}_j) = \gamma_{ij}. \tag{2.1.65}$$

This is commonly called the $3+1$ Arnowitt-Deser-Misner (ADM) metric and α, β^i are referred to as the lapse and shift vector in this context. The line element and metric are commonly written as,

$$\mathrm{d}s^2 = -\alpha^2 \mathrm{d}t^2 + \gamma_{ij} \left[\mathrm{d}x^i + \beta^i \mathrm{d}t\right] \left[\mathrm{d}x^j + \beta^j \mathrm{d}t\right], \tag{2.1.66}$$

$$g_{\mu\nu} = \begin{pmatrix} -\alpha^2 + \beta^i \beta_i & \beta_i \\ \beta_j & \gamma_{ij} \end{pmatrix}, \tag{2.1.67}$$

$$g^{\mu\nu} = \frac{1}{\alpha^2} \begin{pmatrix} -1 & \beta^i \\ \beta^j & \alpha^2 \gamma^{ij} - \beta^i \beta^j \end{pmatrix}, \tag{2.1.68}$$

and using Cramer's rule for metric determinant,

$$g^{00} = \frac{\det\{\gamma_{ij}\}}{\det\{g_{\mu\nu}\}}, \tag{2.1.69}$$

we get the important relationship,

$$\sqrt{-g} = \alpha \sqrt{\gamma}, \tag{2.1.70}$$

where g and γ are the determinants of $g_{\mu\nu}$ and γ_{ij} respectively.

2.1.6 ADM Equations

Now that we have some coordinates suitable for the spacetime foliation we can find the Arnowitt-Deser-Misner (ADM) evolution equations for $\mathcal{K}_{ij}$ and γ_{ij}. First simplifying the Lie derivative $\mathcal{L}_t$ along t^μ using,

$$\mathcal{L}_t \boldsymbol{T} = \partial_t \boldsymbol{T}, \tag{2.1.71}$$

for any tensor $\boldsymbol{T}$ as $\partial_\nu t^\mu = 0$. This can be used to expand the Lie derivative along m^μ,

$$\mathcal{L}_m = \mathcal{L}_t - \mathcal{L}_\beta = \partial_t - \mathcal{L}_\beta, \tag{2.1.72}$$

and the ADM equations can be written by substituting $\mathcal{L}_m \to \partial_t - \mathcal{L}_\beta$ in the normal evolution equations in section 2.1.4 for $\boldsymbol{\mathcal{K}}$ and $\boldsymbol{\gamma}$. The ADM equations are,

$$\partial_t \mathcal{K}_{ij} = \mathcal{L}_\beta \mathcal{K}_{ij} - \mathcal{D}_j \mathcal{D}_i \alpha + \alpha \left[\mathcal{R}_{ij} + \mathcal{K}\mathcal{K}_{ij} - 2\mathcal{K}_i^k \mathcal{K}_{kj} + 4\pi \left[\gamma_{ij} \left[\mathcal{S} - \rho\right] - 2\mathcal{S}_{ij}\right]\right], \tag{2.1.73}$$

$$\partial_t \gamma_{ij} = \mathcal{L}_\beta \gamma_{ij} - 2\alpha \mathcal{K}_{ij}. \tag{2.1.74}$$

Unfortunately, these PDEs turn out to be ill-posed [8]; this means that the time evolution of these equations does not generally depend smoothly on the initial data.

2.1.7 BSSN

To tackle the ill-posedness of the ADM equations in section 2.1.6 we now discuss the Baumgarte-Shapiro-Shibata-Nakamura (BSSN) formalism [9] The first step in BSSN is to decompose the 3-metric into the conformal metric $\tilde{\gamma}_{ij}$ and the conformal factor χ,

$$\tilde{\gamma}_{ij} = \chi \gamma_{ij}, \tag{2.1.75}$$

$$\det\{\tilde{\gamma}_{ij}\} = \tilde{\gamma} = \chi^3 \gamma = 1, \tag{2.1.76}$$

with the above being the convention used in GRChombo described in section 3.2.1. Other conventions include factors such as $\tilde{\gamma}_{ij} = \psi^{-4}\gamma_{ij}$ or $\tilde{\gamma}_{ij} = e^{-\phi}\gamma_{ij}$. Along with this the extrinsic curvature $\mathcal{K}_{ij}$ is conformally decomposed with χ and modified to be trace free,

$$\tilde{A}_{ij} = \chi\left[\mathcal{K}_{ij} - \frac{1}{3}\mathcal{K}\gamma_{ij}\right], \tag{2.1.77}$$

so that $\tilde{A}_{ij}\gamma^{ij} = 0$. During an evolution the condition $\mathrm{tr}\,\tilde{A}_{ij} = 0$ (and soemtimes $\tilde{\gamma} = 1$) is enforced which is observed to improve numerical stability; it is unclear why this works beyond heuristic arguments. As discussed later in section 2.1.10, the definition of $\chi = \gamma^{-1/3}$ is good for black hole simulations where $\gamma \to \infty$ but $\chi \to 0$. For example the isotropic Schwarzschild metric has,

$$\gamma = \left[1 + \frac{M}{2r}\right]^{12}, \tag{2.1.78}$$

$$\chi = \left[\frac{r}{\frac{M}{2} + r}\right]^{4}. \tag{2.1.79}$$

The next step is to introduce the conformal connection functions as auxiliary variables,

$$\tilde{\Upsilon}^{i} = \tilde{\gamma}^{jk}\tilde{\Upsilon}^{i}{}_{jk} = -\partial_i\tilde{\gamma}^{ij}, \tag{2.1.80}$$

$$\tilde{\Upsilon}^{i}{}_{jk} = \frac{1}{2}\tilde{\gamma}^{il}\left[\partial_j\tilde{\gamma}_{kl} + \partial_k\tilde{\gamma}_{lj} - \partial_l\tilde{\gamma}_{jk}\right] = \Upsilon^{i}{}_{jk} + \left[\delta^{i}_{j}\partial_k + \delta^{i}_{k}\partial_j - \gamma^{il}\gamma_{jk}\partial_l\right]\ln\sqrt{\chi}, \tag{2.1.81}$$

where $\Gamma^{i}{}_{jk}$ are the Christoffel symbols of Σ_t as shown in Eq. (2.1.16). This reduces the set of vacuum evolution variables to $\{\chi, \tilde{\gamma}_{ij}, \mathcal{K}, \tilde{\mathcal{A}}_{ij}, \tilde{\Upsilon}^{i}\}$. It is conventional to use $-\partial_i\tilde{\gamma}^{ij}$ to evaluate the conformal connection coefficients when they appear in the RHS of an equation, but $\partial_j\tilde{\Upsilon}^{i}$ is calculated by differentiating the evolution variable $\tilde{\Upsilon}^{i}$. One final necessity, not included in the CCZ4 formulation discussed later, is to add multiples of the constraint equations (in section 2.1.4) to the evolution equations to change the characteristic matrix and improve stability.

The BSSN formalism is not the only way to find a well-posed set of evolution equations for general relativity. Another strongly hyperbolic formalism is the generalised harmonic gauge [10] [11] [12] [13] with,

$$\Box x^{\mu} = H^{\mu}, \tag{2.1.82}$$

for some functions H^{μ}.

2.1.8 Z4 Formalism

The Z4 formalism [14] generalises the Einstein equation to include an unphysical field Z_μ, along with damping terms parameterised by κ_1, κ_2,

$$R_{\mu\nu} + \nabla_\mu Z_\nu + \nabla_\nu Z_\mu - \kappa_1\left[n_\mu Z_\nu + n_\nu Z_\mu - [1+\kappa_2]g_{\mu\nu}n^{\alpha}Z_\alpha\right] = 8\pi G\left[T_{\mu\nu} - \frac{1}{2}Tg_{\mu\nu}\right]. \tag{2.1.83}$$

Of course regular General Relativity is recovered by setting $Z_\mu = 0$. It can be shown that achieving $Z_\mu = 0$ whilst dynamically evolving Z_μ is equivalent to solving the constraints. Z_μ is subjected to a wave equation, transporting constraint violation off the computational domain. It can be shown that the system is driven to $Z_\mu = 0$ for $k_1 > 0$ and $k_2 < -1$. It is much cheaper to evolve the variables Z_μ, driven to zero, than to solve four elliptic PDEs for the constraints $\{\mathcal{H}, \mathcal{M}^{i}\}$ on each timestep.

2.1.9 CCZ4

Merging the conformal decomposition of the BSSN formalism with the constraint damping Z4 formalism gives the conformal covariant Z4 (CCZ4) formalism. The additional modifications,

$$\Theta = -n \cdot Z = -\alpha Z^0, \tag{2.1.84}$$

$$\hat{\Upsilon}^i = \tilde{\Upsilon}^i + \frac{2\gamma^{ij} Z_j}{\chi}, \tag{2.1.85}$$

are made, leaving us with the following set of vacuum evolution variables $\{\chi, \tilde{\gamma}_{ij}, \mathcal{K}, \tilde{\mathcal{A}}_{ij}, \hat{\Upsilon}^i, \Theta\}$. Notably the pair of variables $\mathcal{R}_{ij} + \mathcal{D}_{(i} Z_{j)}$ and its traced version $\mathcal{R} + \boldsymbol{\mathcal{D}} \cdot \boldsymbol{Z}$, always appear together; separately they would ruin strong hyperbolicity but together they do not. The evolution equations can now be found in the CCZ4 scheme by applying a 3+1 decomposition to the Z4 modified Einstein equation (2.1.83) and proceding as in the BSSN formalism. To illustrate this, we derive the equation of motion for χ in the CCZ4 formalism. Using Eqs. (1.3.118) and (2.1.56) with $\chi^{-3} = \gamma$ we obtain,

$$\mathcal{L}_m \gamma = \gamma \gamma^{ij} \mathcal{L}_m \gamma_{ij} = -2\gamma\alpha\gamma^{ij}\mathcal{K}_{ij} = -2\gamma\alpha\mathcal{K}. \tag{2.1.86}$$

This can be used to simplify the Lie derivative of χ,

$$\mathcal{L}_m \chi = \mathcal{L}_{\partial_t} \chi - \mathcal{L}_\beta \chi, \tag{2.1.87}$$

$$= (\partial_t)^i \partial_i \chi + \omega\chi\partial_i (\partial_t)^i - \beta^i \partial_i \chi - \omega\chi\partial_i\beta^i, \tag{2.1.88}$$

$$= \partial_t \chi - \beta^i \partial_i \chi + \frac{2}{3}\chi\partial_i\beta^i, \tag{2.1.89}$$

$$\mathcal{L}_m \chi = \mathcal{L}_m \gamma^{-\frac{1}{3}}, \tag{2.1.90}$$

$$= -\frac{1}{3}\gamma^{-\frac{4}{3}} \mathcal{L}_m \gamma, \tag{2.1.91}$$

$$= \frac{2}{3}\gamma^{-\frac{1}{3}}\alpha\mathcal{K}, \tag{2.1.92}$$

$$= \frac{2}{3}\chi\gamma\alpha\mathcal{K}, \tag{2.1.93}$$

where Eq. (1.3.31) has been used with $\boldsymbol{\mathcal{T}} = \chi$ as χ is a scalar density of weight $\omega = -2/3$. Re-arranging gives the equation of motion for χ,

$$\partial_t \chi = \beta^i \partial_i \chi + \frac{2\chi}{3}\left[\alpha\mathcal{K} - \partial_i\beta^i\right]. \tag{2.1.94}$$

A similar process returns the remaining CCZ4 equations but care should be taken to include the Z4 terms $(\Theta, \hat{\Upsilon}^i)$ where they are needed. The complete list of CCZ4 equations used in simulations with

GRChombo (section 3.2.1) are given below:

$$\partial_t \chi = \beta^i \partial_i \chi + \frac{2\chi}{3}\left[\alpha \mathcal{K} - \partial_i \beta^i\right], \tag{2.1.95}$$

$$\partial_t \tilde{\gamma}_{ij} = \beta^k \partial_k \tilde{\gamma}_{ij} + \tilde{\gamma}_{kj}\partial_i \beta^k + \tilde{\gamma}_{ik}\partial_j \beta^k - \frac{2}{3}\tilde{\gamma}_{ij}\partial_k \beta^k - 2\alpha \tilde{\mathcal{A}}_{ij}, \tag{2.1.96}$$

$$\begin{aligned}\partial_t \mathcal{K} = {} & \beta^k \partial_k \mathcal{K} + \alpha\left[\mathcal{R} + 2\boldsymbol{\mathcal{D}}\cdot\boldsymbol{Z} + \mathcal{K}\left[\mathcal{K} - 2\Theta\right]\right] - 3\alpha\kappa_1\left[1+\kappa_2\right]\Theta \\ & - \chi\tilde{\gamma}^{kl}\mathcal{D}_k\mathcal{D}_l\alpha + 4\pi G\alpha\left[\mathcal{S} - 3\rho\right],\end{aligned} \tag{2.1.97}$$

$$\begin{aligned}\partial_t \tilde{\mathcal{A}}_{ij} = {} & \beta^k \partial_k \tilde{\mathcal{A}}_{ij} + \chi\left[\alpha\left[\mathcal{R}_{ij} + 2\mathcal{D}_{(i}Z_{j)} - 8\pi G\mathcal{S}_{ij}\right] - \mathcal{D}_i\mathcal{D}_j\alpha\right]^{TF} \\ & + \tilde{\mathcal{A}}_{ij}\left[\alpha\left[\mathcal{K} - 2\Theta\right] - \frac{2}{3}\mathcal{K}^2\right] + 2\tilde{\mathcal{A}}_{k(i}\partial_{j)}\beta^k - 2\alpha\tilde{\gamma}^{kl}\tilde{\mathcal{A}}_{ik}\tilde{\mathcal{A}}_{lj},\end{aligned} \tag{2.1.98}$$

$$\partial_t \Theta = \beta^k \partial_k \Theta + \frac{1}{2}\alpha\left[\mathcal{R} + 2\boldsymbol{\mathcal{D}}\cdot\boldsymbol{Z} - \tilde{\mathcal{A}}_{kl}\tilde{\mathcal{A}}^{kl} + \frac{2}{3}\mathcal{K}^2 - 2\Theta\mathcal{K}\right] - \kappa_1\alpha\Theta\left[2+\kappa_2\right] - Z^k\partial_k\alpha - 8\pi G\alpha\rho, \tag{2.1.99}$$

$$\begin{aligned}\partial_t \hat{\Upsilon}^i = {} & \beta^k\partial_k\hat{\Upsilon}^i + \frac{2}{3}\left[\partial_k\beta^k\left[\tilde{\Upsilon}^i + 2\kappa_3\frac{Z^i}{\chi}\right] - 2\alpha\mathcal{K}\frac{Z^j}{\chi}\right] - 2\alpha\kappa_1\frac{Z^i}{\chi} \\ & + 2\tilde{\gamma}^{ij}\left[\alpha\partial_j\Theta - \Theta\partial_j\alpha\right] - 2\tilde{\mathcal{A}}^{ij}\partial_j\alpha - \alpha\left[\frac{4}{3}\tilde{\gamma}^{ij}\partial_j\mathcal{K} + 3\tilde{\mathcal{A}}^{ij}\frac{\partial_j\chi}{\chi}\right] \\ & - \left[\tilde{\Upsilon}^j + 2\kappa_3\frac{Z^j}{\chi}\right]\partial_j\beta^i + 2\alpha\tilde{\Upsilon}^i{}_{jk}\tilde{\mathcal{A}}^{jk} + \tilde{\gamma}^{jk}\partial_j\partial_k\beta^i + \frac{1}{3}\tilde{\gamma}^{ij}\partial_k\partial_j\beta^k - 16\pi G\alpha\tilde{\gamma}^{ij}\mathcal{S}_j,\end{aligned} \tag{2.1.100}$$

$$\partial_t\varphi = \beta^k\partial_k\varphi - \alpha\Pi,. \tag{2.1.101}$$

In the CCZ4 equations there is an additional parameter κ_3 premultiplying terms in the evolution of $\hat{\Upsilon}^i$ which experimentally were found to lead to instabilities in black hole simulations [15]. Setting $\kappa_3 < 1$ stabilises the simulation but at the cost of covariance. Later on it was realised that setting $\kappa_3 = 1$ and $\alpha\kappa_1 \to \kappa_1$ retains covariance as well as numerical stability **??**.

The CCZ4 scheme proves several benefits.

- Any initial data that does not satisfy the constraints will generally not do so during evolution when using the BSSN formalism either. Given that superposition of solutions in GR does not generally give a new solution, but does approximate one for separated compact objects, all the simulated binaries considered in this work will have non constraint satisfying initial data.
- The use of the CCZ4 scheme will also help simulations continue to satisfy the constraints even if they do initially satisfy them; one reason being that finite resolution imposes some small deviation from the continuum solution. More importantly, the use of adaptive mesh refinement (discussed in section 3.2.1) introduces interpolation errors into the simulation at the boundary of the different grid resolution levels.
- Sommerfeld boundary conditions (discussed in section 3.1.2) used are inexact in GR and will introduce errors at the outer boundary that ruin constraint satisfaction.

In all the cases above, the CCZ4 system forces the evolution towards constraint satisfaction, despite the numerical errors and approximations. There is a caveat, even if a simulation satisfies the constraints, there is no guarentee it is the desired solution to Einstein's equation.

2.1.10 Gauge Conditions

The lapse α and shift β^i are freely specifiable on a hypersurface Σ_t being gauge variables, however they must be chosen carefully along with a suitable initial Cauchy surface Σ_{t_0} and initial data. Σ_{t_0} should be a smooth non-intersecting Cauchy surface as described in section 2.1.1 and contain smooth initial

data. It is also wise to avoid singularities (both coordinate and physical) on this surface. As an example, consider the simulation of a single Schwarzschild black hole. Figure 2.2 (left) shows how an initial Cauchy surface could extend to the singularity for ingoing Eddington-Finkelstein coordinates. In this work Σ_{t_0} is chosen to be in the isotropic gauge as in figure 2.2 (right); not only does this allow trivial swapping between spherical polar and Cartesian (used in simulations) coordinates but also provides an initial Cauchy surface free of physical singularities and easy to compute. However, for a poor choice of lapse function, even a well chosen Σ_{t_0} can advance to the physical singularity in finite simulation time.

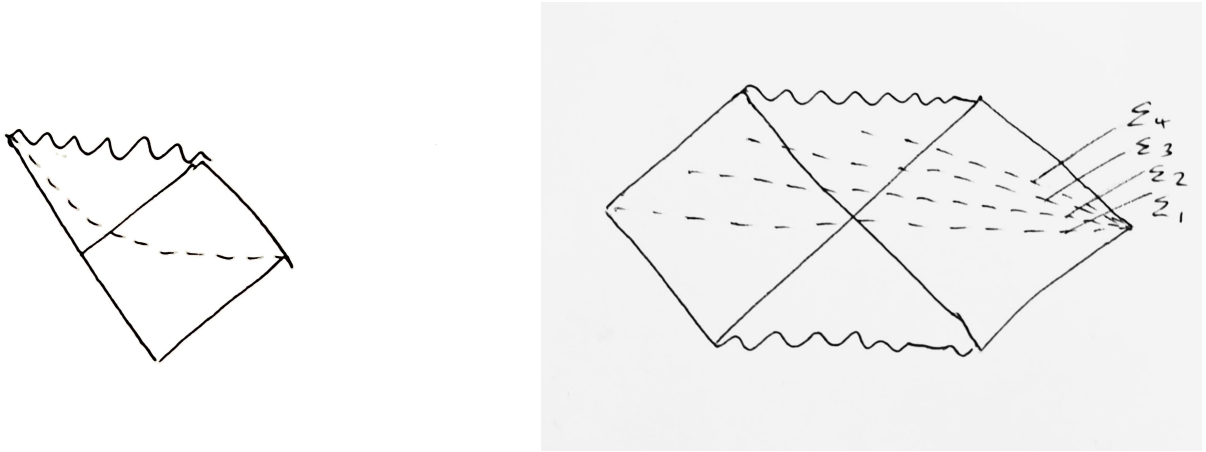

Figure 2.2: Penrose Diagrams, Σ_{t_0} dashed, Left: Ingoing Eddington-Finkelstein Coordinates, Right: Isotropic Coordinates.

Lapse Slicing Conditions

The simplest lapse choice would be to enforce $\alpha = 1$, called geodesic slicing, with the hypersurface following integral curves of n^μ; given that geodesics can converge this can lead to hypersurface self-intersection which breaks the definition of a Cauchy surface and the simulation will likely fail. Another problem is that a black hole singularity can be reached in finite simulation time.

An alternative slicing condition is the maximal slicing condition which keeps the volume element $\sqrt{-g}$ constant along geodesics. This means as $\gamma \to \infty$ nearing a singularity $\alpha \to 0$ from Eq. (2.1.70), causing the hypersurface to advance more slowly before a singularity is reached as demonstrated in Fig. (2.3). This property is called singularity avoiding and is crucial for numerical stability unless using excision[1]. Maximal slicing can be implemented by forcing $\mathcal{K} = \partial_t \mathcal{K} = 0 \, \forall \, t$ which requires a slow elliptic solve for α at each timestep. Instead of performing this slow elliptic solve, α is promoted to an evolution variable and is evolved along with every other simulation variable. To do this we can pick an algebraic slicing condition of the Bona-Masso type,

$$\mathcal{L}_m \alpha = \partial_t \alpha - \beta^i \partial_i \alpha = -\alpha^2 f(\alpha) \mathcal{K}. \tag{2.1.102}$$

Using this with $f = 2\alpha^{-1}$ gives,

$$\mathcal{L}_m \alpha = \partial_t \alpha - \beta^i \partial_i \alpha = -2\alpha \mathcal{K}, \tag{2.1.103}$$

which is called 1+log slicing; this is very common in Numerical Relativity codes. In practice 1+log slicing is strongly singularity avoiding reaching $\alpha = 0$ before the singularity. This is modified in the CCZ4 scheme to,

$$\partial_t \alpha = -2\alpha \left[\mathcal{K} - 2\Theta \right] + \beta^i \partial_i \alpha. \tag{2.1.104}$$

[1]Excision is the practice of cutting singularities out of the computational domain while supplying suitable boundary conditions about the excised region

Using Gaussian normal coordinates $\beta^i = 0$ and provided $\Theta = 0$, the 1+log slicing condition reduces to,

$$\alpha = 1 + \ln \gamma, \tag{2.1.105}$$

giving the slicing condition it's name [16].

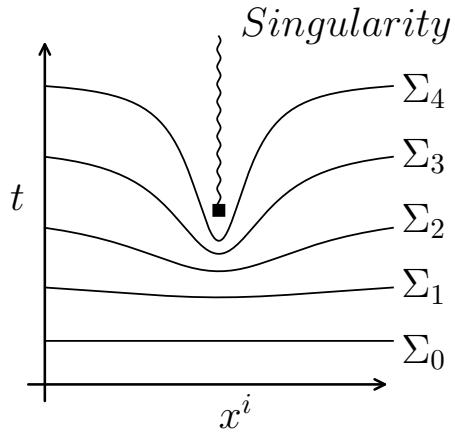

Figure 2.3: Diagram showing the time evolution of a hypersurface using a singularity avoiding slicing condition. The vertical squiggled line represents a physical singularity that is formed at some point in spacetime, potentially from the collapse of matter to a black hole.

Shift Conditions

The simplest choice for the shift vector would be $\beta^i = 0$ but this can cause great stretching and shearing of integral curves of m^μ in the neighbourhood of a singularity as in Fig. (2.3); the effect of this is that neighbouring gridpoints may have large differences in field values leading to inaccurate and unstable evolutions.

Another negative side effect is that the computational domain can fall inside an event horizon in black hole simulations. To counteract this we want to employ a shift vector that minimises hypersurface shear σ_{ij} which can be defined as [17],

$$\sigma_{ij} := \perp_i^\mu \perp_j^\nu \left[\nabla_{(\mu} n_{\nu)} - \frac{1}{3} \gamma^{ab} \nabla_{(a} n_{b)} \gamma_{\mu\nu} \right], \tag{2.1.106}$$

where σ_{ij} is tracefree corresponding to shearing rather than inflation or expansion. Minimising the total shear Σ,

$$\Sigma = \int \sigma_{ij} \sigma^{ij} \sqrt{\gamma} \, \mathrm{d}x^3, \tag{2.1.107}$$

with respect to β^i leads to an elliptic PDE to be solved for each β^i at each time step that minimises shear,

$$\delta\Sigma = 0 \rightarrow \mathcal{D}_i \sigma^{ij} = 0. \tag{2.1.108}$$

This is known as the minimal distortion shift condition. Promoting the β^i to evolution variables is computationally cheaper than solving a set of PDEs at each time step. A very common choice is to promote the elliptic PDE for β^i into a hyperbolic equation via introducing a $\partial_t^2 \beta^i$ term and an artificial damping term parameterised by η. This becomes a damped wave equation and is supposed to transport

away any part of β^i which does not satisfy $\mathcal{D}_i \sigma^{ij} = 0$. This works well with Sommerfeld (outgoing wave) boundary conditions given in section 3.1.2. The standard Gamma driver shift condition is,

$$\partial_t \beta^i = F B^i, \tag{2.1.109}$$

$$\partial_t B^i = \partial_t \tilde{\Gamma}^i - \eta B^i, \tag{2.1.110}$$

where $F = 3/4$ and $\eta = 1$ are used throughout this work.

Moving Puncture Gauge

The moving puncture gauge is the combination of the 1+log slicing lapse condition in Eq. (2.1.103) and the Gamma driver shift condition in Eqs. (2.1.109) and (2.1.110). In 2006, the moving puncture gauge allowed for the first successful simulation of a back hole binary [18] in the CCZ4 formalism[2] without the use of excision. Even though $\chi \to 0$, or $\gamma \to \infty$, at the centre of a black hole, as long as a minimum value for χ (such as $\chi = 10^{-4}$) is enforced a simulation can run. Even thought it is unphysical to modify a physical variable, any errors caused by this are localised to well within the event horizon and as a result do not propagate away from the puncture.

Not only does the moving puncture gauge safeguard the divergence of fields at the puncture, but it allows the puncture to move; hence the name *moving* puncture gauge. Near the puncture, the lapse α becomes vanishingly small and the 1+log slicing condition in Eq. (2.1.103) becomes,

$$\partial_t \alpha = \beta^i \partial_i \alpha, \tag{2.1.111}$$

which causes the puncture to move. Assigning spatial coordinates $x^i_{\text{punc}}(t)$ to the puncture, we know that

$$\alpha(x^i_{\text{punc}}) = 0, \tag{2.1.112}$$

$$\frac{\mathrm{d}}{\mathrm{d}t}\alpha(x^i_{\text{punc}}) = \frac{\partial}{\partial t}\alpha + \left(\left.\frac{\partial x^i}{\partial t}\right|_{x^i = x^i_{\text{punc}}} \right) \frac{\partial}{\partial x^i}\alpha = 0, \tag{2.1.113}$$

which can be compared to Eq. (2.1.111) to show that

$$\beta^i = -\frac{\partial}{\partial t} x^i_{\text{punc}}\,. \tag{2.1.114}$$

This shows that the puncture must move along integral curves of $-\beta^i$.

[2]It should be noted that a black-hole binary had been sucessfully simulated before by [19] in 2003 with co-rotating coordinates and [13] in 2005 using the generalised harmonic gauge.

2.2 Mathematical Modelling of Boson Stars

2.2.1 The Action

The Boson Stars considered are a complex Klein Gordon Scalar field, φ, minimally coupled to gravity. The action is the Einstein-Hilbert vacuum action plus the matter action for curved space,

$$S = \int_{\mathcal{M}} [\mathcal{L}_{EH} + \mathcal{L}_M] \sqrt{-g}\, \mathrm{d}x^4, \tag{2.2.1}$$

$$\mathcal{L}_{EH} = \frac{c^4}{16\pi G} R, \tag{2.2.2}$$

$$\mathcal{L}_M = -\frac{1}{2} g^{\mu\nu} \nabla_\mu \varphi^* \nabla_\nu \varphi - \frac{1}{2} V(|\varphi|^2), \tag{2.2.3}$$

Here V is the Klein-Gordon potential and it's effect on boson stars is discussed in [20] [21]. Some common choices of potentials are,

$$V_{\text{mini}} = \frac{m^2 c^2}{\hbar^2} |\varphi|^2, \tag{2.2.4}$$

$$V_{\text{int}} = \frac{m^2 c^2}{\hbar^2} |\varphi|^2 + \frac{1}{2} \Lambda_4 |\varphi|^4, \tag{2.2.5}$$

$$V_{\text{soli}} = \frac{m^2 c^2}{\hbar^2} |\varphi|^2 \left(1 - \frac{|\varphi|^2}{2\sigma^2}\right)^2, \tag{2.2.6}$$

where $\hbar$ and c are given for completeness but will be set to unity later. Considering only the m^2 term, which corresponds to the squared mass of the particle in the quantum theory, we get a massive wave equation linear in φ, leading to so called *mini* Boson stars. Having $\Lambda_4 \neq 0$ gives *self-interacting* stars which have a nonlinear wave equation corresponding to particle creation and annihilation at the quantum level; self interacting potentials can include higher order terms in φ such as $|\varphi|^6$, $|\varphi|^8$ and more. These self interacting potentials tend to have star solutions with a higher density. Finally, Eq. (2.2.6) describes the *solitonic* potential, giving rise to boson stars with compactness comparable to neutron stars. Solitonic boson stars and their gravitational wave signatures have been studied in [22].

Varying the action with respect to the metric and scalar field return the Einstein field equation and the Klein Gordon equation of curved space respectively,

$$R_{\mu\nu} - \frac{1}{2} R g_{\mu\nu} = \frac{8\pi G}{c^4} T_{\mu\nu}, \tag{2.2.7}$$

$$g^{\mu\nu} \nabla_\mu \nabla_\nu \varphi = \frac{\partial V}{\partial |\varphi|^2} \varphi. \tag{2.2.8}$$

Collectively these are known as the Einstein-Klein-Gordon (EKG) equations. From Eq. (1.4.79), the boson-specific stress energy tensors are,

$$T_{\mu\nu} := -2 \frac{\delta \mathcal{L}_M}{\delta g^{\mu\nu}} + g_{\mu\nu} \mathcal{L}_M, \tag{2.2.9}$$

$$T_{\mu\nu} = \frac{1}{2} \nabla_\mu \varphi^* \nabla_\nu \varphi + \frac{1}{2} \nabla_\nu \varphi^* \nabla_\mu \varphi - \frac{1}{2} g_{\mu\nu} \left[g^{\alpha\beta} \nabla_\alpha \varphi^* \nabla_\beta \varphi + V \right]. \tag{2.2.10}$$

Comparison of Boson Stars to Neutron Stars

Boson stars differ greatly to neutron stars; studying neutron stars requires the fermionic, or ordinary fluid, stress tensor $\boldsymbol{T}_F$;

$$T_F^{\mu\nu} = \left[\rho c^2 + P\right] \frac{u^\mu u^\nu}{c^2} + P g^{\mu\nu} + 2 u^{(\mu} q^{\nu)} + \pi^{\mu\nu} + \dots . \tag{2.2.11}$$

The continuity equation from Eq. (1.4.34), $\nabla_\nu T^{\mu\nu} = 0$, returns the highly nonlinear relativistic Navier-Stokes equations of curved space. The viscosity term $\pi^{\mu\nu}$ and heat flux q^μ are often omitted for simplicity. The remaining variables ρ, P and u^μ are the fluid density, pressure and worldline tangent. Just as in flat space, the Navier-Stokes equations can develop shockwaves and the use of sophisticated shock capturing schemes is required, unlike the linear Klein-Gordon equation which is linear in the principal part.

2.2.2 Solitons

A soliton is a wave packet that exhibits particle-like behaviour. More precisely, in classical field theory, a soliton is a field or set of fields in a localised configuration that travels at constant speed without dispersing. This is a property of solutions to the linear wave equation but many solitonic solutions exist for non-linear differential equations as well. For our purposes, we look for solitons in the Einstein-Klein-Gordon (EKG) system which are self gravitating localised scalar field and metric configurations. In the case of the real scalar field it was shown that there are no long lived solitons [23]; however promoting the field to a complex scalar we can find a spherically symmetric stationary soliton with the following configuration,

$$\varphi = \Phi(r)e^{i\omega t}, \tag{2.2.12}$$

in spherical polar coordinates $x^\mu \in \{t, r, \theta, \phi\}$. Traditionally, the polar areal gauge has been used for the metric's ansatz,

$$g_{\mu\nu}\mathrm{d}x^\mu \mathrm{d}x^\nu = -a^2(r)\mathrm{d}t^2 + b^2(r)\mathrm{d}r^2 + r^2\left[\mathrm{d}\theta^2 + \sin^2\theta \mathrm{d}\phi^2\right], \tag{2.2.13}$$

where the boundary condition $b^2(0) = 1$ is demanded to avoid a conical singularity at the origin. However an isotropic gauge is more useful for simulations due to easier conversion to Cartesian space-coordinates, for more information on isotropic coordinates see section 1.4.5. The polar areal solution must then be transformed into an isotropic solution. Alternatively, the approach taken in this report, is to start with an isotropic ansatz,

$$g_{\mu\nu}\mathrm{d}x^\mu \mathrm{d}x^\nu = -\Omega^2(r)\mathrm{d}t^2 + \Psi^2(r)\mathrm{d}\boldsymbol{x}^2, \tag{2.2.14}$$

where $\mathrm{d}\boldsymbol{x}^2$ denotes the euclidean 3D line element; this changes between spherical polar or Cartesian coordinates trivially. This ends up being slightly harder to solve for numerically, but no conversion to isotropic coordinates is needed afterwards.

To get a set of ODEs to solve for the functions $\{\Omega(r), \Psi(r), \Phi(r)\}$ we must turn to the Einstein equation and Klein Gordon equation. The Einstein equations for $\{\mu, \nu\} = \{0, 0\}, \{1, 1\}, \{2, 2\}$ are the only components that give unique non-zero equations in spherical symmetry; they are,

$$\frac{\Omega^2\left[r\Psi'^2 - 2\Psi\left[r\Psi'' + 2\Psi'\right]\right]}{r\Psi^4} = 4\pi G\left[\Omega^2\left[\frac{P'^2}{\Psi^2} + V\right] + \omega^2 P^2\right], \tag{2.2.15}$$

$$\frac{2\Psi\Psi'\left[r\Omega' + \Omega\right] + r\Omega\Psi'^2 + 2\Psi^2\Omega'}{r\Psi^2\Omega} = 4\pi G\left[P'^2 - \Psi^2 V + \frac{\omega^2 P^2\Psi^2}{\Omega^2}\right], \tag{2.2.16}$$

$$r\left[-\frac{r\Psi'^2}{\Psi^2} + \frac{r\Psi'' + \Psi'}{\Psi} + \frac{r\Omega'' + \Omega'}{\Omega}\right] = -4\pi G r^2\Psi^2\left[\frac{P'^2}{\Psi^2} + V - \frac{\omega^2 P^2}{\Omega^2}\right], \tag{2.2.17}$$

where the Einstein tensor $G_{\mu\nu} = R_{\mu\nu} - \frac{1}{2}Rg_{\mu\nu}$ and the stress tensor $T_{\mu\nu}$ are on the left and right respectively. Substituting the metric ansatz Eq. (2.2.14) and the field ansatz Eq. (2.2.12) into Eq. (2.2.8), the Klein Gordon equation becomes,

$$g^{\mu\nu}\nabla_\mu\nabla_\nu\varphi = \frac{\partial V}{\partial|\varphi|^2}\varphi, \tag{2.2.18}$$

$$\frac{1}{\sqrt{-g}}\partial_\mu\left[\sqrt{-g}g^{\mu\nu}\partial_\nu\Phi(r)e^{i\omega t}\right] = \frac{\partial V}{\partial|\varphi|^2}\Phi(r)e^{i\omega t}, \tag{2.2.19}$$

$$\Phi'' = \Phi\Psi^2\left[V' - \frac{\omega^2}{\Omega^2}\right] - \Phi'\left[\frac{\Omega'}{\Omega} + \frac{\Psi'}{\Psi} + \frac{2}{r}\right]. \tag{2.2.20}$$

Simplifying the Einstein Equations and combining with the Klein Gordon equation we get three ODES to solve; the EKG system has been reduced to two second order ODES and a first order ODE,

$$\Omega' = \frac{\Omega}{r\Psi' + \Psi}\left[2\pi G r \Psi\left[\Phi'^2 - \Psi^2 V + \frac{\omega^2\Phi^2\Psi^2}{\Omega^2}\right] - \Psi' - \frac{r\Psi'^2}{2\Psi}\right], \tag{2.2.21}$$

$$\Psi'' = \frac{\Psi'^2}{2\Psi} - \frac{2\Psi'}{r} - 2\pi G\left[V\Psi^3 + \Phi'^2\Psi + \frac{\omega^2\Phi^2\Psi^3}{\Omega^2}\right], \tag{2.2.22}$$

$$\Phi'' = \Phi\Psi^2\left[V' - \frac{\omega^2}{\Omega^2}\right] - \Phi'\left[\frac{\Omega'}{\Omega} + \frac{\Psi'}{\Psi} + \frac{2}{r}\right]. \tag{2.2.23}$$

This is turned into a set of five first order ODES to numerically integrate from $r = 0$ out to large radius. Note that if we had used the polar areal ansatz in Eq. (2.2.13) the equation for Φ would also be first order; reducing the EKG system to four first order ODES.

2.2.3 3+1 Klein Gordon System

Now let us project the Klein Gordon equation in a 3+1 split to get the evolution equations. The first step is to turn the second order Klein-Gordon equation into two first order differential equations (in time),

$$\partial_t\varphi = ... \quad \text{and} \quad \partial_t\Pi = ..., \tag{2.2.24}$$

where Π is the foliation dependant definition of conjugate momentum to the complex scalar field defined by,

$$\Pi := -\mathcal{L}_n\varphi. \tag{2.2.25}$$

Above, $\boldsymbol{n}$ is the unit normal vector to Σ_t. Decomposing the Klein Gordon Equation gives,

$$\nabla^\mu\nabla_\mu\varphi = V'\varphi = \frac{1}{\sqrt{-g}}\partial_\mu\left[\sqrt{-g}\left[\gamma^{\mu\nu} - n^\mu n^\nu\right]\partial_\nu\varphi\right] = \frac{1}{\sqrt{-g}}\partial_\mu\left[\sqrt{-g}\left[\mathcal{D}^\mu\varphi - n^\mu\mathcal{L}_n\varphi\right]\right]. \tag{2.2.26}$$

The term with $\mathcal{D}^\mu$ simplifies like,

$$\frac{1}{\sqrt{-g}}\partial_\mu\left[\sqrt{-g}\mathcal{D}^\mu\varphi\right] = \frac{1}{\alpha\sqrt{\gamma}}\partial_\mu\left[\alpha\sqrt{\gamma}\mathcal{D}^\mu\varphi\right] = \mathcal{D}_\mu\mathcal{D}^\mu\varphi + \mathcal{D}^\mu\varphi\,\partial_\mu\ln\alpha, \tag{2.2.27}$$

and the remainder becomes

$$-\frac{1}{\sqrt{-g}}\partial_\mu\left[\sqrt{-g}n^\mu\mathcal{L}_n\varphi\right] = -\left[\nabla\cdot n + n\cdot\partial\right]\mathcal{L}_n\varphi = -\mathcal{K}\Pi + \mathcal{L}_n\Pi. \tag{2.2.28}$$

Combining these results, the Klein Gordon equation becomes,

$$\mathcal{L}_m\Pi = -\mathcal{D}^\mu\varphi\,\partial_\mu\alpha + \alpha\left[\mathcal{K}\Pi - \mathcal{D}_\mu\mathcal{D}^\mu\varphi + V'\varphi\right], \tag{2.2.29}$$

$$\mathcal{L}_m\varphi = -\alpha\Pi. \tag{2.2.30}$$

where $\mathcal{L}_m = \alpha\mathcal{L}_n$ for a scalar field. Using the CCZ4 formalism (covered in section 2.1.9), the equations of motion for the scalar field are

$$\partial_t\varphi = \beta^k\partial_k\varphi - \alpha\Pi, \tag{2.2.31}$$

$$\partial_t\Pi = \beta^k\partial_k\Pi - \chi\tilde{\gamma}^{ij}\partial_i\varphi\partial_j\alpha + \alpha\left[\chi\tilde{\Upsilon}^k\partial_k\varphi + \frac{1}{2}\tilde{\gamma}^{lk}\partial_k\chi\partial_l\varphi - \chi\tilde{\gamma}^{ij}\partial_i\partial_j\varphi + \mathcal{K}\Pi + V'\varphi\right]. \tag{2.2.32}$$

The final matter term we must decompose is the Klein-Gordon stress tensor in Eq. (2.2.10) with Eqs. (2.1.45), (2.1.46) and (2.1.47).

$$\rho = n^\mu n^\nu T_{\mu\nu} = \frac{1}{2}|\Pi|^2 + \frac{1}{2}\gamma^{ij}\mathcal{D}_i\varphi^*\mathcal{D}_j\varphi + \frac{1}{2}V(|\varphi|^2), \tag{2.2.33}$$

$$S_i = -\perp_i^\mu n^\nu T_{\mu\nu} = \frac{1}{2}\left[\Pi^*\mathcal{D}_i\varphi + \Pi\mathcal{D}_i\varphi^*\right], \tag{2.2.34}$$

$$S_{ij} = \perp_i^\mu\perp_j^\nu T_{\mu\nu} = \mathcal{D}_{(i}\varphi\mathcal{D}_{j)}\varphi^* - \frac{1}{2}\left[\gamma^{ij}\mathcal{D}_i\varphi\mathcal{D}_j\varphi^* - |\Pi|^2 + V(|\varphi|^2)\right]. \tag{2.2.35}$$

2.2.4 Klein Gordon's Noether Charge

The complex scalar field has a conserved quantity called the Noether charge. The Noether charge represents the number of particles minus the number of antiparticles described by the field theory. In a numerical simulation a conserved quantity can be used to check the quality of a simulation as with good resolution the total charge should be conserved.

The Noether charge of the complex scalar field is associated with the following U(1) symmetry,

$$\varphi \to \varphi e^{i\epsilon} \approx \varphi + i\epsilon\varphi, \tag{2.2.36}$$

$$\varphi^* \to \varphi^* e^{-i\epsilon} \approx \varphi^* - i\epsilon\varphi^*, \tag{2.2.37}$$

which leaves the Lagrangian unchanged and therefore the total action. The associated conserved current j and current density $\mathcal{J}$ are then,

$$j^\mu = \frac{\delta\mathcal{L}}{\delta\nabla_\mu\varphi}\delta\varphi + \frac{\delta\mathcal{L}}{\delta\nabla_\mu\varphi^*}\delta\varphi^*, \tag{2.2.38}$$

$$j^\mu = ig^{\mu\nu}\left[\varphi\nabla_\nu\varphi^* - \varphi^*\nabla_\nu\varphi\right], \tag{2.2.39}$$

where the current satisfies the conservation equation,

$$\nabla_\mu j^\mu = 0. \tag{2.2.40}$$

Using Eq. (1.3.141), the conservation equation can be re-written as,

$$\nabla_\mu j^\mu = \frac{1}{\sqrt{-g}}\partial_\mu\left(\sqrt{-g}j^\mu\right) = \frac{1}{\sqrt{-g}}\partial_\mu\mathcal{J}^\mu = 0, \tag{2.2.41}$$

where $\mathcal{J}^\mu = \sqrt{-g}j^\mu$ is the current expressed as a tensor density. Therefore,

$$\partial_\mu\mathcal{J}^\mu = 0, \tag{2.2.42}$$

is also true and even in curved space the current $\boldsymbol{\mathcal{J}}$ obeys a conservation equation; this means there must be some conserved charge $\mathcal{Q}$ associated with the current. Integrating Eq. (2.2.42) over a manifold $\mathcal{M}$ gives,

$$\int_{\mathcal{M}} \partial_\mu\mathcal{J}^\mu \mathrm{d}x^4 = 0, \tag{2.2.43}$$

$$\int_{t_0}^{t_1}\left[\int_{\Sigma_t}\partial_0\mathcal{J}^0\mathrm{d}x^3\right]\mathrm{d}t = -\int_{t_0}^{t_1}\left[\int_{\Sigma_t}\partial_i\mathcal{J}^i\mathrm{d}x^3\right]\mathrm{d}t, \tag{2.2.44}$$

$$\int_{t_0}^{t_1}\left[\int_{\Sigma_t}\partial_0\mathcal{J}^0\mathrm{d}x^3\right]\mathrm{d}t = -\int_{t_0}^{t_1}\left[\int_{\partial\Sigma_t}\hat{s}_i\mathcal{J}^i\mathrm{d}x^2\right]\mathrm{d}t, \tag{2.2.45}$$

$$\int_{t_0}^{t_1}\left[\int_{\Sigma_t}\partial_0\mathcal{J}^0\mathrm{d}x^3\right]\mathrm{d}t = 0, \tag{2.2.46}$$

where the flat space divergence theorem was used and $\hat{\boldsymbol{s}}$ is the flat space normal to $\partial\Sigma_t$, the boundary of Σ_t. The term containing $\hat{s}_i\mathcal{J}^i$ integrates to zero over $\partial\Sigma_t$ due to $\mathcal{J}$ vanishing on $\partial\Sigma_t$. The $\mathcal{J}^0$ term can be simplified by permuting the time derivative using,

$$\partial_0\int_{\Sigma_t}\mathcal{J}^0\mathrm{d}x^3 = \int_{\Sigma_t}\partial_0\mathcal{J}^0\mathrm{d}x^3 + \lim_{\Delta x^0\to 0}\left[\frac{1}{\Delta x^0}\int_{\Delta\Sigma_t}\left[\mathcal{J}^0 + \Delta x^0\partial_0\mathcal{J}^0\right]\mathrm{d}x^3\right], \tag{2.2.47}$$

where the last term vanishes as $\mathcal{J}$ vanishes on $\Delta\Sigma_t$ near $\partial\Sigma$, and Eq. (2.2.46) becomes,

$$\int_{t_0}^{t_1}\left[\partial_0\int_{\Sigma_t}\mathcal{J}^0\mathrm{d}x^3\right]\mathrm{d}t = 0, \tag{2.2.48}$$

and the formula for the conserved charge Q can be read off as,

$$\partial_0 Q = 0, \tag{2.2.49}$$

$$Q = \int_{\Sigma_t} \mathcal{J}^0 \mathrm{d}x^3. \tag{2.2.50}$$

The charge density $\mathcal{Q}$ is defined as,

$$Q := \int_{\Sigma_t} \mathcal{Q}\sqrt{\gamma}\,\mathrm{d}x^3, \tag{2.2.51}$$

$$\mathcal{Q} = \frac{\mathcal{J}^0}{\sqrt{\gamma}} = \frac{\sqrt{-g}j^0}{\sqrt{\gamma}} = \alpha j^0, \tag{2.2.52}$$

where Eq. (2.1.70), saying $\sqrt{-g} = \alpha\sqrt{\gamma}$, was used. Finally we get an expression for the total Noether charge $N = Q$,

$$N = i\int_{\Sigma_t} \sqrt{-g}\left[\varphi\nabla^0\varphi^* - \varphi^*\nabla^0\varphi\right]\mathrm{d}x^3. \tag{2.2.53}$$

Using $\sqrt{-g} = \alpha\sqrt{\gamma}$ again and $\alpha\nabla^0\varphi = -n_\mu\nabla^\mu\varphi = \Pi$ from Eq. (2.2.25) we get the following neat formula,

$$N = i\int_{\Sigma_t} \left[\varphi\Pi^* - \varphi^*\Pi\right]\sqrt{\gamma}\,\mathrm{d}x^3. \tag{2.2.54}$$

Equivalently, the Noether charge density $\mathcal{N}$ is ,

$$\mathcal{N} = i\left(\varphi\Pi^* - \varphi^*\Pi\right). \tag{2.2.55}$$

The ideas of this section concerning conserved charges are extended in section **??** with applications to continuity equations in energy, momentum, angular momentum and Noether charges for spin-1 Proca fields. The results of this section have all been derived for an infinite volume where only a charge density $\mathcal{Q}$ needs be considered. Section **??** considers continuity equations in a finite volume V so must also consider the flux density $\mathcal{F}$ of conserved particles through ∂V (the boundary of V) and the source density $\mathcal{S}$ (creation and destruction of $\mathcal{Q}$) in V.

2.2.5 Boosted Boson Stars and Black Holes

Let us now consider a moving star, this corresponds to boosting a stationary soliton solution. There is no unique way of doing this as any coordinate transformation that reduces to a Minkowski spacetime boost at large radius is valid. All the degrees of freedom we have can be absorbed into a coordinate gauge choice so it makes sense to choose the trivial, constant valued boost, with rapidity $\chi = \mathrm{arctanh}(v)$ for a velocity v, from Special Relativity. Using Cartesian coordinates, the boost matrix $\mathbf{\Lambda}$ for a boost in the x direction is,

$$\Lambda^\mu_{\ \nu} = \exp\begin{pmatrix} 0 & -\chi & 0 & 0 \\ -\chi & 0 & 0 & 0 \\ 0 & 0 & 1 & 0 \\ 0 & 0 & 0 & 1 \end{pmatrix} = \begin{pmatrix} \cosh(\chi) & -\sinh(\chi) & 0 & 0 \\ -\sinh(\chi) & \cosh(\chi) & 0 & 0 \\ 0 & 0 & 1 & 0 \\ 0 & 0 & 0 & 1 \end{pmatrix}, \tag{2.2.56}$$

as discussed in section 1.4.1. Declaring the boosted frame and lab frame (in which the star is moving) to have coordinates x^μ and $\tilde{x}^\mu$,

$$\tilde{x}^\mu = [\Lambda^{-1}]^\mu_{\ \nu} x^\nu, \tag{2.2.57}$$

where both x^μ and $\tilde{x}^\mu$ agree on an origin. The metric transforms via the tensor transformation law like,

$$\tilde{g}_{\mu\nu}(\tilde{x}^\sigma) = \frac{\partial x^\alpha}{\partial \tilde{x}^\mu}\frac{\partial x^\beta}{\partial \tilde{x}^\nu} g_{\alpha\beta}(\tilde{x}^\sigma) = \Lambda^\alpha_{\ \mu}\Lambda^\beta_{\ \nu} g_{\alpha\beta}(\tilde{x}^\sigma), \tag{2.2.58}$$

where the inverse boost matrix $\mathbf{\Lambda}^{-1}$ can be found simply by $\mathbf{\Lambda}^{-1}(\chi) = \mathbf{\Lambda}(-\chi)$ which is equivalent to a boost in the opposite direction. We choose the boosted soliton's initial Cauchy surface to be the level set of $\tilde{t} = 0$, an instance of time in the lab frame. The coordinates and metric transform as,

$$x^\mu = \{t, x, y, z\} = \{\tilde{t}\cosh(\chi) + \tilde{x}\sinh(\chi), \tilde{x}\cosh(\chi) + \tilde{t}\sinh(\chi), \tilde{y}, \tilde{z}\}, \tag{2.2.59}$$

$$g_{\mu\nu} = \mathrm{diag}\{-\Omega^2, \Psi^2, \Psi^2, \Psi^2\}, \tag{2.2.60}$$

$$\tilde{g}_{\mu\nu} = \begin{pmatrix} -\Omega^2\cosh^2(\chi) + \Psi^2\sinh^2(\chi) & \sinh(\chi)\cosh(\chi)\left[\Omega^2 - \Psi^2\right] & 0 & 0 \\ \sinh(\chi)\cosh(\chi)\left[\Omega^2 - \Psi^2\right] & \Psi^2\cosh^2(\chi) - \Omega^2\sinh^2(\chi) & 0 & 0 \\ 0 & 0 & \Psi^2 & 0 \\ 0 & 0 & 0 & \Psi^2 \end{pmatrix}, \tag{2.2.61}$$

as the star is at rest using coordinates x^μ rather than $\tilde{x}^\mu$. Comparing this boosted metric to the $3+1$ decomposed metric in Eq. (2.1.67) we can read off the shift vector $\tilde{\beta}_i$, the 3-metric $\tilde{\gamma}_{ij}$ and obtain the lapse and metric determinant,

$$\tilde{\alpha}^2 = \frac{\Psi^2\Omega^2}{\Psi^2\cosh^2(\chi) - \Omega^2\sinh^2(\chi)}, \tag{2.2.62}$$

$$\tilde{\gamma} = \det\tilde{\gamma}_{ij} = \Psi^4\left[\Psi^2\cosh^2(\chi) - \Omega^2\sinh^2(\chi)\right]. \tag{2.2.63}$$

Finally, the conformal 3-metric with unit determinant is,

$$\bar{\gamma}_{ij} = \tilde{\gamma}^{-\frac{1}{3}}\begin{pmatrix} \Psi^2\cosh^2(\chi) - \Omega^2\sinh^2(\chi) & 0 & 0 \\ 0 & \Psi^2 & 0 \\ 0 & 0 & \Psi^2 \end{pmatrix}, \tag{2.2.64}$$

where normally $\tilde{\gamma}_{ij}$ is the conformal 3-metric, but to avoid confusion it is denoted $\bar{\gamma}_{ij}$ in this section. Turning our attention to the matter fields now we only need to change the coordinate dependence, like $\varphi(x) \to \varphi(\tilde{x})$, given that φ and Π are (complex) scalar fields. Given that $\tilde{t} = 0$ describes a time slice in the lab frame (where the star has non-zero velocity), $t = \tilde{x}\sinh(\chi)$ in the rest frame and we get the following boosted complex scalar field,

$$\varphi = \Phi(r)e^{i\omega\tilde{x}\sinh(\chi)}, \tag{2.2.65}$$

where r is the radius in the boosted frame; $r = \sqrt{\tilde{x}^2\cosh^2(\chi) + \tilde{y}^2 + \tilde{z}^2}$. Note the field is modulated by an oscillatory phase now with wavenumber $k = \omega\tilde{x}\sinh(\chi)$; nodal planes in $\mathrm{Re}(\varphi)$ appear perpendicular to velocity. The conjugate momentum $\tilde{\Pi}$, defined in Eq. (2.2.25), in the rest frame it becomes,

$$\tilde{\Pi}(\tilde{x}^\mu) = -\mathcal{L}_{\tilde{n}}\varphi(\tilde{x}^\mu) = -\frac{1}{\tilde{\alpha}}\tilde{m}\cdot\tilde{\partial}\varphi = -\frac{1}{\tilde{\alpha}}\left[\tilde{\partial}_0 - \tilde{\beta}^i\tilde{\partial}_i\right]\Phi(r)e^{i\omega t}. \tag{2.2.66}$$

Inconveniently we can not simply evaluate $\tilde{\Pi}$ in the lab frame from Π in the co-moving frame as the two frames have a different spacetime foliation and the normal vector as $\boldsymbol{n} \neq \tilde{\boldsymbol{n}}$ and is genuinely changed; not just transforming components under coordinate transformation. Explicitly writing the contra-variant components of the shift vector,

$$\tilde{\beta}^i = \left(\frac{\sinh(\chi)\cosh(\chi)\left[\Omega^2 - \Psi^2\right]}{\Psi^2\cosh^2(\chi) - \Omega^2\sinh^2(\chi)}, 0, 0\right), \tag{2.2.67}$$

and using the following derivative formulae,

$$\partial_{\tilde{t}} = \cosh(\chi)\partial_t + \sinh(\chi)\partial_x, \tag{2.2.68}$$

$$\partial_{\tilde{x}} = \cosh(\chi)\partial_x + \sinh(\chi)\partial_t, \tag{2.2.69}$$

$$\partial_t\varphi = \Phi\partial_t e^{i\omega t} = i\omega\Phi e^{i\omega t}, \tag{2.2.70}$$

$$\partial_x\varphi = \frac{\partial r}{\partial x}\Phi' e^{i\omega t} = \frac{x}{r}\Phi' e^{i\omega t}, \tag{2.2.71}$$

we get an expression for the conjugate momentum of a boosted star. Again, setting $\tilde{t} = 0$ gives the conjugate momentum on the surface $\tilde{t} = 0$ to be used as initial conditions,

$$\widetilde{\Pi} = -\frac{1}{\tilde{\alpha}}\left[\left[\sinh(\chi) - \tilde{\beta}^1\cosh(\chi)\right]\frac{\tilde{x}\cosh(\chi)}{r}\Phi' + i\omega\left[\cosh(\chi) - \tilde{\beta}^1\sinh(\chi)\right]\Phi\right]e^{i\omega\tilde{x}\sinh(\chi)}. \tag{2.2.72}$$

The penultimate ingredient is the intrinsic curvature $\tilde{\boldsymbol{K}}$, defined in Eq. (2.1.10). Similarly to the conjugate momentum, the definition of $\tilde{\boldsymbol{K}}$ depends on the spacetime foliation so using $K_{ij} = 0$ in the stars rest frame and using the tensor transformation to conclude that $\tilde{K}_{ij} = 0$ in the lab frame is incorrect. Instead the components $\tilde{K}_{ij}$ must be calculated from scratch with the correct normal vector $\boldsymbol{n}$ as follows,

$$\tilde{\mathcal{K}}_{\mu\nu} := -\frac{1}{2}\mathcal{L}_{\tilde{n}}\tilde{\gamma}_{\mu\nu} = -\frac{1}{2\tilde{\alpha}}\mathcal{L}_{\tilde{m}}\tilde{\gamma}_{\mu\nu} = -\frac{1}{2\tilde{\alpha}}\left[\tilde{m}\cdot\tilde{\partial}\tilde{\gamma}_{ij} + \tilde{\gamma}_{ik}\tilde{\partial}_j\tilde{m}^k + \tilde{\gamma}_{jk}\tilde{\partial}_i\tilde{m}^k\right]. \tag{2.2.73}$$

The explicit form for the components of $\tilde{K}_{ij}$ are

$$\widetilde{\mathcal{K}}_{xx} = \frac{1}{\tilde{\alpha}}\cosh^2(\chi)\sinh(\chi)\frac{x}{r}\frac{\left[v^2\Omega^2\Omega' + \Psi\Omega\Psi' - 2\Psi^2\Omega'\right]}{\Psi^2\Omega}, \tag{2.2.74}$$

$$\widetilde{\mathcal{K}}_{xy} = \frac{1}{\tilde{\alpha}}\cosh(\chi)\sinh(\chi)\frac{y}{r}\frac{\left[\Omega\Psi' - \Psi\Omega'\right]}{\Psi\Omega}, \tag{2.2.75}$$

$$\widetilde{\mathcal{K}}_{xz} = \frac{1}{\tilde{\alpha}}\cosh(\chi)\sinh(\chi)\frac{z}{r}\frac{\left[\Omega\Psi' - \Psi\Omega'\right]}{\Psi\Omega}, \tag{2.2.76}$$

$$\widetilde{\mathcal{K}}_{yy} = -\frac{1}{\tilde{\alpha}}\sinh(\chi)\frac{x}{r}\frac{\Psi'}{\Psi}, \tag{2.2.77}$$

$$\widetilde{\mathcal{K}}_{zz} = \widetilde{\mathcal{K}}_{yy}, \tag{2.2.78}$$

where the $\{x, y, z\}$ need to be expanded in terms of $\{\tilde{x}, \tilde{y}, \tilde{z}\}$ and $r = \sqrt{x^2 + y^2 + z^2}$.

The final object needed is the three-dimensional connection symbols $\Upsilon^i{}_{jk}$, these are calculated numerically after the initial data is loaded in using the definition from Eq. (1.3.77),

$$\Upsilon^i_{jk} = \frac{1}{2}\gamma^{im}\left(\partial_k\gamma_{jm} + \partial_j\gamma_{mk} - \partial_m\gamma_{jk}\right). \tag{2.2.79}$$

The boost formalism described here can be applied to a Black Hole spacetime by setting,

$$\varphi = 0, \tag{2.2.80}$$

$$\Pi = 0, \tag{2.2.81}$$

$$\Omega = \frac{1 - \frac{M}{2r}}{1 + \frac{M}{2r}}, \tag{2.2.82}$$

$$\Psi = \left[1 + \frac{M}{2r}\right]^2, \tag{2.2.83}$$

corresponding to the isotropic Schwarzschild black hole given in section 1.4.5.

Chapter 3

Numerical Methods and GRChombo

3.1 Numerical Methods

3.1.1 Numerical Discretisation of Spacetime

There are many ways to time evolve a field theory on a spatial surface. Some popular numerical methods include spectral methods, finite element models and finite volume methods. The method used throughout this work is the finite difference framework. This models a continuous spacetime with a discrete lattice of points; usually this lattice is cubic or cuboidal. A field $\phi(x^\mu)$ on a manifold $\mathcal{M}$ is expressed as a set of discrete values ϕ^n_{ijk}, for integer $\{n, i, j, k\}$, on a set of discrete lattice points with coordinates $(x^n_{ijk})^\mu$. In uniform Cartesian coordinates $(x^n_{ijk})^\mu = \{n\Delta t, i\Delta x, j\Delta y, k\Delta z\}$ where Δt, Δx, Δy and Δz represent the grid spacing. In the limit that the grid spacing tends to zero, the lattice and discretised fields should converge to the continuum solution. For a detailed introduction to numerical methods the reader is directed to [24].

To calculate gradients on a lattice, we can consider a two dimensional manifold spanned by coordinates $\{t, x\}$. We can no longer employ the traditional definition of $\mathrm{d}f/\mathrm{d}x$,

$$\frac{\mathrm{d}f}{\mathrm{d}x} := \lim_{\delta x \to 0} \left(\frac{f(x+\delta x) - f(x)}{\delta x} \right), \tag{3.1.1}$$

as there no longer exist two points x and $x + \delta x$ that are infinitesimally close to each other. Derivatives are now calculated by comparing gridpoints a finite distance from each other. To elucidate this idea, a formula for the second derivative is calculated. First we pick five lattice points, equally spaced by Δx, with coordinates $\{x_{-2}, x_{-1}, x_0, x_1, x_2\}$, and writing $f(x_i) = f_i$. Then using the well known formula for the Taylor expansion of a function about a point x_0,

$$f(x) = f(x_0) + (x - x_0)f'(x_0) + \frac{(x-x_0)^2}{2!}f''(x_0) + \frac{(x-x_0)^3}{3!}f'''(x_0) + \dots, \tag{3.1.2}$$

we can write,

$$f_2 \approx f_0 + 2\Delta x f'_0 + 2(\Delta x)^2 f''_0 + \frac{4}{3}(\Delta x)^3 f'''_0 + \frac{2}{3}(\Delta x)^4 f''''_0, \tag{3.1.3}$$

$$f_1 \approx f_0 + \Delta x f'_0 + \frac{1}{2}(\Delta x)^2 f''_0 + \frac{1}{6}(\Delta x)^3 f'''_0 + \frac{1}{24}(\Delta x)^4 f''''_0, \tag{3.1.4}$$

$$f_0 \approx f_0, \tag{3.1.5}$$

$$f_{-1} \approx f_0 - \Delta x f'_0 + \frac{1}{2}(\Delta x)^2 f''_0 - \frac{1}{6}(\Delta x)^3 f'''_0 + \frac{1}{24}(\Delta x)^4 f''''_0, \tag{3.1.6}$$

$$f_{-2} \approx f_0 - 2\Delta x f'_0 + 2(\Delta x)^2 f''_0 - \frac{4}{3}(\Delta x)^3 f'''_0 + \frac{2}{3}(\Delta x)^4 f''''_0, \tag{3.1.7}$$

where the Taylor expansions are truncated at terms of order $(\Delta x)^4$. The equations above can be inverted to give,

$$\left.\frac{\mathrm{d}^2 f}{\mathrm{d}x^2}\right|_{x_0} := f''_0 = \frac{-f_2 + 16f_1 - 30f_0 + 16f_{-1} - f_{-2}}{12(\Delta x)^2} + \mathcal{O}(\Delta x^4). \tag{3.1.8}$$

An approximation for the second derivative using a discrete sum of neighbouring points, also called a stencil, has been obtained. Adding terms of order $(\Delta x)^5$ in the Taylor expansion for f_i would not affect the result as the pairs of terms $\{f_2, f_{-2}\}$ and $\{f_1, f_{-1}\}$ appear in equal amounts; therefore Eq. (3.1.8) is correct up to a Taylor expansion of order $(\Delta x)^6$. Given that f''_0 appears with a $(\Delta x)^2$ and Eq. (3.1.8) is correct until terms of order $(\Delta x)^6$, then the expression is accurate up to fourth order. Any other derivative to any order accuracy (in any dimension) can be calculated in a similar fashion. In the limit that the grid spacing $\Delta x \to 0$ the approximations for the derivatives approach the exact continuum limit while higher order accurate stencils approach the continuum limit more quickly.

3.1.2 Boundary Conditions

Another artefact of evolving field equations over a volume on a computer is that the volume must have finite size; a computer does not have infinite memory to store an infinite amount of gridpoints. The usual way to deal with this problem is to enforce an algebraic condition on the fields on a surface surrounding the region of interest. Alternatively, an infinite volume can be modelled if coordinates are used which compactify the volume to some finite region, this corresponds to the grid spacing Δx diverging or resolution becoming infinitely low towards the boundary.

Common boundary conditions include Dirichlet (fixed value), Von-Neumann (fixed derivative) or some mix of these conditions. It is common to re-categorise boundary conditions into sub-categories with informative names such as reflective, periodic or symmetric.

As an example in one spatial dimension, symmetric boundary conditions for a field ϕ about a point x_n could be implemented by creating extra *ghost cells* beyond the desired simulation domain with coordinates $\{x_{n+1}, x_{n+2}, x_{n+3}, ...\}$ and setting,

$$\phi_{n+1} = \pm\phi_{n-1}, \quad \phi_{n+2} = \pm\phi_{n-2}, \quad \phi_{n+3} = \pm\phi_{n-3}, \quad ..., \tag{3.1.9}$$

where the $+$ or $-$ sign is taken for even or odd parity variables and $\phi_i = \phi(x_i) = \phi(i * \Delta x)$. These extra ghost cells allow the calculation of derivatives at x_n using stencils, as shown in section 3.1.1; without these ghost cells the stencil would not be able to access points x_m where $m > n$. The number of ghost cells should be chosen to be the minimum required to allow the calculation of derivative stencils at each point in the simulation domain. The desired location of the boundary condition does not have to coincide with a gridpoint. As an example, modifying the symmetric boundary condition to be centred on $x_n + \Delta x/2$ instead results in,

$$\phi_{n+1} = \pm\phi_{n}, \quad \phi_{n+2} = \pm\phi_{n-1}, \quad \phi_{n+3} = \pm\phi_{n-2}, \quad ... . \tag{3.1.10}$$

Generic boundary conditions can be imposed by assigning values to ghost cells similarly to above. Although the examples given in this section are in one dimension, the ideas generalise to arbitrary dimensions straightforwardly.

Sommerfeld Boundary Conditions

A very useful type of boundary condition is the Sommerfeld boundary condition [25], used to approximate an outgoing wave being transmitted through the boundary condition. Sommerfeld boundary conditions can be derived from studying the solution to the wave equation in spherical symmetry in flat space,

$$-\frac{1}{v^2}\partial_t^2\Psi + \gamma^{ij}\mathcal{D}_i\mathcal{D}_j\Psi = -\frac{1}{v^2}\partial_t^2\Psi + \frac{1}{\sqrt{-\gamma}}\partial_i\left(\sqrt{\gamma}\gamma^{ij}\partial_j\Psi\right) = -\partial_t^2\Psi + \frac{1}{r^2}\partial_r\left(r^2\partial_r\Psi\right) = 0, \tag{3.1.11}$$

for some field Ψ with wavespeed v. In spherical polar coordinates, $\gamma^{ij} = \text{diag}\{1, r^{-2}, r^{-2}\text{cosec}^2(\theta)\}$, and Eq. (3.1.11) has an outgoing wave solution,

$$\Psi(r,t) = \Psi_\infty + \frac{A}{r}\psi(r - vt), \tag{3.1.12}$$

for an asymptotic value Ψ_∞ and arbitrary constant A. In differential form this can be written as,

$$\frac{1}{v}\partial_t\Psi + \partial_r\Psi + \frac{1}{r}(\Psi - \Psi_\infty) = 0. \tag{3.1.13}$$

The equation of motion for Ψ can be used to write ∂_t in terms of spatial derivatives and field values giving the new boundary condition which can be applied numerically as a regular mixed type boundary condition. Typically one-sided stencils are needed to avoid sampling non-existent gridpoints.

In general relativity, Sommerfeld boundary conditions are commonly used with $v = c = 1$ (the speed of light) to avoid reflections of matter and gravitational waves from the boundary of a simulation. It should be noted that Sommerfeld boundary conditions are approximate in general relativity for a number of reasons.

- Sommerfeld boundary conditions are derived in spherical symmetry and flat space; spacetimes often asymptote to spherically symmetric flat space, but this is only approximately true for finite radii.
- Matter doesn't always obey a wave equation or propagate at the speed of light.
- Gravitational waves only obey a linear wave equation under special circumstances such as specific wave shapes (such as Brill waves) and small amplitude waves in flat space; again this problem is alleviated at large radius in an asymptotically flat space.

It has been found experimentally in my work that ensuring the boundary conditions are sufficiently far away from any compact objects is very important in maintaining accuracy of the simulation when using Sommerfeld boundary conditions.

3.1.3 The Method of Lines

Assuming adequate boundary conditions are in place, the time evolution of initial data ϕ^n_{ijk} covering a spacelike computational grid can be done by applying a time integration scheme to the PDE governing the field $\phi(x^\mu)$. There are many ways to do this and the reader is directed to [24] for a comprehensive introduction. A common method is the method of lines (MoL).

The MoL reduces the dimensionality of the PDE problem to a set of ODEs in time at each gridpoint (with coordinate $\boldsymbol{x}_{ijk}$). Spatial derivatives are treated as a function on each gridpoint; their evaluation is done using the derivative stencils described in section 3.1.1. For example, consider the partial differential equation,

$$\partial_t \phi(\boldsymbol{x}, t) = \hat{O}\phi(\boldsymbol{x}, t) + f(\phi, \boldsymbol{x}, t), \tag{3.1.14}$$

where $\hat{O}$ is some spatial derivative operator, f is a function and $\boldsymbol{x}$ are spacelike coordinates. Using the MoL, the operator $\hat{O}$ is discretised (in space only) on a grid like,

$$\hat{O}\phi(\boldsymbol{x}, t) \Rightarrow (\hat{O}\phi)_{ijk}(t), \tag{3.1.15}$$

where $(\hat{O}\phi)_{ijk}(t) \approx \hat{O}\phi(\boldsymbol{x}_{ijk}, t)$ is a sum of field values at neighbouring gridpoints generated by the method of finite differences. Discretising the function f on the grid gives the following ODE for each gridpoint with spatial indices $\{i, j, k\}$,

$$\partial_t \phi_{ijk}(t) \approx (\hat{O}\phi)_{ijk}(t) + f_{ijk}(\phi, t) := F_{ijk}(\phi, t), \tag{3.1.16}$$

where $F_{ijk}(\phi, t)$ is treated as the discretisation of a continuum function $F(\phi, \boldsymbol{x}, t)$.

3.1.4 Integration of ODEs

To perform the time evolution of the ODE (3.1.16), we need to pick a time integration method for an ODE. The obvious choice might be to discretise the time integral like,

$$\partial_t \phi^n_{ijk} = \frac{\phi^{n+1}_{ijk} - \phi^n_{ijk}}{\Delta t}, \tag{3.1.17}$$

where Δt is the time-step of evolution. This can be substituted into Eq. (3.1.16) to give,

$$\phi^{n+1}_{ijk} = \phi^n_{ijk} + F^n_{ijk}\Delta t, \tag{3.1.18}$$

which is an explicit scheme; the desired future field values ϕ^{n+1}_{ijk} are given by an explicit formula in terms of the previous values ϕ^n_{ijk}. This is known as the Euler method and is often unstable; it can be shown to

be completely unstable no matter how small Δt is taken to be for $F^n_{ijk} = A\phi^n_{ijk}$ for positive constant A. There is nothing stopping us instead writing,

$$\phi^{n+1}_{ijk} - F^{n+1}_{ijk}\Delta t = \phi^n_{ijk}, \tag{3.1.19}$$

which is known as an implicit scheme as the desired future field values ϕ^{n+1}_{ijk} are given by an implicit equation. This is called the backwards Euler method and is often stable, but only first order accurate in time. This can be improved to the second order accurate Crank-Nicolson method,

$$\phi^{n+1}_{ijk} - \frac{1}{2}F^{n+1}_{ijk}\Delta t = \phi^n_{ijk} + \frac{1}{2}F^n_{ijk}\Delta t, \tag{3.1.20}$$

but is still implicit in ϕ^n_{ijk}. The problem with implicit methods is that the F^{n+1}_{ijk} are some combination of the ϕ^{n+1}_{ijk} at $\boldsymbol{x}_{ijk}$ and multiple other neighbouring gridpoints around $\boldsymbol{x}_{ijk}$; the number of gridpoints increases with higher order accurate derivative stencils. Solving the set of simultaneous equations in Eq. (3.1.20), for example, requires inverting a large (albeit sparse) matrix whose size scales with the number of gridpoints. This can be done in a single step if the F^n_{ijk} are linear in ϕ^n. For non-linear PDEs the F^n_{ijk} are non-linear in ϕ^n_{ijk}; in the best case one can linearise Eq. (3.1.20) and the ϕ^{n+1}_{ijk} can be solved with an iterative method, in the worst case the implicit scheme is impossible to solve.

A stable and explicit method can be obtained by seeking a higher order accurate time derivative. In a similar fashion to the derivation of Eq. (3.1.8), one can write,

$$\phi^n_{ijk} = \phi^n_{ijk}, \tag{3.1.21}$$

$$\phi^{n-1}_{ijk} = \phi^n_{ijk} - \Delta t\dot{\phi}^n_{ijk} + \frac{1}{2}(\Delta t)^2\ddot{\phi}^n_{ijk}, \tag{3.1.22}$$

$$\phi^{n-2}_{ijk} = \phi^n_{ijk} - 2\Delta t\dot{\phi}^n_{ijk} + 2(\Delta t)^2\ddot{\phi}^n_{ijk}, \tag{3.1.23}$$

where the dot represents a time derivative and the Taylor expansion has been given up to $(\Delta t)^2$ terms. Rearranging, these give

$$\partial_t\phi^n_{ijk} = \frac{-3\phi^n_{ijk} + 4\phi^{n-1}_{ijk} - \phi^{n-2}_{ijk}}{6\Delta t}. \tag{3.1.24}$$

Substituting this into Eq. (3.1.16) gives an explicit equation for ϕ^n_{ijk},

$$\phi^n_{ijk} = \frac{4}{3}\phi^{n-1}_{ijk} - \frac{1}{3}\phi^{n-2}_{ijk} - 2F_{ijk}\Delta t, \tag{3.1.25}$$

where the index n has been omitted from F_{ijk} as is it can be replaced with any combination $aF^n_{ijk} + bF^{n-1}_{ijk} + cF^{n-2}_{ijk}$, provided $a + b + c = 1$, such as $F^n_{ijk} = \frac{4}{3}F^{n-1}_{ijk} - \frac{1}{3}F^{n-2}_{ijk}$. Even thought this method is explicit it requires two sets of initial data, ϕ^{n-1}_{ijk} and ϕ^{n-2}_{ijk} and one must take care to check if the choice of F_{ijk} gives a stable scheme.

The Runge Kutta Method

The Runge-Kutta method is an explicit ODE integration scheme that can be made accurate to arbitrary order in Δt. For an ODE of the form,

$$\frac{\mathrm{d}\phi}{\mathrm{d}t} = F(\phi, t), \tag{3.1.26}$$

the widely used fourth order accurate Runge-Kutta (RK4) method first calculates four intermediate rates of change $\{k_1, k_2, k_3, k_4\}$,

$$k_1 = F(\phi, t), \tag{3.1.27}$$

$$k_2 = F(\phi + \frac{1}{2}k_1\Delta t, t + \frac{1}{2}\Delta t), \tag{3.1.28}$$

$$k_3 = F(\phi + \frac{1}{2}k_2\Delta t, t + \frac{1}{2}\Delta t), \tag{3.1.29}$$

$$k_4 = F(\phi + k_3\Delta t, t + \Delta t). \tag{3.1.30}$$

These are then summed in a way that calculates $\phi(t+\Delta t)$ from $\phi(t)$ removing errors up to and including $(\Delta t)^4$ terms,

$$\phi(t+\Delta t) = \phi(t) + \frac{1}{6}\left(k_1 + 2k_2 + 2k_3 + k_4\right)\Delta t + \mathcal{O}(\Delta t^5). \tag{3.1.31}$$

A similar procedure can be done for any desired accuracy with higher order methods becoming quite involved. The simplicity of this RK4 scheme along with its robustness has led to it being one of the most popular methods for integrating ODEs. Lower order Runge-Kutta methods also exist, for example the first order RK1 method which is equivalent to the Euler method in Eq. (3.1.18). Another common Runge-Kutta method is the second order accurate RK2 method also called the midpoint method.

3.2 GRChombo

3.2.1 Overview of GRChombo

GRChombo [26] [27] is an open-source fully non-linear Numerical Relativity (NR) code built on top of Chombo, a PDE solver with adaptive mesh refinement (AMR). GRChombo is written in C++ making extensive use of templating, classes and object oriented programming. GRChombo also supports vectorisation and parallelisation with OpenMP and MPI for efficient scaling to large problems suitable for use on supercomputer clusters. Current public examples of GRChombo include a black hole binary with separate spins, a single Kerr black hole and a compact real scalar configuration.

The AMR in Chombo relies on the Berger-Oliger style AMR [28] with block-structured Berger-Rigoutsos grid generation [29]. The labelling of which regions to regrid, called tagging, is specifiable by the user. A common tagging criterion (used in this work) is to define a gradient sensitive quantity $\aleph$ in terms of a grid variable ψ,

$$\aleph = \Delta x \sqrt{\frac{\left|\sum_{ij}(\partial_i\partial_j\psi)(\partial_i\partial_j\psi)\right|}{\left|\sum_k(\partial_k\psi)(\partial_k\psi)\right| + \epsilon}}, \tag{3.2.1}$$

for grid spacing Δx and small positive constant ϵ to avoid division by zero. Some threshold ψ_0 is prespecified and any gridpoint where $\aleph > \psi_0$ is flagged (or tagged) for regridding. If a box[1] has a greater fraction of its cells tagged than a *fill_ratio* parameter then the box will be covered by the next inner AMR level; in this work *fill_ratio* $= 0.7$. The reason for premultiplying by Δx is so that as the grid spacing gets smaller on deeper levels the tagging criterion is not flagged unless gradients become more extreme.

In order to evolve a spatial hypersurface according to the Einstein equation, GRChombo uses either the BSSN formalism [30] [31] described in section 2.1.7 or the CCZ4 formalism [14] [15]. A summary of the CCZ4 formulation is given in section 2.1.9 along with the equations of motion used in this work. The conformal factor used is $\chi = \gamma^{-\frac{1}{3}}$ where γ is the metric determinant from Eq. (2.1.9) on the three dimensional hypersurface Σ_t. The time evolution scheme is the method of lines (section 3.1.3) using fourth order spatial derivatives (section 3.1.1) and Runge Kutta fourth order time integration (section 3.1.4). While sixth order spatial derivatives have been implemented, they are not used in this work due to the increasing number of ghost cells needed. Kreiss-Oliger dissipation [32] is used to suppress high frequency noise occurring from interpolation, regridding of AMR and high field gradients inside black hole regions. As described in section 2.1.10, the moving puncture gauge with conformal factor χ is used to evolve moving black hole singularities.

The code can use Sommerfeld, periodic, reflective and extrapolating boundary conditions. Simulations in this work all use some combination of Sommerfeld boundary conditions for boundaries far away and symmetric boundary conditions in a plane of symmetry. Headon collisions of identical objects can use *octant* symmetry, three planes of symmetry on the planes $x = 0$, $y = 0$ and $z = 0$. This means one

[1] Each AMR level is subdivided into cuboids, often of side lengths 8, 16, or 32 gridpoints, called boxes. These boxes can be evolved forward one time step without sharing memory making them compatible with MPI.

only needs to simulate the region $x > 0$, $y > 0$ and $z > 0$ with symmetric boundary conditions on the symmetry planes; the overall problem size (or number of gridpoints) decreases by a factor of eight. Similarly, some headon collisions of non-similar objects can use *quadrant* symmetry, reducing the problem size by four. The inspiral of two dissimilar compact objects often has one plane of symmetry, the plane of inspiral; *bitant* symmetry can be used to half the problem size. For all the pre-mentioned symmetries, a suitable rest frame must be used aligning with the symmetries of the initial data. In the case that the colliding objecst have spin the mentioned symmetries may be broken; in the worst case scenario there are no plane of symmetry for generic orbits with misaligned spins.

A selection of diagnostic tools have been implemented in GRChombo. These include a black hole horizon finder, gravitational wave extraction and the calculation of the ADM mass, ADM momentum, Noether charges and energy-momentum densities and fluxes. The diagnostic for the angular momentum density and flux are derived in section **??**.

While GRChombo can be used to simulate traditional spacetimes, such as binary black hole inspirals [33], it excels at simulating novel physics due to its adaptable code structure and AMR. The advantage of AMR is that regions needing higher resolution are assigned (and de-assigned) dynamically during run time; this requires no a priori knowledge or pre-determined grid structure unlike other NR codes such as Lean [34] or Einstein-Toolkit [35] [36] [37]. AMR is especially useful for matter simulations that can develop features requiring high resolution in unexpected places. GRChombo has also successfully simulated ring-like configurations [38] and inhomogeneous spacetimes [39] which would be difficult to model with a conventional pre-specified grid structure.

Simulation Units

GRChombo defaults to geometric units with $c = G = 1$, but the value of Newton's gravitational constant G can be changed if desired. Planck's constant does not arise in vacuum General Relativity, but does appear when the Klein Gordon equation for a scalar fields as in section 2.2.1. Following the conventions of section 1.1.3, Planks reduced constant $\hbar$ is also set to unity and Planck units are used.

As given in section 2.2.1, the Lagrangian for a self-interacting boson star is proportional to,

$$g^{\mu\nu}\partial_\mu\varphi\partial_\nu\bar{\varphi} + m^2|\varphi|^2 + \frac{1}{2}\Lambda_4|\varphi|^4, \tag{3.2.2}$$

in natural units; of course setting $\Lambda_4 = 0$ returns a mini boson star. For a constant κ, Setting $m \to \kappa m$ with $\varphi \to \kappa^{-1}\varphi$, $x^\mu \to \kappa^{-1}x^\mu$[2] and $\Lambda_4 \to \kappa^4\Lambda_4$ leaves the Lagrangian unchanged. Similarly for the solitonic boson star with Lagrangian,

$$g^{\mu\nu}\partial_\mu\varphi\partial_\nu\bar{\varphi} + m^2|\varphi|^2\left(1 - \frac{|\varphi|^2}{2\sigma^2}\right), \tag{3.2.3}$$

the total Lagrangian is unchanged under $m \to \kappa m$, $x^\mu \to \kappa^{-1}x^\mu$ and $\sigma \to \kappa^{-1}\sigma$. This means that changing the boson particle mass m gives a solution of the same equation but with rescaled coordinates, field values and scalar field parameters. To account for this one parameter freedom, from now on the coordinates $\hat{x}^\mu = x^\mu \cdot m$, scalar field $\hat{\varphi} = \varphi \cdot m$ and solitonic parameter $\hat{\sigma} = \sigma \cdot m$ will be used; the circumflex over these units will now be dropped for convenience. This is equivalent to setting $m = 1$; if boson stars with particle mass other than $m = 1$ are desired they can be obtained by rescaling the appropriate solution of the $m = 1$ Klein-Gordon equation.

3.2.2 Boson Star Initial Data

We now seek to solve the EKG ODEs (2.2.21), (2.2.22) and (2.2.23) numerically to obtain initial data for a single static boson star. The system can be reduced to a set of five first order ODEs with five boundary

[2]It has been assumed that the coordinates x^μ have the dimension of length such as Cartesian coordinates; instead we can demand that $g^{\mu\nu}\partial_\mu\partial_\mu \to \kappa^2 g^{\mu\nu}\partial_\mu\partial_\mu$ which is generally true even for dimensionless coordinates such as angles.

conditions. For a physical star we would like to impose $\Phi(0) = \Phi_c$, $\Phi'(0) = 0$, $\Phi(r \to \infty) \to 0$, $\Omega'(0) = 0$, $\Omega(r \to \infty) \to 1$, $\Psi'(0) = 0$ and $\Psi(r \to \infty) \to 1$ to be regular at the origin and match the Schwarzschild vacuum solution at large radius; however this is seven boundary conditions and we can only impose five. The condition $\Omega(0)' = 0$ cannot be specified as Eq. (2.2.21) is first order in derivatives of Ω but given that r and Ψ' both vanish at the origin then Ω' must also vanish at the origin automatically. One more boundary condition can be removed by asking for the boson star solution to match the isotropic Schwarzschild solution in Eq. (1.4.54) at large radius and therefore,

$$\Omega_\infty = \left(\frac{1 - \frac{M_{\rm BS}}{2r}}{1 + \frac{M_{\rm BS}}{2r}}\right) \quad \& \quad \Psi_\infty = \left(1 + \frac{M_{\rm BS}}{2r}\right)^2 \tag{3.2.4}$$

where $M_{\rm BS}$ can be interpreted as the mass of the boson star; this mass will not enter the boundary condition so can be safely ignored. Combining the two equations above gives

$$\sqrt{\Psi_\infty}\,(1 + \Omega_\infty) = 2 \tag{3.2.5}$$

for a vacuum spacetime. Imposing the single condition $\sqrt{\Psi(\infty)}\,(1 + \Omega(\infty)) = 2$, rather than both $\Omega(\infty) = 1$ and $= \Psi(\infty) = 1$, then gives asymptotic flatness in just one boundary condition. One final point of importance is the frequency ω turns the Klein-Gordon ODE into an eigenvalue problem, admitting only discrete values of ω.

The problem has now been reduced to five ODEs with the following five boundary conditions,

$$\{\Phi(0), \Phi'(0), \Psi'(0), \Omega(0), \sqrt{\Psi(\infty)}\,(1 + \Omega(\infty))\,; \omega\} = \{\Phi_c, 0, 0, \Omega_0, 2; \omega_0\}, \tag{3.2.6}$$

subjected to the condition of an eigenvalue $\omega = \omega_0$. The first attempt to find the radial profile $\{\Phi(r), \Omega(r), \Psi(r)\}$ of the boson star was to use a relaxation method as it trivially incorporates the above two-point boundary conditions. In practice this method did not work well with the eigenvalue problem in ω. Unlike with a shooting method, there was no obvious way of telling whether the guess ω was larger or smaller than the correct value. Even if this problem were overcome, a numerical solution with relaxation is computationally slow, even with Successive Over-Relaxation [40]; perhaps a multigrid method could work here but a simpler method was used.

Shooting Method

To find the initial data for a single Boson star, a c++ script was written using the RK4 method in section 3.1.4 to integrate the EKG system taking five initial conditions, and eigenvalue guess ω_0,

$$\{\Phi(0), \Phi'(0), \Psi(0), \Psi'(0), \Omega(0); \omega\} = \{\Phi_c, 0, \Psi_c, 0, \Omega_0; \omega_0\}. \tag{3.2.7}$$

Unfortunately Ω_0 and Ψ_c are unknown a priori, but guessing any values reasonably close to unity, such as $\omega_0 = 0.5$ and $\Psi_c = 2$, still give a boson star. This will generally result in the following asymptotic metric,

$$g_{\mu\nu}(r \to \infty) \to \text{diag}(-A^2, B^2, B^2, B^2), \tag{3.2.8}$$

for constant A and B.

Before we discuss how to find the correct value of ω, there is a subtle numerical problem to address. Using spherical polar coordinates in flat space, the Klein-Gordon equation (2.2.8) with $V = m^2|\varphi|^2$ and ansatz $\varphi = \Phi_{flat}(r)e^{\mathrm{i}\omega t}$ reduces to,

$$\frac{1}{\sqrt{-g}}\partial_\mu\left(\sqrt{-g}g^{\mu\nu}\partial_\nu\right)\varphi = \frac{\partial V}{\partial|\varphi|^2}\varphi, \tag{3.2.9}$$

$$\partial_t\left(g^{tt}\partial_t\right)\Phi_{flat}(r)e^{\mathrm{i}\omega t} + \frac{1}{r^2}\partial_r\left(r^2 g^{rr}\partial_r\right)\Phi_{flat}(r)e^{\mathrm{i}\omega t} = m^2\Phi_{flat}(r)e^{\mathrm{i}\omega t}, \tag{3.2.10}$$

$$\omega^2\Phi_{flat}(r) + \frac{1}{r^2}\partial_r\left(r^2\partial_r\right)\Phi_{flat}(r) = m^2\Phi_{flat}(r), \tag{3.2.11}$$

$$\tag{3.2.12}$$

where $\sqrt{-g} = r^2 \sin(\theta)$, $g^{tt} = -1$ and $g^{rr} = 1$. This has general solution,

$$\Phi_{flat}(r) = \frac{1}{r}\left(C_1 e^{-r\sqrt{m^2-\omega^2}} + C_2 e^{r\sqrt{m^2-\omega^2}}\right), \tag{3.2.13}$$

for the amplitude $\Phi_{flat}(r)$ specified by two constants C_1 and C_2. Due to finite resolution during numerical integration, at large radius C_2 will never be exactly zero and will eventually grow (along increasing radius) and spoil the numerical integration; even though this behaviour was derived in flat space it is still present in curved space with spherical symmetry - especially at such large radius that space is approximately flat. In practice, the scalar field Φ decays to some small[3] value and is effectively zero within numerical noise. At this point the coefficient C_2 is excited by noise and starts to grow exponentially. At a radius r_* when the growing mode is deemed to be dominating, usually detected by an axis crossing ($\Phi(r_*) = 0$) or a turning point ($\Phi'(r_*) = 0$), the conditions $\Phi(r > r_*) = \Phi'(r > r_*) = 0$ are enforced during integration. This creates a vacuum for $r > r_*$ and the spacetime is equivalent to the Schwarzschild spacetime. After this radius, an exponentially growing stepsize is used to reach radii of order 10^8 to 10^{10} and the values $A = \Omega_\infty = \sqrt{-g_{00}}$ and $B = \Psi_\infty = \sqrt{g_{ii}}$ can be read off.

Interval bisection was used to find the correct value of ω, ω_0, to machine precision; for the ground state we can tell that $\omega > \omega_0$ if $\Phi(r)$ develops a turning point before an axis crossing and $\omega < \omega_0$ if $\Phi(r)$ develops an axis crossing before a turning point. To find the n'th excited state, which has n axis crossing for $\Phi(r)$ and $\Phi(r \to \infty) \to 0$, a similar scheme is followed to find the eigenvalue ω_n. If $\Phi(r)$ has $n+1$ axis crossings then $\omega > \omega_n$ and if $\Phi(r)$ has n axis crossings followed by a turning point then $\omega < \omega_n$. This method of doing a numerical integration and iteratively restarting to get closer to the target solution is known as a shooting method.

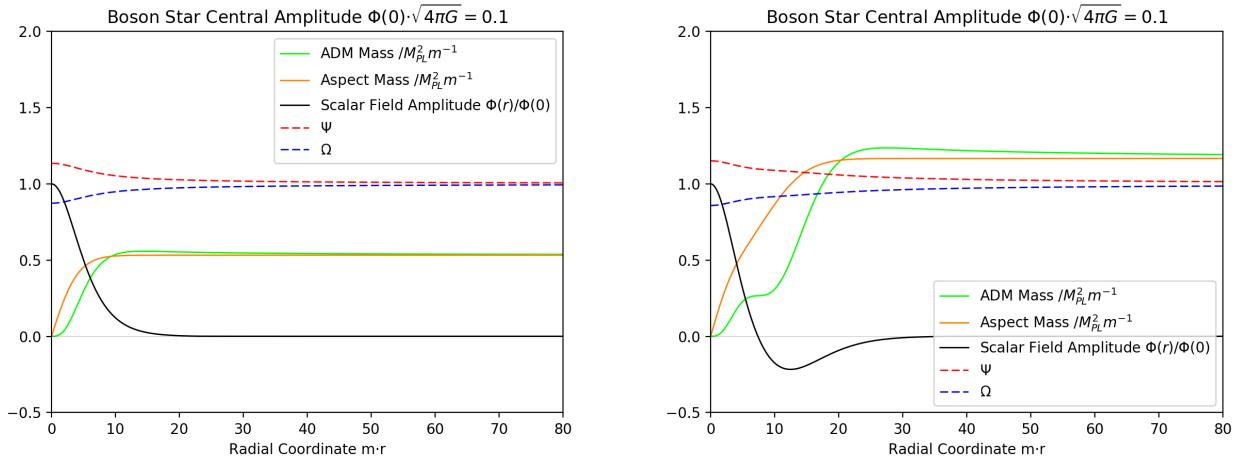

Figure 3.1: Boson Star radial profile, Left: Ground state, Right: 1st Excited state

Putting everything together, a boson star solution with eigen value ω_0 (or ω_n for excited stars) and asymptotic metric Eq. (3.2.8) can be obtained. To find a star with asymptotic metric $\eta_{\mu\nu}$ of flat space, the initial conditions are iteratively improved like $\Omega_c \to \Omega_c/\Omega_\infty$ and $\Psi_c \to \Psi_c/\Psi_\infty$; the interval bisection for ω is then restarted. This is iterated three to five times which leaves $A = \Omega_\infty = 1$ and $B = \Psi_\infty = 1$ to high precision and the isotropic boson star profile has been created. This whole process requires a few seconds runtime for a high resolution 200,000 grid-point simulation on a regular laptop.

Figure 3.2a shows the numerically obtained radial profile of a mini boson star ($\Lambda = 0$) and an excited mini boson star. Note two mass definitions are plotted; the ADM mass (calculated as a function of

[3]Small meaning roughly twenty orders of magnitude smaller than the central density $\Phi(0)$ for a mini boson star. This gets a little less small for dense solitonic stars but it still a good approximation to zero.

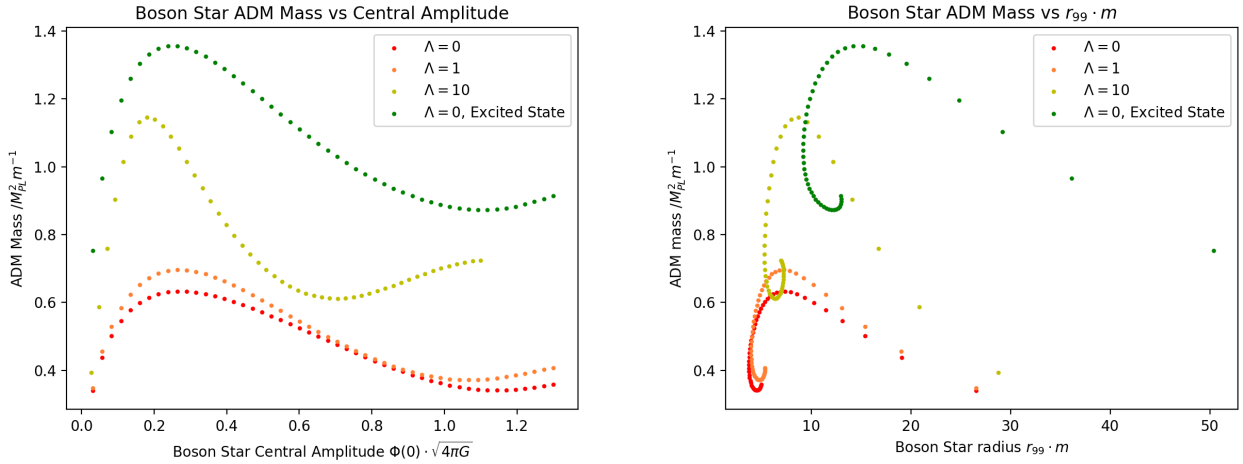

Figure 3.2: Boson star trends, Left: ADM mass vs $\Phi(0)$, Right: ADM mass vs r_{99}

finite r) and the aspect mass [REF] [I THINK I NEED TO WRITE OUT THIS SOMEWHERE ITS ONLY A FEW LINES]. Polytropic fluid stars were also simulated as a preliminary test of the code; they are much easier to create not needing to solve an eigenvalue problem and don't have an asymptotically growing mode. Figure (3.3a) shows how the ADM mass of boson stars varies with central amplitude $\Phi(0)$ and r_{99}, the radius which $\Phi(r_{99}) = \Phi(0)/100$. It should be noted that the mini boson star (with $\Lambda = 0$) case agrees with the known maximum mass, the Kaup limit [41] $M_{max} \approx 0.633 M_{PL}^2 m^{-1}$ with the highest measured mass being $M_{max} = 0.63299(3) M_{PL}^2 m^{-1}$ corresponding to a central amplitude of $\sqrt{4\pi G}\Phi(0)_{max} = 0.271(0)\ m^{-1}$.

While many different boson stars have been made to test the initial data code, all the following evolutions use the same boson star with parameters $\Lambda = 0$, $\sqrt{4\pi G}\Phi(0) = 0.1\ m^{-1} \rightarrow \Phi(0) \approx 0.0282\ m^{-1}$ and ADM mass $M = 0.532(7)\ M_{\rm PL}^2 m^{-1}$. This is as the stars are heavy enough to form black holes under collisions and large deformations, but stable enough to not collapse to a black hole for moderate perturbations.

3.2.3 Single Star Evolution

As a check that the initial from section 3.2.2 is correct, a mini boson star with central density $\Phi(0) = 0.02820\ m^{-1}$ is evolved in time in three spatial dimensions. The simulation has a physical domain size $L = 1024\ m^{-1}$ with $N = 320$ gridpoints on AMR level zero with grid spacing $\Delta x = 3.2\ m^{-1}$. The AMR is allowed up to six extra levels; the finest level (level six) has a grid spacing of $\Delta x = 0.05\ m^{-1}$. The star is supposed to remain in the centre of the grid and not change as it is a rest frame soliton; this is observed through evolution with GRChombo. Figure (3.4a) shows the global maximum value of $|\varphi|$ and Fig. (3.4b) shows the total integral of the Noether charge N over the grid. As can be seen, $|\varphi|_{max}$ is constant to $\sim 0.7\%$ and N is conserved to the $\sim 0.07\%$ level until time $t = 350\ m^{-1}$.

3.2.4 Superposition of Initial Data

In order to simulate a spacetime consisting of two stars (or a star and a black hole) we must choose a way of superposing the initial data of two objects, centred at $x^{(1)}$ and $x^{(2)}$. For some field $\psi^{(j)}$ associated with the compact object at $x^{(j)}$,

$$\psi^{(j)} = \psi(x - x^{(j)}), \tag{3.2.14}$$

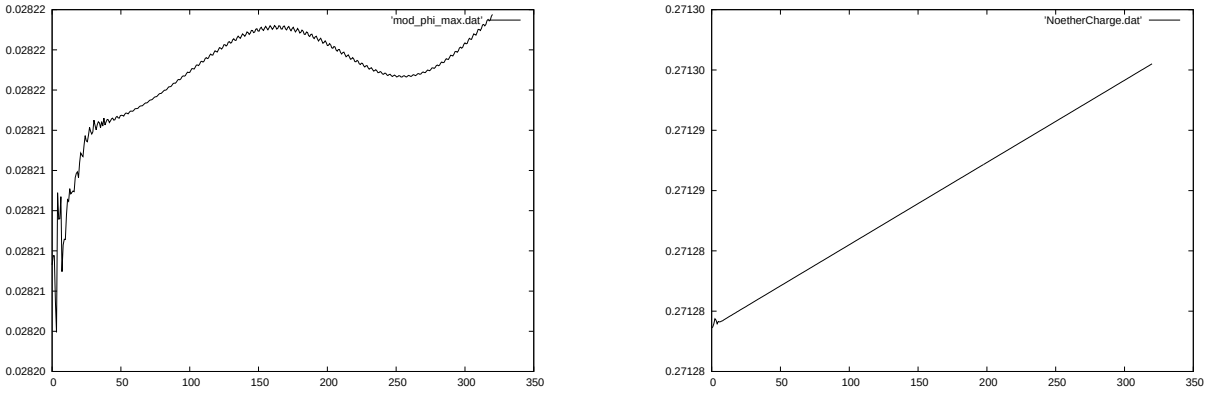

Figure 3.3: Left: Maximum of $|\varphi|$ during evolution, Right: Total integrated Noether charge N.

where ψ refers to the object centred about the origin. Taking two compact objects with fields φ, Π, γ_{ij}, $\mathcal{K}_{ij}$, α and β^i, a naive superposition scheme was chosen;

$$\varphi = \varphi^{(1)} + \varphi^{(2)}, \tag{3.2.15}$$

$$\Pi = \Pi^{(1)} + \Pi^{(2)}, \tag{3.2.16}$$

$$\mathcal{K}^i_j = \mathcal{K}^{(1)}{}^i_j + \mathcal{K}^{(2)}{}^i_j, \tag{3.2.17}$$

$$\gamma_{\mu\nu} = \gamma^{(1)}_{\mu\nu} + \gamma^{(2)}_{\mu\nu} - \delta_{\mu\nu}, \tag{3.2.18}$$

$$\beta_i = \beta^{(1)}_i + \beta^{(2)}_i, \tag{3.2.19}$$

$$\alpha = \sqrt{\alpha^2_{(1)} + \alpha^2_{(2)} - 1}, \tag{3.2.20}$$

$$\chi = \det\left(\gamma^{(1)}_{\mu\nu} + \gamma^{(2)}_{\mu\nu} - \delta_{\mu\nu}\right)^{-1/3}, \tag{3.2.21}$$

where the super-scripts $^{(1)}$ and $^{(2)}$ refer to the separate compact objects. The extrinsic curvature is chosen to be superposed with mixed indices so that it implies the trace $\mathcal{K}$ is also superposed. If one of the compact objects is a black hole the lapse $\alpha \to 0$ on the horizon; this is circumvented by setting,

$$\alpha = \sqrt{\chi}, \tag{3.2.22}$$

ensuring that the lapse is real and non-negative for a all of Σ_t.

Superposing two solutions in general relativity usually no longer satisfies the Einstein equation, the Hamiltonian constraint Eq. (2.1.50) and momentum constraints Eq. (2.1.52) are violated. For asymptotically flat compact objects, the constraint violation reduces to zero as the object separation tends to infinity. In the case of finite separations, the CCZ4 scheme in section 2.1.9 aims to drive the constraint violation towards zero and hence a true solution of Einstein's equation. The collisions of compact objects in section(S) 3.2.5 use this naive superposition scheme. Section [REF] [MALAISE PAPER SECTION] explores a technique to improve the naive superposition of compact objects.

3.2.5 Collisions of Boson Stars

Both a headon collision and a grazing collision of two boson stars are simulated using the superposition scheme given in section 3.2.4. The two stars are identical, each has a central density of $\Phi(0) = 0.02820$ and an ADM mass $M = 0.532(7)\ M^2_{\rm PL} m^{-1}$. The stars are placed at positions $x^i = \pm\{40, 0, 0\}\ m^{-1}$ in the headon case and $x^i = \pm\{40, 8, 0\}\ m^{-1}$ in the grazing case and are boosted together with respective

velocities $v^i = \mp\{0.1, 0, 0\}$ in both cases. A speed of $v = 0.1$ corresponds to a rapidity of $\psi = 0.1003353$ (4 s.f.). The simulations have a physical domain size of $L = 512\ m^{-1}$ with $N = 256$ gridpoints on AMR level zero, this gives a coarse grid resolution of $\Delta x = 2\ m^{-1}$. There are up to five extra AMR levels giving a finest grid resolution of $\Delta x = 1/16\ m^{-1}$.

Headon Collision

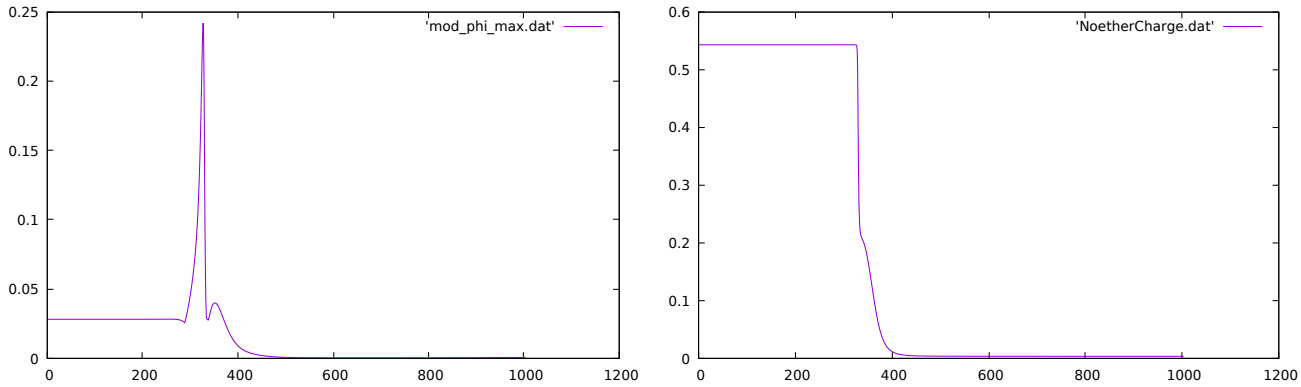

Figure 3.4: Left: Maximum of $|\varphi|$ during evolution, Right: Total integrated Noether charge N.

Figure (3.5a) shows $|\varphi|_{max}$, the global maximum value of $|\varphi|$, and the total Noether charge N as a function of time for the headon collision. At time $t \approx 289\ m^{-1}$, $|\varphi|_{max}$ rapidly increases and collapses to a black hole. At time $t \approx 327\ m^{-1}$, there is a temporal maximum in $|\varphi|_{max}$ as the resolution limit of the simulation is reached and the scalar field is dissipated by the Kreiss-Oliger dissipation mentioned in section 3.2.1. This dissipation can also be seen in the Noether charge plot at a time of $t \approx 326\ m^{-1}$ where the total charge that should remain constant but begins to fall. The lack of sufficient resolution inside the black hole is not problematic for the external simulation; the errors accumulated are trapped inside the event horizon. Fig. (3.5a) shows that the total Noether charge rapidly decays to zero as it falls into the black hole and is dissipated due to finite resolution effects.

The gravitational wave extraction at radius $r = 140\ m^{-1}$ is given in figure 3.6a. A spin-weighted spherical harmonic decomposition of the Newman-Penrose scalar Ψ_4 [REF] [DO I NEED TO REF THIS?] has been done and the $m, l = 2, 0$ and $m, l = 2, 2$ modes are plotted.

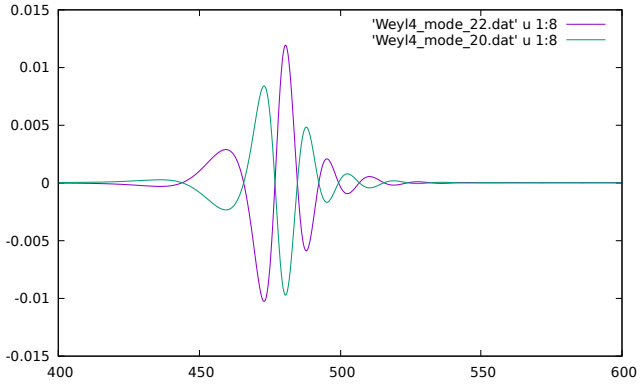

Figure 3.5: Gravitational wave signal of the headon boson star collision. The $m, l = 2, 2$ and $m, l = 2, 0$ spin weighted spherical harmonic modes of the Ψ_4 Newman-Penrose scalar are given.

The dynamics of the two boson stars are shown in Fig. (3.9a) which plots the scalar field modulus $|\varphi|$ on the x, y plane. The stars collide at at time $275\ m^{-1} < t < 300\ m^{-1}$; the collision time of two point

masses (with the same initial conditions) has been simulated in Newtonian gravity giving a collision time of $t = 287.6\ m^{-1}$. Soon after collision, an over-density of scalar field is developed which subsequently collapses to a black hole. The black hole then accretes the surrounding scalar field; the scalar field can be seen to be composed of higher order spherical harmonic modes at later times. DO I MENTIONT THIS IS BECAUSE HIGHER ORDER MODES HAVE SLWOER DECAY RATE? I THINK I HAVE SHOWN THIS

Grazing Collision

Figure (3.7a) plots $|\varphi|_{max}$ and the total Noether charge (N) versus time for the grazing collision. At time $t \approx 309\ m^{-1}$, $|\varphi|_{max}$ rapidly increases and a black hole is soon formed. The black hole is assumed to be spinning due to the collapsing matter containing angular momentum. At time $t \approx 356\ m^{-1}$ there is a temporal maximum in $|\varphi|_{max}$; similarly to the headon collision, this is caused by diverging resolution requirements towards the black hole centre and usually does not affect the exterior spacetime. Consequently, the Noether charge plot shows a fall in charge at a time of $t \approx\ m^{-1}$; for a well resolved simulation N should remain constant.

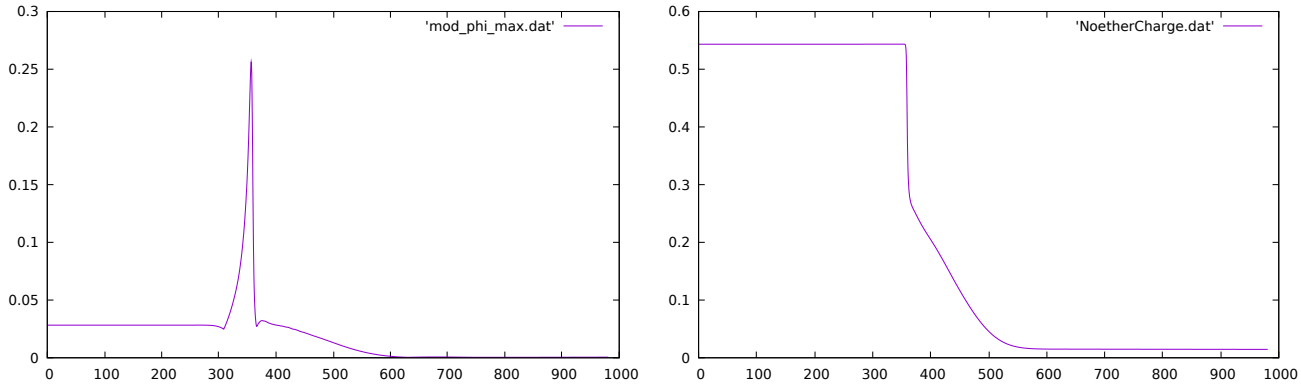

Figure 3.6: Left: Maximum of $|\varphi|$ during evolution, Right: Total integrated Noether charge N.

A simulation of the grazing collision with point masses has been done using Newtons laws. The time taken for closest approach (with separation $s = 2.33\ m^{-1}$) is $t = 315.8\ m^{-1}$; at this separation the finite sized stars would collide. Snapshots of the grazing boson star collision using numerical relativity are shown in Fig. (3.10a) plotting the scalar field modulus $|\varphi|$ on the x, y plane. The stars collide at time $300\ m^{-1} < t <\ m^{-1}$ which is in good agreement with the Newtonian approximation. Soon after collision, an over-density of scalar field develops and collapses to a black hole; this black hole is thought to be spinning due to the angular momentum of the collapsing matter. The black hole subsequently accretes most of the surrounding scalar field leaving a quasi-long-lived rotating toroidal scalar field configuration surrounding the black hole. This late time toroidal scalar field configuration will be referred to as a *toroidal wig* due to it being "fake" hair. The late time toroidal wig seems to settle to a rotationally symmetric configuration, with no quadrupole moment, and does not emit a gravitational wave signal; this can be seen in the figure 3.8a which plots the $m, l = 2, 2$ and $m, l = 2, 0$ modes of Ψ_4.

Figure (3.9a) shows the late time Noether charge of the grazing and headon collisions. In contrast to the headon collision, the decay of N in the grazing case is slower and reaches a value approximately 7 times greater. Using linear extrapolation, the Noether charge of the grazing collision decays to zero at time $t \approx 12500\ m^{-1}$ and hence the toroidal wig has an approximate lifespan of $12000\ m^{-1}$.

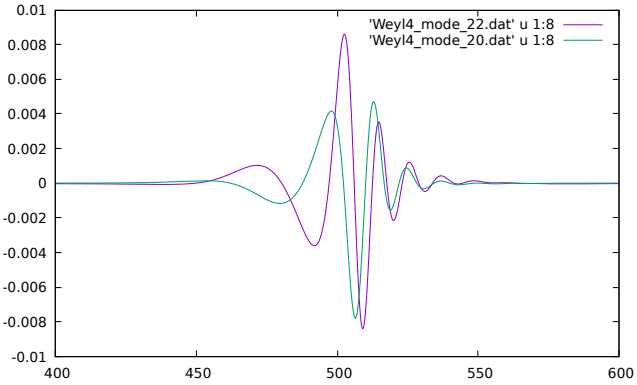

Figure 3.7: Gravitational wave signal of the grazing boson star collision. The $m, l = 2, 2$ and $m, l = 2, 0$ spin weighted spherical harmonic modes of the Ψ_4 Newman-Penrose scalar are given.

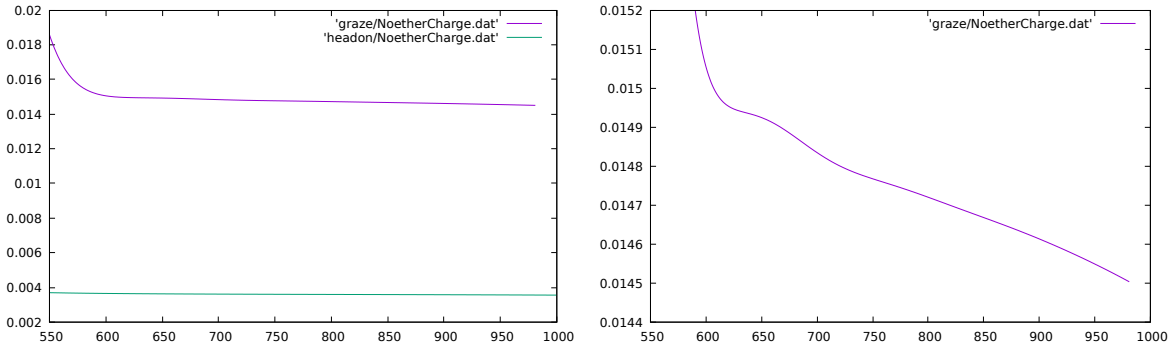

Figure 3.8: Left: Comparison of late time Noether charge N between headon collision and grazing collision of two boson stars. Right: Late time plot of the Noether charge of the grazing collision only.

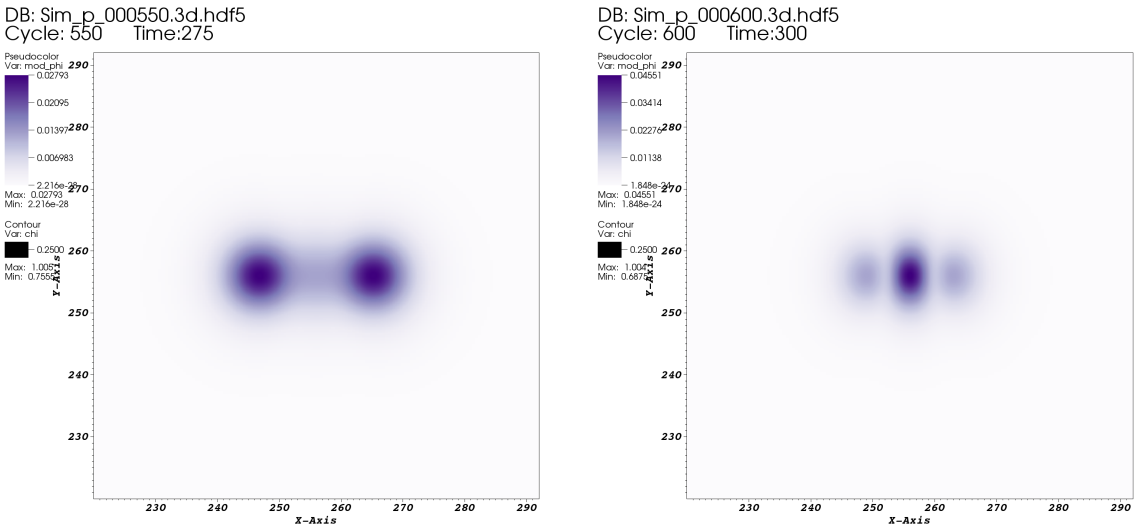

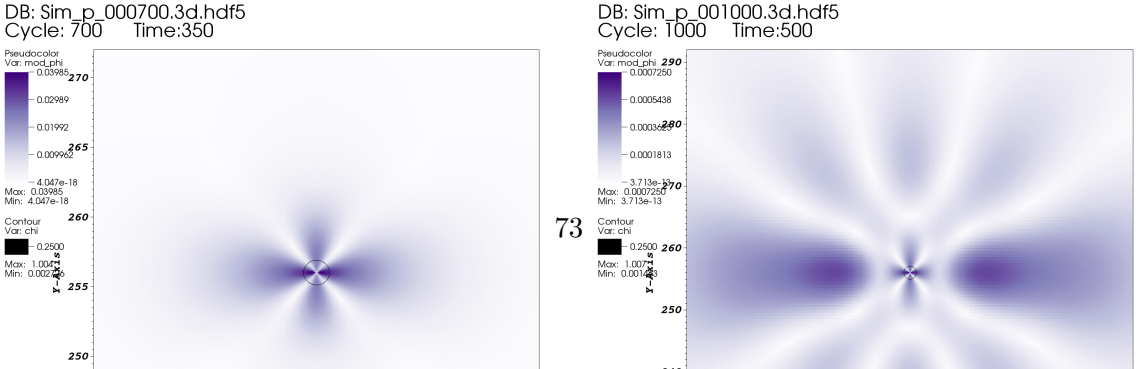

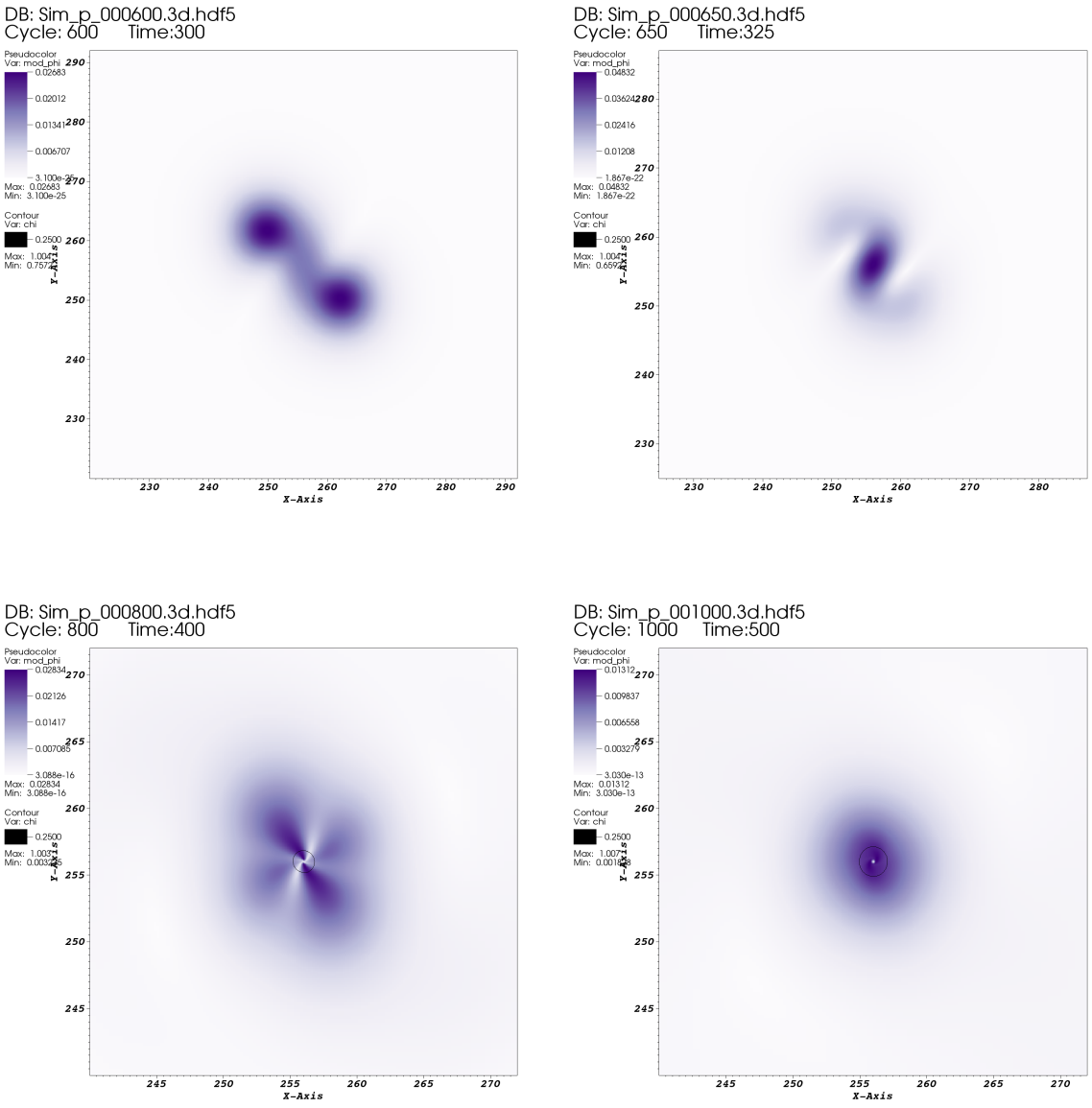

Figure 3.10: Field plots of $|\varphi|$ during evolution at four different times for the grazing boson star collision. Time $t = 300\ m^{-1}$ and $t = 325\ m^{-1}$ show snapshots momentarily before and after the collision. The Newtonian estimate of collision time is $t = 315.8\ m^{-1}$. Time $t = 400\ m^{-1}$ shows the scalar field accreting into the recently formed black hole. Time $t = 500\ m^{-1}$ shows the scalar field surrounding the black hole a little later; this is called a *toroidal wig*. Both the plots of $t = 400\ m^{-1}$ and $t = 500\ m^{-1}$ display a contour plot of $\chi = 0.25$ acting as a very approximate marker for the event horizon.

Chapter 4

STUFF TO DO

check tensor vs tensor field

3+1 stress tensor is wrong for klein gordon? check it again

add a sections with intro reading such as books alcubbiere baumgarte, adn GR stuff like sean caroll, tong, harvey ..

ADD TO CONVENTIONS THAT LATE LATIN INDECES (I,J,K,...) SYMBOLISE 3D OBJECTS IN 4D SPACE ASWELL AS 3D OBJECST IN 3D SPACE

CHECK THE 3+1 SPLIT STRESS TENSOR AGREES WITH PAPERS ...

CHECK CURLY VS SMOOTH BRACKETS FOR SETS AND VECTORS ALL OVER

REF THE ADM METRIC?

make a note of the dx form notation but don't go into depth, maybe hint at intergating over a mfold?

MAYBE ADD Z4 LAGRANGEAN OR UNDERSTAND IT BETTER? LOOK AT MARKUS/KATY THESIS?

MAKE SOME UNIFORM CONVENTION FOR STRESS TENSOR, MAYBE RHO FOR ENERGY DENSITY MAYBE EPSILON? SIMILAR FOR THE MOMENTA AND THE PROJECTED TENSOR? its in the ccz4 equations too ...

fig or Fig in figure referneceing? use Fig but no brackets around figures]

DECIDE ON A FACTOR OF 16PI IN TEH MATTER LAGRANGEAN OF GR BETWEEN THE INTRO SECTION AND THE LATER SECTION. PROBABLY USE R/16PI RATHER THAN 16PI*MATTER ...

standardise complex phi, bar or star for conjugate? or dagger??

MAKE SURE I CREDIT MIREN FOR THE TIME EVOLUTION OF THE SCALAR FIELD

SORT OUT MY RANDOM USE OF ITALICS

IF SR SECTION GETS BOOSTS, MUST REFERENCE THEM FROM THE BOOSTED STARS SECTION

IF THE MASS RESCALING THING (M) IS EXPLAINED IN THE GRCHOMBO SECTION MAYBE IT CAN BE REMOVED IN THE Q PAPER SECTION?

NAME THE SECTIONS AND CHAPTERS PROPERLY

CAN REFERENCE THE ASPECT MASS FROM THE MALAISE PAPER

CHECK THE INTRO SECTION OF MALAISE AND BOSON STARS DONT DOUBLE COVER TOO MUCH STUFF

CHECK HAM AND MOM CONSTRAINT ARE CALLED H ADN M EVERYWHERE

DEFINE PDE OR ODE SOMEWHERE

IN GR OR INTRO MAYBE PUT REFS TO GR TEXTBOOKS, DEFO FOR NR TEXTBOOK BAUMGARTE AND ALCUBIERE

<><><><><><><><><> important <><><><><><><><><><> MAYBE PROPERLY DO THE PENROSE DIAGRAMS IN GAUGE SECTION - could steal from smith knight

FOR BOSON MASS M CHECK EVERYWHERE WE HAVE $x = 20m^{-1}$ rather than $x = 20m$ (for example)

DEFINE ASPECT MASS SOMERWHERE

FIX THE LINES IN THE TABLE IN AFTERGLOW PAPER - COMPARE TO ORIGINAL PAPER

MAYBE THERE IS TOO MUCH DOUBLE COVER OF QFS STUFF IN APPENDIX OF AFTERGLOW PAPER

CHECK FOR BROKEN CREF IN AFTERGLOW PAPER, SOME REFERENCES ARE EMPTY IN TYPE (BUT HYPERLINKING STILL WORKS)

CTRL+F THE WORD PAPER (MAYBE WORK - MAYEB LETTER) TO ENSURE WE ALWAYS REFER TO A THESIS

USE TEXTSC FOR NAMES LIEK GRCHOMBO OR C++, CHECK THE BH PAPER FOR CONVENTIONS

MAYEB MAKE THE PROOF OF G$^{M}UNUISINVERSEOFG_{M}UNUABITCLEARERR$?

M-DIMENSIONAL OR M DIMENSIONAL ?

MAYBE WRITE A BIT ON WHY GEODEICS ARE IMPORTANT AT THE END OF THE GEODESIC SECTION? LINK TO GR AND INERTIAL FRAMES.

CHECK NON-AFFINE GEODESIC SOMETIME

CHECK THE DISTRIBUTIVE AND ASSOCIATIVITY BIT FOR DIFF OPERATORS <><><><><> IMPORTANT, CHECK IF LIE DERIV CAN USE FUNCTIONS IN DISTRIBUTIVITY???

MAYBE DISTINGUISH BETWEEN : AND CDOT FOR THE INNER PRODUCT, WITHOUT A METRIC WE MUST USE : NOT CDOT

FIX ALL THE PLACES THE DIV THEOREM OR THE DIV OF A TENSOR IS USED AND REFERENCES MAYBE?

CHECK THE RIGHT GAMMA (HAT GAMMA VS TILDE GAMMA) IS USED ALL OVER THE CCZ4 EQNS - ESPACIALLY THE KLEIN GORDON EQUATION. CHECK THE KLEIN GORDON IN CCZ4 IS EVEN CORRECT

<><><><><><> SUPER IMPORTANT - CHECK BEFORE SUBMIT <><><><><><><><><><> CHECK THE K1 K3 STUFF IN CCZ4 AND SEE WHAT I USE IN GRCHOMBO

FIX THE BROKEN REF IN CCZ4

GREEK INDECES IN 3+1 SECTION

CHECK MY GAUGE EVOLUTION VS GRCHOMBO

READ AND IMPLEMENT ULIS COMENT ABOUT CHARACTORISTICS (AND PUT INTO NUMERICAL SECTION BOUNIDARY CONDITIONS)

<><><><><><><> FOR ULI TO READ <><><><><><><><><> THE GR SECTION CCZ4 AND GAUGE CONDITIONS

Bibliography

Bibliography

[1] D. J. Kaup, "Klein-Gordon Geon," *Phys. Rev.*, vol. 172, pp. 1331–1342, 1968.

[2] R. Brito, V. Cardoso, C. A. Herdeiro, and E. Radu, "Proca stars: gravitating bose–einstein condensates of massive spin 1 particles," *Physics Letters B*, vol. 752, pp. 291–295, 2016.

[3] J.-w. Lee and I.-g. Koh, "Galactic halos as boson stars," *Physical Review D*, vol. 53, no. 4, p. 2236, 1996.

[4] F. E. Schunck and E. W. Mielke, "General relativistic boson stars," *Classical and Quantum Gravity*, vol. 20, no. 20, p. R301, 2003.

[5] A. Einstein *et al.*, "On the electrodynamics of moving bodies," *Annalen der physik*, vol. 17, no. 10, pp. 891–921, 1905.

[6] G. C. McVittie, "The mass-particle in an expanding universe," *Monthly Notices of the Royal Astronomical Society*, vol. 93, pp. 325–339, 1933.

[7] D. Hilbert, "Die grundlagen der physik [foundations of physics]," *Nachrichten von der Gesellschaft der Wissenschaften zu Göttingen–Mathematisch-Physikalische Klasse*, vol. 3, p. 395, 1915.

[8] S. Frittelli and R. Gómez, "Ill-posedness in the einstein equations," *Journal of Mathematical Physics*, vol. 41, no. 8, pp. 5535–5549, 2000.

[9] T. W. Baumgarte and S. L. Shapiro, "On the Numerical integration of Einstein's field equations," *Phys. Rev. D*, vol. 59, p. 024007, 1998. gr-qc/9810065.

[10] D. Garfinkle, "Harmonic coordinate method for simulating generic singularities," *Phys. Rev. D*, vol. 65, p. 044029, 2002. gr-qc/0110013.

[11] D. Garfinkle, "Harmonic coordinate method for simulating generic singularities," *Physical Review D*, vol. 65, no. 4, p. 044029, 2002.

[12] F. Pretorius, "Numerical relativity using a generalized harmonic decomposition," *Class. Quantum Grav.*, vol. 22, pp. 425–452, 2005. gr-qc/0407110.

[13] F. Pretorius, "Evolution of Binary Black-Hole Spacetimes," *Phys. Rev. Lett.*, vol. 95, p. 121101, 2005. gr-qc/0507014.

[14] C. Gundlach, G. Calabrese, I. Hinder, and J. M. Martín-García, "Constraint damping in the z4 formulation and harmonic gauge," *Classical and Quantum Gravity*, vol. 22, no. 17, p. 3767, 2005.

[15] D. Alic, C. Bona-Casas, C. Bona, L. Rezzolla, and C. Palenzuela, "Conformal and covariant formulation of the z4 system with constraint-violation damping," *Phys. Rev. D*, vol. 85, p. 064040, Mar 2012.

[16] M. Alcubierre, *Introduction to 3+ 1 numerical relativity*, vol. 140. Oxford University Press, 2008.

[17] L. Smarr and J. W. York Jr, "Kinematical conditions in the construction of spacetime," *Physical Review D*, vol. 17, no. 10, p. 2529, 1978.

[18] M. Campanelli, C. O. Lousto, P. Marronetti, and Y. Zlochower, "Accurate evolutions of orbiting black-hole binaries without excision," *Phys. Rev. Lett.*, vol. 96, p. 111101, Mar 2006.

[19] B. Brügmann, W. Tichy, and N. Jansen, "Numerical simulation of orbiting black holes," *Phys. Rev. Lett.*, vol. 92, p. 211101, 2004. gr-qc/0312112.

[20] F. E. Schunck and E. W. Mielke, "General relativistic boson stars," *Class. Quant. Grav.*, vol. 20, pp. R301–R356, 2003.

[21] S. L. Liebling and C. Palenzuela, "Dynamical Boson Stars," *Living Rev. Rel.*, vol. 15, p. 6, 2012.

[22] C. Palenzuela, P. Pani, M. Bezares, V. Cardoso, L. Lehner, and S. Liebling, "Gravitational Wave Signatures of Highly Compact Boson Star Binaries," *Phys. Rev. D*, vol. 96, no. 10, p. 104058, 2017.

[23] A. Diez-Tejedor and A. X. Gonzalez-Morales, "No-go theorem for static scalar field dark matter halos with no noether charges," *Physical Review D*, vol. 88, no. 6, p. 067302, 2013.

[24] Press, William H. and Teukolsky, Saul A. and Vetterling, William T. and Flannery, Brian P., *Numerical recipes in C (2nd ed.): the art of scientific computing*. New York, NY, USA: Cambridge University Press, 1992.

[25] M. Alcubierre, B. Brügmann, P. Diener, M. Koppitz, D. Pollney, E. Seidel, and R. Takahashi, "Gauge conditions for long-term numerical black hole evolutions without excision," *Phys. Rev. D*, vol. 67, p. 084023, 2003. gr-qc/0206072.

[26] T. Andrade, L. A. Salo, J. C. Aurrekoetxea, J. Bamber, K. Clough, R. Croft, E. de Jong, A. Drew, A. Duran, P. G. Ferreira, P. Figueras, H. Finkel, T. França, B.-X. Ge, C. Gu, T. Helfer, J. Jäykkä, C. Joana, M. Kunesch, K. Kornet, E. A. Lim, F. Muia, Z. Nazari, M. Radia, J. Ripley, P. Shellard, U. Sperhake, D. Traykova, S. Tunyasuvunakool, Z. Wang, J. Y. Widdicombe, and K. Wong, "Grchombo: An adaptable numerical relativity code for fundamental physics," *Journal of Open Source Software*, vol. 6, no. 68, p. 3703, 2021.

[27] K. Clough, P. Figueras, H. Finkel, M. Kunesch, E. A. Lim, and S. Tunyasuvunakool, "Grchombo: numerical relativity with adaptive mesh refinement," *Classical and Quantum Gravity*, vol. 32, no. 24, p. 245011, 2015.

[28] M. J. Berger and J. Oliger, "Adaptive mesh refinement for hyperbolic partial differential equations," *Journal of computational Physics*, vol. 53, no. 3, pp. 484–512, 1984.

[29] M. Berger and I. Rigoutsos, "An algorithm for point clustering and grid generation," *IEEE Transactions on Systems, Man, and Cybernetics*, vol. 21, no. 5, pp. 1278–1286, 1991.

[30] M. Shibata and T. Nakamura, "Evolution of three-dimensional gravitational waves: Harmonic slicing case," *Phys. Rev. D*, vol. 52, pp. 5428–5444, 1995.

[31] T. W. Baumgarte and S. L. Shapiro, "Numerical integration of einstein's field equations," *Physical Review D*, vol. 59, no. 2, p. 024007, 1998.

[32] H.-O. Kreiss and J. Oliger, *Methods for the approximate solution of time dependent problems*. No. 10, International Council of Scientific Unions, World Meteorological Organization, 1973.

[33] M. Radia, U. Sperhake, E. Berti, and R. Croft, "Anomalies in the gravitational recoil of eccentric black-hole mergers with unequal mass ratios," *Physical Review D*, vol. 103, no. 10, p. 104006, 2021.

[34] U. Sperhake, "Binary black-hole evolutions of excision and puncture data," *Phys. Rev. D*, vol. 76, p. 104015, 2007. gr-qc/0606079.

[35] F. Löffler, J. Faber, E. Bentivegna, T. Bode, P. Diener, R. Haas, I. Hinder, B. C. Mundim, C. D. Ott, E. Schnetter, *et al.*, "The einstein toolkit: a community computational infrastructure for relativistic astrophysics," *Classical and Quantum Gravity*, vol. 29, no. 11, p. 115001, 2012.

[36] M. Zilhão and F. Löffler, "An Introduction to the Einstein Toolkit," *Int. J. Mod. Phys. A*, vol. 28, p. 1340014, 2013. arXiv:1305.5299 [gr-qc].

[37] Einstein Toolkit webpage: http://einsteintoolkit.org/.

[38] T. Helfer, J. C. Aurrekoetxea, and E. A. Lim, "Cosmic string loop collapse in full general relativity," *Phys. Rev. D*, vol. 99, p. 104028, May 2019.

[39] J. C. Aurrekoetxea, K. Clough, R. Flauger, and E. A. Lim, "The effects of potential shape on inhomogeneous inflation," *Journal of Cosmology and Astroparticle Physics*, vol. 2020, pp. 030–030, may 2020.

[40] A. Hadjidimos, "Successive overrelaxation (sor) and related methods," *Journal of Computational and Applied Mathematics*, vol. 123, no. 1-2, pp. 177–199, 2000.

[41] D. J. Kaup, "Klein-gordon geon," *Phys. Rev.*, vol. 172, pp. 1331–1342, Aug 1968.

[42] blank